# Development of Nanocomposite Based Bioelectrodes using Alcohol Oxidase and Laccase as Biocatalysts for Bioelectronic Applications

A Thesis

*Submitted in partial fulfilment of the requirements for the degree of*

**Doctor of Philosophy**

*By*

**MADHURI DAS**

Centre for Energy
Indian Institute of Technology Guwahati
Guwahati-781039, Assam, India
December, 2014

*Dedicated to*

*My*

*Beloved Parents*

**Centre for Energy**

**Indian Institute of Technology Guwahati**

Guwahati - 781039, Assam, INDIA

# STATEMENT

I do hereby declare that the matter incorporated in this thesis is the result of investigations carried out by me in the Centre for Energy, Indian Institute of Technology Guwahati, India, under the guidance of **Prof. Pranab Goswami**.

In keeping with the general practice of reporting scientific observations, due acknowledgements have been made wherever the work described is based on the findings of other investigators.

December, 2014

**Madhuri Das**

**Roll No. 09615106**

भारतीय प्रौद्योगिकी संस्थान गुवाहाटी, गुवाहाटी-781 039
INDIAN INSTITUTE OF TECHNOLOGY GUWAHATI
Department of Biotechnology
Guwahati - 781 039, India

Phone: +91-361-2582202 (Biotech)
+91-361-2583126 (Energy)
Fax: +91-361-2690762
+91-361-2582249 (Biotech)
E-mail: pgoswami@iitg.ernet.in

**Prof. Pranab Goswami**
Professor & Head
Centre for Energy

CENTRE FOR ENERGY

# Certificate

This is to certified that the thesis entitled "**Development of Nanocomposite Based Bioelectrodes using Alcohol Oxidase and Laccase as Biocatalysts for Bioelectronic Applications**" that is being submitted by **Madhuri Das** (Roll No. 09615106) for the award of the degree of Doctor of Philosophy is an authentic record of the results obtained from the research work carried out under my supervision in the Centre for Energy, Indian Institute of Technology Guwahati, Assam, India.

The results incorporated in this thesis have not been submitted to any other University or Institute for the award of any degree.

**Dr. Pranab Goswami**
Professor
(Research Supervisor)

December, 2014

# ACKNOWLEDGEMENT

*Taking the opportunity of this column, I would like to express my sincere gratitude to all those who directly or indirectly helped me in successful completion of my Phd.*

*With immense pleasure, I wish to express my deep sense of gratitude and indebtedness to my supervisor Prof. Pranab Goswami, Department of Biotechnology, HoC Centre for Energy, IIT Guwahati for his valuable guidance, constant encouragement, constructive criticism advice and countless help throughout the period of my research work and preparation of the thesis.*

*I would like to express my sincere gratitude to Prof. Pinakeswar Mahanta ,Prof Aloke K Ghoshal, former HoC of the Centre for Energy, IIT Guwahati and my doctoral committee Prof. Pinakeswar Mahanta, Prof. Vikas K Dubey and Prof. PK Iyer whose guidance and encouragement were motivation factor during the thesis work.*

*I am very grateful to my seniors Dr. A.Kiran Kumar, Dr. Susuvan Chatterjee, Dr. Anil Sharma, Dr. Preety Vatsyayan, Dr. Urmila Saxena, Seraj Ahmad, friends Dr. Mitun Chakraborty, Somasekhar Reddy; juniors Ankana, Priyanki, Mrinal, Santhosh, Priyamvada, Babina, Naveen, Sharbani, Abdul, Farhan, Phurpa for their help, support and encouragement in completing my phd work.*

*I am grateful to the past and present staff members of Centre for Energy Dr. Lepakshi Barbora, Dhiren Huzuri, Dr. Pankaj Kalita, Archana Rajbonshi, Gitanjali Hazarika, Bornali Malakar and research scholar of Centre for energy for their constant support and help. I am also thankful to my friends, Rajesh, Arghya, Ashish for their help and with whom I share tons of fond memories in the IITG campus.*

*I thank Ministry of Human Resource and Development (MHRD), Govt of India and Indian Institute of Technology Guwahati for providing all the financial assistances and providing me the platform to carry out my research smoothly.*

*I would like to thank Centre for excellence facility of Department of Biotechnology, Central Instruments Facility, Control lab, Electronics and Electrical Engineering, Chemical Engineering, IIT Guwahati for providing the access to various facilities without which this study would not be feasible.*

*Lastly, I express my deep sense of gratitude to my parents, my brother for their unconditional love, help, co-operation and moral support during the course of investigation. Thanks to the Almighty for his blessings bestowed upon me to complete this thesis*

**Madhuri Das**

# ABSTRACT

This study aims at fabricating alcohol oxidase (AOx) based bioelectrode for biosensors and biofuel cell application. An octameric AOx (Mw ~675 kDa) from *Pichia pastoris*, immobilized on multiwalled carbon nanotubes- nafion (MWCNT-Nf) matrix and encapsulated with polyethylenimine (PEI) on gold electrode (AuE), showed a redox peak at 0.21 V (vs. Ag/AgCl electrode at pH 7.5) for oxidation of alcohol. Studies on response of AuE-MWCNT-Nf-AOx-PEI bioelectrodes for alcohol showed a linear response in the range of 8 μM–42 μM, response time of 55 s for steady state current, and detection limit of 5 μM. The electron transfer rate constant ($K_s$) of $1.69 \pm 0.15\ s^{-1}$ was observed for the bioelectrode, indicating facilitation of the electron transfer between AOx and AuE. The bioelectrode retained ~ 90% of the original response even after four weeks when stored in potassium phosphate buffer pH 7.5 at 4 °C. In another work, laccase from *Trametes versicolor* was immobilized in a nanocomposite matrix comprising of osmium tetroxide on poly 4-vinylpyridine, MWCNT, nafion and carbon black on glassy carbon electrode for detection of pyrocatechol in environmental samples. The laccase bioelectrode exhibited a linear response against pyrocatechol in the range of 3.98 -16.71 nM with a detection limit of 2.82 nM and storage stability of upto 3 weeks. The $K_s$ and surface concentration of the ionic species of the bioelectrode were $0.67\ s^{-1}$ and $1.32 \times 10^{-8}$ mol $cm^{-2}$, respectively. The response of the constructed biosensor was generated at 0.14 V from the electrocatalyzed reduction of 1,2-benzoquinone formed from the biocatalyzed oxidation of pyrocatechol. The AOx based bioanode was utilized for generating power from methanol substrate in a fuel cell setup using air breathed laccase biocathode. The matrix containing MWCNT, carbon paste and nafion was used as electroactive support for immobilization of the enzymes on toray carbon paper as supporting electrode in the fabrication of the bioelectrodes. PEI was used to electrostatically

stabilize the AOx. The enzymatic biofuel cell generated an open circuit potential of 0.61 (±0.02) V with a maximum power density of 46 (±0.002) μW $cm^{-2}$ at an optimum of 1 M methanol, 25 °C and an internal resistance of 0.024 μΩ. The operation and storage half life ($t_{1/2}$) of the EFC were 17.22 h and 52 days, respectively at a fixed load of 1.85 Ω. To achieve efficient oxidation of the fuel methanol, a bioanode was developed by immobilizing FAD based AOx and NAD-dependent formaldehyde dehydrogenase and formate dehydrogenase on the surface of a graphite electrode electropolymerised with methylene green (MG) as electron transfer mediator. A composite matrix containing MWCNT, carbon powder and nafion was used as electroactive support for immobilization of the enzyme. MG was employed as electron transfer mediator on the anodic surface that reduced significantly the oxidation potential of NADH, which is the cofactor of the dehydrogenases used in the enzyme cascade. It showed a power density of 2.5 $mW/cm^2$ and open circuit potential of 0.901 V at room temperature and neutral pH condition. The result demonstrated the potential of the AOx based cascade enzyme assembly as anodic catalysts for efficient generation of power from methanol fuel substrate in a laccase biocathode based biofuel cell assembly.

.

# CONTENTS

# LIST OF SCHEMES

# LIST OF FIGURES

# LIST OF TABLES

# LIST OF ABBREVIATIONS

| | |
|---|---|
| A | Electrode surface area |
| ABTS | [2,2′-azino-bis(3-ethylbenzothiazoline-6-sulfonic acid)] |
| ADH | Alcohol dehydrogenase |
| AOx | Alcohol oxidase |
| AuE | Gold electrode |
| BSA | Bovine serum albumin |
| CB | Carbon black |
| CHIT | Chitosan |
| CNT | Carbon nanotube |
| CNF | Carbon nanofibre |
| CNTF | Carbon nanotube forest |
| CP | Carbon powder |
| CV | Cyclic voltametry |
| DET | Direct electron transfer |
| DPV | Differential pulse voltametry |
| DL | Detection limit |
| DMFCs | Direct methanol fuel cell |
| EDP | Electrodeposition paints |
| EDX | Energy-dispersive X-ray spectroscopy |
| EFC | Enzymatic fuel cell |
| EIS | Electrochemical impedance spectroscopy |
| ET | Electron transfer |

| | |
|---|---|
| FAD | Flavin adenine dinucleotide |
| FDH | Formaldehyde dehydrogenase |
| FIA | Flow injection analysis |
| FtDH | Formate dehydrogenase |
| FESEM | Field emission scanning electron microscope |
| FRA | Frequency response analyser |
| GC | Gas chromatography |
| GCE | Glassy carbon electrode |
| GE | Graphite electrode |
| GDH | Glucose dehydrogenase |
| GDL | Gas diffusion layer |
| GOx | Glucose oxidase |
| HRP | Horseradish peroxidase |
| $H_2O_2$ | Hydrogen peroxide |
| ID | Inner diameter |
| KPBS | Potassium phosphate buffer solution |
| LBL | Layer by layer |
| LDH | Lactate dehydrogenase |
| MB | Methylene blue |
| MBTH | 3-methyl-2-benzothiazolinone hydrazone |
| MCM | Mesoporous silica sieve |
| MDP | Meldola's blue |
| $MgSO_4$ | Magnesium sulphate |
| MEA | Membrane electrode assembly |
| MET | Mediated electron transfer |

| | |
|---|---|
| MG | Methylene green |
| MP | Microperoxidase |
| $M_{ox}$ | Mediator oxidized |
| $M_{red}$ | Mediator rduced |
| MTFE | Mercury thin flilm electrode |
| MWCNT | Multiwalled carbon nanotube |
| NAD | Nicotinamide adenine dinucleotide (oxidized) |
| NADH | Nicotinamide adenine dinucleotide phosphate (reduced) |
| NaF | Sodium fluoride |
| Nf | Nafion |
| NiCNFs | Nickel nanoparticle loaded carbon nanofibers |
| $NaN_3$ | Sodium azide |
| N-OMC | Nitrogen-containing ordered mesoporous carbon |
| OCP | Open circuit potential |
| OD | Outer diameter |
| $OsO_4$P4VP | Osmium tetraoxide polyvinyl pyridine |
| PB | Prussian Blue |
| PDA | Polydopamine |
| PAMAM | Polyamidoamine |
| PANI | Polyaniline |
| PEI | Polyethylenimine |
| PPY | Polypyrrole |
| $PPY_{ox}$ | Overoxidized non-conducting polypyrrole |
| PSSG | (3-mercaptopropyl)-trimethoxysilane sol–gel |
| PVA | Polyvinyl alcohol |

| | |
|---|---|
| PQQ | Pyrroloquinoline quinone |
| R | Gas constant |
| RT | Room temperature |
| SAM | Self assembled monolayers |
| SC | Selectivity coefficient |
| SD | Standard deviation |
| SEM | Scanning electron microscopy |
| SiNW | Silicon nonowire |
| SWCNT | Single walled carbon nanotube |
| T | Temperature |
| TB | Toluidine blue |
| TCP | Toray carbon paper |
| TTF | Tetrathiafulvalene |
| U | Urea |
| UA | Uric acid |
| UV-Vis | UV-Visible |
| $ZnSO_4$ | Zinc sulphate |

# LIST OF SYMBOL

| | |
|---|---|
| $K_m$ | Michaelis-Menten constant |
| $t_{1/2}$ | Half- life |
| ε | Extinction coefficient |
| λ | Wavelength |
| n | Number of electrons |
| *G | Free energy |
| ΔS | Entropy |
| D | Decimal reduction time |
| Eo’ | Apparent standard potential |
| $E_p$ | Peak potential |
| $E_{pa}$ | Anodic peak potential |
| $E_{pc}$ | Cathodic peak potential |
| F | Faraday constant |
| f | Fill factor |
| $I_{sc}$ | Short circuit current |
| $I_c$ | Response in the absence of interferent |
| $I_{c+1}$ | Response in the presence of interferent |
| $I_{pa}$ | Anodic peak current |
| $I_{pc}$ | Cathodic peak current |
| p*I* | Isoelectric point |
| $K_{cat}$ | Turnover number |

| | |
|---|---|
| $K_s$ | Rate constant |
| **[**L] | Linear range |
| [DL] | Detection limit |
| [RT] | Response time |
| $R_{tn}$ | Resistance at maximum power density |
| $R_2$ | Regression coefficient |
| $R_{ct}$ | Charge transfer resistance |
| T | Temperature |
| $Z$ | Impedance |
| $\alpha$ | Charge transfer coefficient |
| $\Delta Ep$ | Peak separation |
| $\nu$ | Potential scan rate |
| $V_{oc}$ | Open circuit voltage |
| $\Gamma$ | Surface concentration of ionic species |

# Chapter 1

## Introduction

# Chapter 1

# Introduction

The research on enzyme based bioelectronics devices has been tremendously growing since the beginning of the last decade with the parallel growth of knowledge on enzyme and advance materials in the field of biotechnology and nanosciences. Among these bioelectronic devices, biosensor and enzymatic fuel cell (EFC) research have attracted wide attention due to their bright application potentials. A biosensor is an analytical tool consisting of biologically active material used in close conjuction with a device that converts a biochemical signal into a qualitative electrical signal. Among the various classes of biosensors the amperometric transducer-based biosensors are widely acclaimed not only for their inherent potential to exhibit the improved functional properties such as fast, label free and sensitive detection of analytes but also for bearing the scope of scaling down their size with tailored low production cost, easy fabrication, and simple operation with low or no sample loss. The EFC on the other hand is a variant of fuel cell and has been recognized as a promising portable and sustainable power source for powering micro scale electronic devices in the field of telecommunications, space, biomedical science and environmental research (Barton et al., 2004). Unlike chemical and microbial fuel cells where respective chemical and microbial catalysts are employed, the EFC utilizes redox enzymes as primary catalysts on the electrode surface to execute the redox reactions for generating power from the supplied fuel substrates. These biofuel cells take readily available substrates from renewable sources and convert them into benign by-products with the generation of electricity at room temperature without using any toxic materials. As a result, they are an excellent alternative to the conventional fuel cells and their application has been projected as a power source for small

scale electronic devices in the field of healthcare, space, environmental studies and consumer electronics.

The enzyme based bioelectrode fabrication is a critical and common issue for the performance of the both amperometric biosensors and enzymatic biofuel cell. One of the major challenges for developing these enzyme-based products to a functionally sustained device is to prolong operational stability owing to the delicate nature of the proteinous enzymes being used in these systems. While, the other issues of enzyme based amperometric biosensors and biofuel cells are the comparatively weak selectivity for the target analyte and the low columbic efficiency of the device, respectively.

In these bioelectronic devices the type redox enzymes chosen is based on the end use of the devices. For EFC, the selection of redox enzymes is based on the choice of substrate being used to generate the power. Emphasis is usually given on cheap and renewable substrates which do not inhibit the enzymatic function and cause interference in the electrochemical reaction. From this perspective, alcohol substrates, primarily methanol and ethanol have received increasing attention for developing chemical and biological fuel cells. The other advantages of the alcohols as fuel substrates are their aqueous solubility and wide availability as these compounds can be readily produced by fermentative or chemical means from cheap renewable substrates. On the other hand, there is also importance of detection of alcohols in different fields. The quantitative detection of alcohols with high sensitivity, selectivity and accuracy are required in clinical and forensic analysis, food, beverage, pulp industries etc. Many analytical methods based on chemical, chromatographic, and spectroscopic principles have been developed for the determination of ethanol. Although, a few of these methods are reliable, they are complex, time consuming and require prior separation processes, expensive instrumentation and trained operators. Such disadvantages may be overcome by using amperometric enzyme based biosensors. However, the biosensors

reported so far for quantitative detection of alcohol are yet to develop properly for commercial applications.

Alcohol dehydrogenase (ADH) has been widely studied to develop alcohol biosensors and alcohol fuel based biofuel cells. However the requirement of supplementing cofactor $NAD^+$ to the ADH bioelectrode for achieving the desired function of these constructs stand as technical hurdle to develop these to a commercially viable product. The other commonly available alcohol oxidizing enzymes namely, alcohol oxidase (AOx) does not require supplementing cofactor during the operation since its co-factor flavin adenine dinucleotide (FAD) is avidly bound to the protein matrix. Considering the above facts, we focus our attention on the studies on the redox enzyme, AOx for both the aforesaid bioelectronic devices. AOx (Alcohol: $O_2$ Oxidoreductase; EC 1.1.3.13) is an oligomeric enzyme consisting of eight identical sub-units arranged in a quasi-cubic arrangement, each containing an avidly bound cofactor, FAD. AOx catalyzes the irreversible conversion of alcohols to the corresponding aldehydes using molecular oxygen as electron acceptor with concomitant formation of hydrogen peroxide as co-product in the reaction. The enzyme has been detected in several genera of yeasts, such as *Candida*, *Pichia*, and *Hansenula*, that utilize methanol as a sole carbon and energy source.

Application of AOx as anodic catalysts for oxidation of substrate alcohol was not known before we initiated this work. Whereas, the enzyme has been reported for developing amperometric alcohol biosensors where, in most cases the response was recorded by using the hydrogen peroxide as the redox indicator formed in the enzymatic reaction. However, the amperometric determination of hydrogen peroxide requires high anodic potential (~ 0.65 V) that induces many electrochemically active species present in serum samples for oxidation leading to false positive signals. Therefore, we would like to focus our research for developing AOx based bioelectrode following 3$^{rd}$ generation principle of direct electron

transfer (Willner et al., 2002) where the electron exchange between the enzyme and the electrode is facilitated at the low native potential of the redox centre of the enzyme. However, the major obstacle for developing AOx based functional 3$^{rd}$ generation bioelectrode for biosensor and biofuel cell applications is the thick protein shell of this multimeric AOx that hampers the electron hopping from the redox centre of the enzyme to the electrodes. We propose nano-fabrication of bioelectrode with highly conductive multiwalled carbon nanotube (MWCNT) to establish the direct electron transfer for developing efficient bioelectrodes for both amperometric alcohol biosensor and alcohol substrate based biofuel cell.

A common problem of EFCs is their low power density caused by the incomplete oxidation of the fuel substrate in the anodic chamber. To address these problem multienzyme cascade consisting of alcohol dehydrogenase, aldehydes dehydrogenase and formate dehydrogenase has been used to completely oxidize methanol to carbon dioxide. The cascade however needs high amount of cofactor NADH to supplement that may levid high operational cost of the fuel cells. To reduce the requirement of NADH and to examine the function of this FAD bound AOx under these enzyme combination, we propose to replace ADH with AOx in the aforementioned enzyme cascade for developing methanol fuel based bioanode for biofuel cell application.

For analyzing the performance of the AOx based bioelectrode in the biofuel cell setup we have selected the commonly used oxygenase enzyme, laccase as $O_2$ reducing catalysts in the cathode due to its certain advantageous over the chemical platinum catalyst as the latter is expensive and requires high over potential for the reduction (Schaetzle et al., 2009). The potential of laccase as biofuel cell catalyst can also be justified for its high thermal tolerance and substrate turnover rate (Kittl et al., 2012). Laccase (benzenediol: oxygen oxidorecuctases, EC 1.10.3.2) is the simplest multi-copper oxidase consisting of four copper atoms and no

other cofactors (Solomon et al 1996). Naturally laccase catalyses the oxidation of phenolic compounds in the presence of molecular oxygen and hence, the present investigation has been extended to study the potential of this robust enzyme as bio recognition element for detection of phenolic compound, namely pyrocatechol (1,2-dihydroxybenzene) in addition to the primary focus of its use as cathodic catalyst in the biofuel cell.

Considering the aforesaid challenges and work plans following objectives have been formulate for the studies embodied in this thesis: (1) Fabrication and characterization of alcohol oxidase based bioelectrode for alcohol biosensing application (2) Fabrication and characterization of laccase based bioelectrode for biosensor application. (3) Development and characterization of AOx and laccase based bioelectrodes for biofuel cell application. (4) Alcohol oxidase linked enzyme cascade as anodic biofuel cell catalyst.

To accomplish these objectives the content of this thesis entitle “Development of nanocomposite based bioelectrodes using alcohol oxidase and laccase as biocatalysts for bioelectronic applications” has been divided into the following chapters.

**Chapter 1: Introduction**

This chapter provides a brief introduction defining the origin of the work that comprises the motivation for pursuing the work, challenges involved and the objectives undertaken to address the challenges.

**Chapter 2: Review of Literature**

This chapter summarizes the progress of the work on the subject as a whole, focusing the gap and important findings on the area.

**Chapter 3: Fabrication and characterization of alcohol oxidase based bioelectrode for alcohol biosensing application**

This chapter describes the fabrication of the AOx bioelectrode on gold electrode using multiwalled carbon bound nanocomposites matrix for developing amperometric alcohol biosensor. The morphological and electrochemical characterization of the fabricated bioelectrode are discussed. The response of the biosensor towards ethanol has been examined and deduced various response parameters. The application of the biosensor for real sample analysis is also demonstrated.

**Chapter 4: Fabrication and characterization of laccase based bioelectrode for biosensor application.**

This chapter describes fabrication of a highly sensitive and stable laccase based amperometric biosensor for detection of pyrocatechol in environmental samples. The detection principle has been elucidated and the response against different common interfering agents has been evaluated.

**Chapter 5: Development and characterization of alcohol oxidase and laccase based bioelectrodes for biofuel cell application.**

This chapter describes the fabrication and characterization of AOx based third generation bioanode and air breathed laccase biocathode using microporous electroactive matrix for immobilization of the enzymes on toray carbon paper. A detailed account on the performance of the EFC fabricated by assembling these two bioelectrodes in fuel cell set up has been described.

**Chapter 6: Alcohol oxidase linked enzyme cascade as anodic biofuel cell catalyst**

This chapter includes the finding on the investigations for developing a bioanode by immobilizing AOx, FDH, FtDH on a graphite electrode containing carbon powder (CP) and multiwalled carbon nanotube (MWCNT) modified electroactive matrix to oxidize methanol to $CO_2$ in the presence of methylene green acting as the NADH electrocatalyst. A detailed account on the performance of the EFC has been incorporated.

Following Chapter 6, overall conclusions of the research work highlighting the significant findings and scope for future work is included, which is followed by a bibliography section.

# Chapter 2

## Review of Literature

# Chapter 2

# Review of Literature

### 2.1 An overview on alcohol oxidase

Alcohol oxidases (Alcohol: $O_2$ Oxidoreductase; EC 1.1.3.x) are flavoenzymes that catalyze the oxidation of alcohols to the corresponding carbonyl compounds with a concomitant release of hydrogen peroxide.

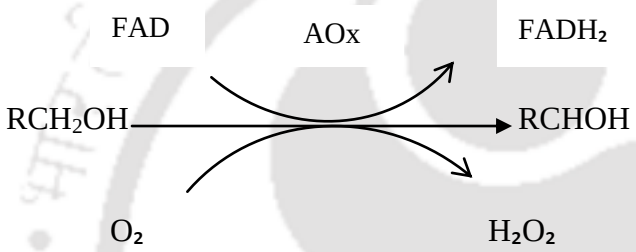


**Scheme 1.1** The reaction scheme on the AOx catalyzed conversion of alcohol to aldehydes.

Based on substrate specificity, alcohol oxidase (AOx) enzymes may be categorized broadly into, (a) short chain alcohol oxidase, (b) long chain alcohol oxidase,(c) aromatic alcohol oxidase, and (d) secondary alcohol oxidase (Kumar and Goswami, 2006). The enzymes belong to short chain alcohol oxidase produced primarily by the methylotropic yeast and are widely known as, methanol oxidase, or ethanol oxidase (EC 1.1.3.13). The AOx produced by the methylotropic yeast *Pichia pastoris* is a homooctameric flavoprotein consisting of eight identical subunits, each containing flavin adenine dinucleotide (FAD) as a prosthetic group. The molecular weight of the enzyme is ~675 kDa (Goswami et al., 2013). AOx enzyme from *Pichia pastoris* has a optimum pH of 7.5 (Couderc and Baratti, 1980). The optimum temperature of the enzyme is 28 to 30 °C and isoelectric point (p*I*) is in the range of 4.0 to 5.7 (Huang et al., 2011). This AOx protein, belong to the group of glucose-methanol-

choline (GMC) family, has an FAD binding domain, a flavin attachment loop, and a substrate binding domain. In addition to these domains, there are two minor domains, namely an FAD-covering loop and an extended FAD-binding domain. The FAD-binding domain is the most conserved region and consists of an ADP-binding motif (βαβ) and a characteristic nucleotide-binding site GXGXXG (amino acids 13–18 of AOx) (Ozimek et al., 2005).

The other functionally complementary well known enzyme that catalyzes the oxidation of alcohol to the corresponding carbonyl compound is alcohol dehydrogenase (ADH) (Alcohol: $NAD^+$ oxidoreductases; EC 1.1.1.1). ADH requires nicotinamide ($NAD^+$ or $NADP^+$) co-factor as terminal electron acceptor in the reaction. The FAD in AOx is avidly associated with the redox center of the enzyme and is involved in transferring the hydride ion originated from alcohol substrate to molecular oxygen leading to the formation of $H_2O_2$. In case of ADH, the cofactor $NAD^+$ needs to be supplied externally in the reaction medium for the catalysis (Azevedo et al., 2005).

## 2.2 Methods for detection of alcohol

### *2.2.1 Conventional analytical methods for detection of alcohol*

Many analytical methods have been developed for the determination of ethanol and other aliphatic alcohols. These include the use of chemical methods such as, gas diffusion flow injection analysis (FIA) system (Kunnecke and Schmid, 1990), colorimetric methods (Mataix and Castro, 2000), chromatographic (Apers et al., 2003) and spectroscopic methods (Mendes et al., 2003). Mataix and Castro (2000) reported a method for the determination of ethanol in wines based on the coupling of pervaporation-chemical derivatisation-photometric detection for ethanol. After separation by pervaporation the ethanol is collected in a $K_2Cr_2O_7$ acceptor stream and the $Cr^{3+}$ formed is driven to the spectrophotometer and monitored at 600

nm. Mendes et al., (2003) reported a fourier transform-near infrared (FT-NIR) and FT-Raman spectrometries used to design partial least squares (PLS) calibration models for the determination of the ethanol content in ethanol biofuel and alcoholic beverages. Kunnecke and Schmid, (1990) combined immobilized AOx with a gas-diffusion membrane in a flow-injection system to greatly enhanced the specificity of ethanol determination. This gas-diffusion flow-injection system with amperometric detection of hydrogen peroxide had a linear range of analysis from 0.0006 up to 60 % (v/v) ethanol. The frequency of analysis was 120–180 samples $h^{-1}$ and the operational half-life of the immobilized enzyme was 8000 injections within 44 h. Apers et al., (2003) determined the ethanol content during the quality control of liquid herbal drug preparations, where capillary headspace GC/MS method of analyses were developed and fully validated. The first step in the determination of the ethanol content was the dilution of the test solution with distilled water to bring the concentration of ethanol within the range 0.0634 to 0.1901 % (v/v).

Some of the aforementioned methods though are precise and reliable, they are complex, time consuming and require previous separation processes, expensive instrumentation and trained operators. Such disadvantages can be overcome by using biosensor devices incorporating enzymes as biorecognition element (Yildiz and Toppare, 2006).

*2.2.2 Biosensors for detection of alcohol*

Biosensor is an analytical device which employs a biological molecule such as enzyme, antibody, DNA as biorecognition element to specifically detect analyte of interest (Thevenot et al., 1999) (Scheme 1.2). It can rapidly and quantitatively detect small volume of analyte in a complex reaction medium. However, biosensors reported so far for quantitative detection of alcohol are yet to develop properly for commercial applications. Alcohol

biosensors described in the literature are largely based on the alcohol oxidizing enzyme, ADH (Zhang and Gorski, 2011). The enzyme catalyzes the conversion of ethanol to acetaldehyde as described above. The reduced cofactor, NADH generated in the enzymatic reaction can be used to measure alcohol electrochemically (Azevedo et al., 2005). A suitable potential is applied for the electrooxidation of NADH for its detection. However, large overvoltages required for electrooxidation of NADH, accumulation of the product dimer on the electrode surface (Bartlett et al., 2002; Moiroux and Elving, 1980) and the need of supplementing the cofactor ($NAD^+$) to the reaction medium are some of the major constrains for utilizing ADH as biorecognition element for developing alcohol biosensor (Vijayakumar et al., 1996).

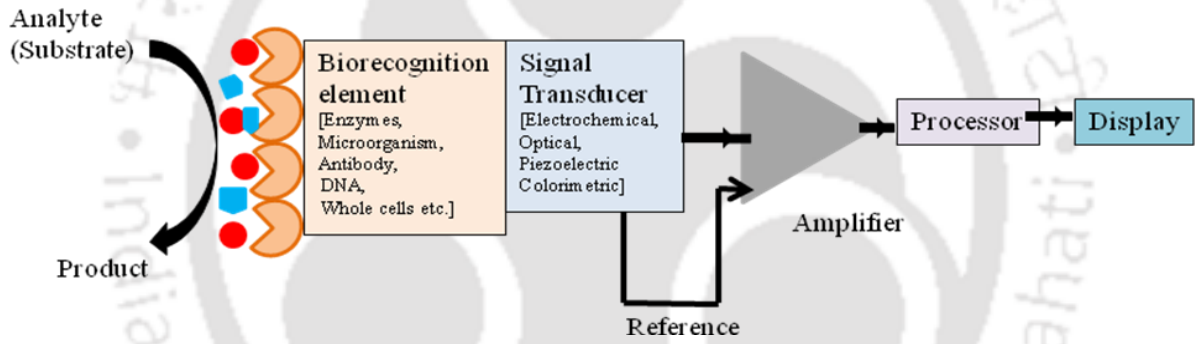


**Scheme 1.2** Schematic representation of a general configuration of biosensors.

AOx as bio-recognition element for sensing alcohol has stimulated interest since the last decade (Azevedo et al., 2005). Some potential advantages of AOx based bio-recognition system are identified among which the irreversible catalytic oxidation of alcohols and the avidly bound flavin-based co-factor to the redox center of the enzyme are pertinent to the biosensor applications. The detection principle involved the measuring of $O_2$ or $H_2O_2$ concentration using optical or electrochemical detections. Various optical biosensors for alcohol have been reported in the past using $O_2$ sensitive compounds, mostly different

ruthenium organic complex (Mitsubayashi et al., 2003). Ruthenium is one of the most common matrices for optical oxygen sensors as it has a high permeability to oxygen, inertness to biological samples, optical transparency, and excellent chemical and mechanical stability (Quaranta et al., 2012). In the optical biosensor, a fibre-optic chemiluminescence method for the determination of ethanol in beverages was proposed. In this method, the $H_2O_2$ formed in the reaction was determined by measuring the luminescence formed by the oxidation of luminol by $H_2O_2$ using $K_3Fe(CN)_6$ as a catalyst (Xie et al., 1992). Hack et al. (2007) reported a dipstick to detect ethanol in saliva. The sensor could monitor cross-reaction and showed a positive color change with very low concentrations of methanol but not ethylene glycol. The dipstick was designed to turn various shades of blue-green from the original white color in a predictable manner. The color change was completed after two minutes of saturation. In the first generation electrochemical (amperometric) detection of alcohol, the oxygen content in the reaction mixture was commonly monitored by using a Clark-type of $O_2$ electrode (Clark et al., 1953). Most oxygen probe bound ethanol sensors consist of an electrode covered by a membrane onto which AOx was immobilised (Akyilmaz and Dinckaya, 2000; Akyilmaz and Dinckaya, 2005). The signal output of the electrode is the difference between the base oxygen level (100 % saturation) and the level attained as a result of oxygen depletion by the enzymatic reaction. The oxygen-based detection, however, has practical inconveniences and limitations such as, poor response, low accuracy and reproducibility, and high background signal that may raise the minimum detection level of the substrate alcohol (Bott 1998).

Many first-generation amperometric AOx based biosensors for alcohol using $H_2O_2$ as electroactive species have also been reported in the last decade (Carelli et al., 2006; Alpeeva et al., 2005; Shkotova et al., 2006; Smutok et al., 2006). Alpeeva et al., (2005) developed a bi-layer bi-enzyme biosensor architecture using different peroxidases and alcohol oxidase

with a sensitivity of 60–98 nA $mM^{-1}$. Shkotova et al., (2006) reported an amperometric biosensor for ethanol detection based on AOx immobilised within electrochemically deposited resydrol polymeric film. The minimal detection limit was $3.5\times10^{-2}$ % (v/v) of total ethanol present in the sample. The biosensor developed had shown potential for ethanol detection in real alcoholic beverages. Carelli et al., (2006) developed an interference-free first generation alcohol biosensor based on a gold electrode modified by an over oxidised non-conducting polypyrrole film and found detection limit of 2.3 µM. Smutok et al., (2006) reported a reagentless bienzyme amperometric biosensor based on AOx/peroxidase and an osmium-complex modified electrodeposition paint with sensitivity of 0.48 $AmM^{-1}$ and 0.2 $AmM^{-1}$ for methanol and ethanol respectively. Vijayakumar et al., (1996), reported an AOx based biosensor using carbon paste/HRP-osmium as a matrix components, with a linear alcohol detection range of 250-2000 µM. Patel et al., (2001) reported Pt/AOx-poly(carbamyl) sulfonate hydrogel bioelectrode for alcohol sensing, showing linear detection range from 10 to 3000 µM. Gulce et al., (2002) characterized a Pt/polyvinyl ferrocenium matrix-$AO_x$ (Batch) based bioelectrode for alcohol detection upto 3000 µM. de Prada et al., (2003) reported a carbon paste matrix–(graphite-teflon)/$AO_x$-HRP-feroccene bioelectrode for alcohol detection showing linear range for alcohol detection from 10 to 750 µM. Gouveia-Caridade et al., (2008) reported a carbon film MWCNT/AOx bioelectrode for alcohol sensing and showed linear range upto 1400 µM. However, the high overpotential of ~0.6 V for the oxidation of $H_2O_2$ in the aforesaid first generation alcohol biosensor causes electrochemical interference in the detection by many electroactive species present in samples leading to false positive signals (Iannello and Iacynych, 1981). To reduce the interference problem the use of an electron transfer mediator either in solution phase or co-immobilized with enzyme on electrode, to shuttle electrons between the redox centers and the electrode with comparatively low potential (~ -0.1Vto 3.0 V) has been proposed, a principle widely known as second

generation biosensors (Azevedo et al., 2005) (Scheme 1.3). In this line, a ferrocene mediator based alcohol biosensor with low working potential was reported that improved the electrochemical selectivity and the detection limits of the biosensor (de Prada et al., 2003). Smutok et al., (2006) reported a bienzyme amperometric biosensor based on AOx/peroxidase and within an osmium-complex electrodeposition paints (EDP). The used redox EDP assures fast electron transfer between the integrated peroxidase and the electrode surface. The linearity was upto 1 mM for methanol, upto 2 mM for ethanol, upto 4 mM for propanol, and upto 8 mM for n butanol. The susceptibity of the mediator to dissolute in the sample solution however, poses hurdle for sensitive detection of the target analytes. Therefore, the focus of alcohol bioelectrode research for biosensor and biofuel cell has been laid on the direct electron transfer principle, widely known as third generation biosensor where the substrate electron is directly transferred from redox site of the enzyme to the electrode (Willner et al., 2002). However, deep embedment of FAD in the protein core prevents direct electrical communication between FAD and electrode (Willner and Willner, 2001). Significantly low flavin midpoint redox potentials (~ −400 mV to +60 mV) in AOx enzymes (Munteanu et al., 2008) are likely to contribute to the criteria suitable for developing third generation alcohol biosensors. Notably, third-generation biosensors offer highly selective and sensitive detection of target analytes. The biosensors operates in a potential window closer to the redox potential of the enzyme and are therefore less prone to interfering reactions (Zhang and Li, 2004).

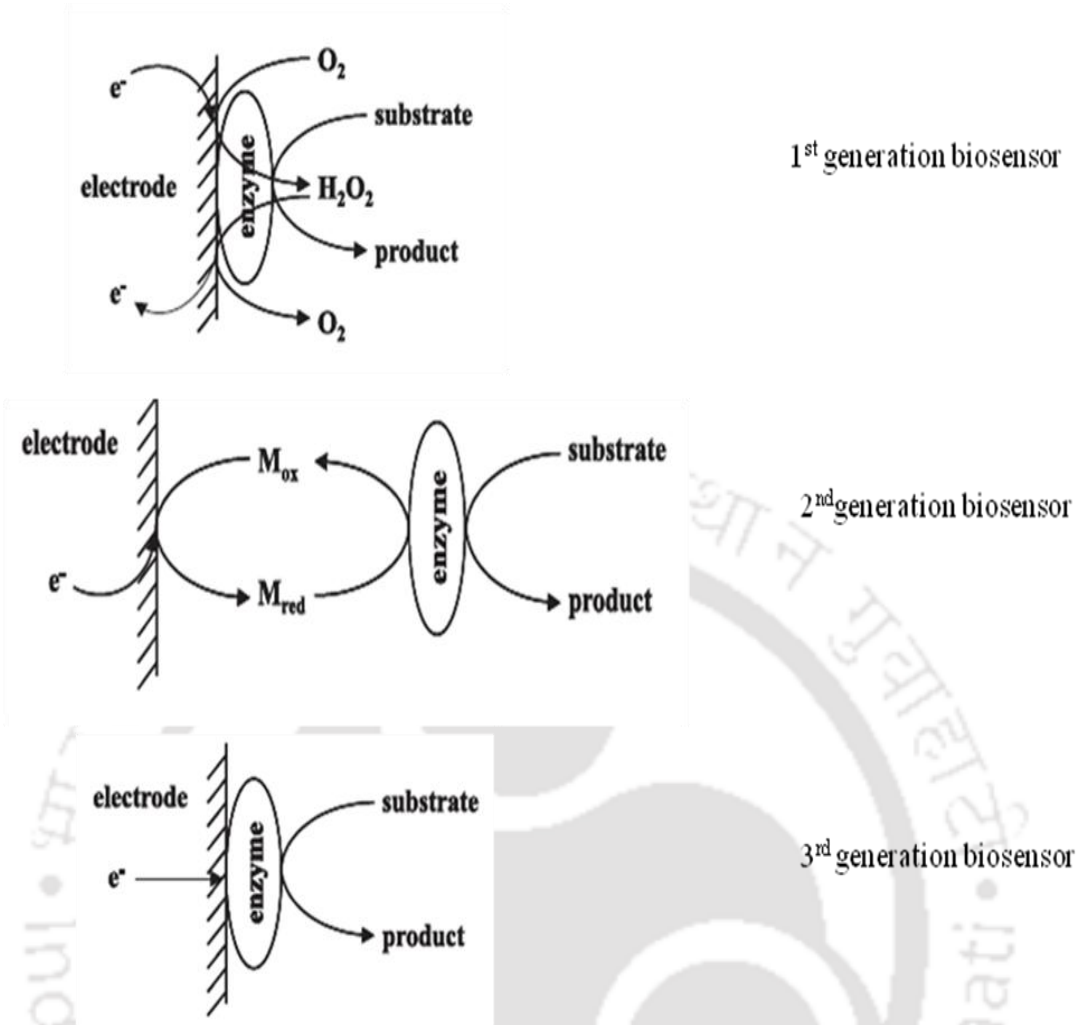


**Scheme 1.3** Schematic representation of three generations of amperometric biosensors ($M_{ox}$, *Mediator oxidized,* $M_{red}$*, Mediator reduced*) (Freire et al., 2003).

One of the major focuses of the AOx-based bioelectrode is to prolong the activity of this complex enzyme on the sensor surface. Vijaykumar et al., (1996) found that 10 % of sensitivity lost after 9 h, in a coupled HRP/AOx based sensor. Patel et al., (2001) found that 32 % of sensitivity lost after 12 measurements carried out in 12 h and 40 % sensitivity lost after 18 days when AOx is immobilized in poly(carbamyl) sulfonate hydrogel. Carelli et al., (2006) reported an AOx based biosensor immobilized in Au/$PPY_{ox}$/glutaraldehyde/BSA. They found that 5 % of sensitivity lost after 6 h of monitoring. The stability of the enzymes

may be enhanced by using suitable biocompatible matrices and immobilization techniques. It is worth mentioning that nanomaterials such as, gold nanoparticles, carbon nanotubes, etc. have recently attracted attention for developing efficient and stable bioelectrode for biosensor applications. Gouveia-Caridade et al., (2008) developed an alcohol biosensor in which AOx was immobilized with BSA on solid MWCNT–carbon film electrode. They noted a significant increase in sensitivity but the biosensor losses 70 % of the initial sensitivity value after three weeks.

**2.3 An overview on enzymatic fuel cell (EFC)**

The production of energy from biologically renewable resources has been a recent focus of many research groups due to obvious reason of global drive for green technology. Enzymatic fuel cell (EFC) represents an approach for such clean energy production because it involve the use of biologically modified electrode surfaces that can harness the electricity by the action of the renewable redox enzymes (Yu and Scott, 2010). EFCs can operate under mild pH and temperature conditions (pH 5–8, 25–37°C), which is in stark contrast to the highly acidic/basic and high-temperature operating conditions of traditional fuel cell (Meredith and Minteer et al., 2012). EFCs employ enzymes instead of conventional noble metals as catalysts. The working principle of EFC is similar with the conventional fuel cells, namely fuel is oxidized at the anode side, and the electrons that are released by the oxidation reaction are driven through an outer electrical circuit, thus generating electric current (Ivanov et al., 2010). Finally, the electrons reach the cathode, where they combine with an oxidant (typically oxygen) and protons to a product (typically water). The development of such biodevices requires significant improvements in terms of efficiency and stability.

First EFCs was reported in 1964 by Kimbe, Yahiro and co-workers (Yahiro 1964). Since then no remarkable progress was visible till 1990s. Willner and Katz reported an EFC

using pyrroloquinoline quinone (PQQ) monolayer-functionalized-Au-electrode as the anode and a microperoxidase-11 (MP-11)-modified Au-electrode as the cathode (Willner, et al., 1998). They used $H_2O_2$ as the cathodic oxidizer and 1,4-dihydronicotinamide adenine dinucleotide as anodic fuel substrate. The biofuel cell generated an OCP of *ca.* 320 mV and a short-circuit current density of *ca.* 30 μA $cm^{-2}$. The maximum electrical power extracted from the cell was 8 μW at an external load of 3 kΩ. Katz and his group further developed a novel glucose/$O_2$ biofuel cell without compartmentalisation between anode and cathode. The anode consisted of a surface reconstituted glucose oxidase monolayer, whereas the cathode was presented by the reconstituted cytochrome c/cytochrome oxidase couple. The system paves the way to develop implantable biofuel cells for biomedical application (Katz et al., 1999).

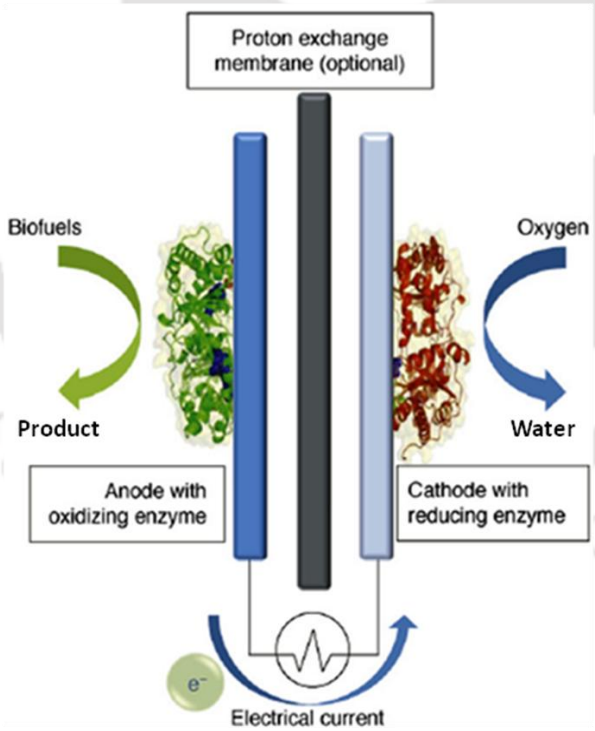


**Scheme 1.4** Schematic illustration of an enzyme-based biofuel cell (Kim et al., 2008).

The interest in developing enzyme based bioelectronics has arisen due to the increasing demand of sustainable implanted medical devices for the healthcare applications such as continuous glucose monitoring, pacemaker etc. (Rigla et al., 2008; Barton et al., 2004; Heller 2004; Willner. 2009). Heller et al., (2004) reported a glucose–$O_2$ cell, consisting of only a pair of 7 mm in diameter and 2 cm long carbon fiber, and a volume of 0.0026 $mm^3$. The cell continuously generates 4.4 µW at 37 °C. When implanted in a grape, it generates 2.4 µW at 25 °C. In six days of operation in the physiological buffer solution, the cell generates about a thousand times more energy than a zinc–air cell would have generated. Portable electronic devices, such as laptops, mobile phones and mp3 players, are new areas to use EFC. Sony has developed a biobattery using sugar as the fuel and enzymes as catalysts to power a Walkman®. Enzymatic bioelectronics show promising applications in various areas (Yu and Scott, 2010). Sakai et al., (2009) when stacked four of the cells together, a power output of 100 mW was achieved, which is enough to run an mp3 player with speakers or a small remote controlled car. For applications on a smaller scale, EFCs operating on high energy density fuels have the potential to power portable electronic devices, though current power densities of most of the reported EFCs are still far from the target figures of ~100 mW. There are different redox enzymes reported so far for developing EFCs and among them glucose oxidase (Yahiro et al., 1964; Ivnitski et al., 2006; Mano, 2008), alcohol dehydrogenase (ADH) (Davis et al., 1983; Palmore et al., 1998; Topcagic and Minteer, 2006), glucose dehydrogenase (Togo et al., 2007; Wang et al., 2012a), fructose dehydrogenase (Murata et al., 2009), aldehyde dehydrogenase (Neto et al., 2013), are used as anodic catalyst whereas, laccase (Barton et al., 2001; Barriere et al., 2006), billirubin oxidase (Topcagic and Minteer, 2006), microperoxidase (Ramanavicius et al., 2008), and horse radish peroxidase (Ramanavicius and Ramanaviciene, 2009 ; Gomez et al., 2010) are reported as cathodic catalysts.

The two major problems in enzyme-based systems are the short lifetime of the enzymes caused by the reduction in their stability in a foreign environment, and the low power densities resulting from a low electron transfer rate from the enzyme active site to the electrode (Kim et al., 2006). The bulk of the research in EFC has been directed to enzyme/electrode integration methods which may alleviate these problems. The short lifetime (a few hours) is an inherent characteristic of enzymes even in their natural environment, but the lifetime may be increased to a few days by adapting suitable immobilization methodology (Minteer et al., 2007).

In the EFC, there are three major losses that contribute towards the overvoltage (or overpotential): activation overpotentials, ohmic losses and mass-transport (concentration) overpotentials (Clauwaert et al., 2008). At low currents, activation (charge transfer) losses dominate; they arise from the energy barrier to charge transfer from the mediator or enzyme to the electrodes. Activation losses can be reduced by improving the electrode catalysis, increasing the electrode surface area, and by optimising the operating conditions (e.g. temperature and pH) (Clauwaert et al., 2008). Ohmic losses are due to the resistance to charge transport through the various components in the cell, including contact resistances. They include both ionic and electronic resistances through the current collectors, electrolytes, membrane and electrodes, as well as the interfaces between these components (Osman et al., 2011). To keep ohmic losses to a minimum, the membrane must possess a low resistance, the gap between the electrodes should be optimal and the components must be well contacted. Concentration losses are caused by resistance to mass transport, leading to large concentration gradients, notably in the vicinity of the electrode surface. These losses tend to dominate at high current densities. They can be lowered by ensuring that the solutions are well-mixed (e.g. by stirring or recirculation) or, in the case of an air-breathing cathode, the ingress of $O_2$ is not severely restricted (Osman, et al., 2011).

One of the most important measures of the performance of an EFC is the coulombic efficiency, which is defined as the ratio of the coulombs transferred from the substrate to the anode, to the theoretical maximum coulombs produced if all of the substrate is oxidized (×100%) (Liu et al., 2005). The major causes of reduced coulombic efficiency have been ascribed as (a) the occurrence of alternative reactions that do not result in current production; (b) build-up of biomass; and (c) crossover of the substrate or mixing of the anodic and cathodic reagents, a particular problem in membrane-less systems (Clauwaert et al., 2008).

*2.3.1 Alcohol substrate based EFC*

Alcohol substrates, primarily methanol and ethanol have received increasing attention for developing chemical and biological fuel cells. The advantages of the alcohols as fuel substrates are their aqueous solubility, low cost, high energy density (Topcagic and Minteer 2006) and wide availability, as these compounds can be readily produced by fermentative or chemical means from cheap renewable substrates (Goswami et al., 2013).

The enzyme commonly used in EFCs for oxidation of the fuel alcohol is $NAD^+$ dependent ADH (Addo et al., 2011) due to its advantages such as, low redox potential (Rincon et al., 2011a) that supports the anode to function at low potential for generating high cell voltage. The challenges commonly encountered in employing ADH for developing operationally stable EFC are the leaching susceptibility of the cofactor $NAD^+$ from the electrode surface (Vijayakumar et al., 1996), and electrode fouling caused by the polymerization of oxidized products on the electrode surface (Cardosi and Liu, 2012) that eventually increase the overvoltage for oxidation of NADH (Bartlett et al., 2002 ; Lee and Tsai, 2009). Hence, redox enzymes with strongly bound cofactor in the reactive center may be an alternative choice for developing operationally stable EFC. In this regard, the enzyme AOx may be projected as potential anodic biocatalyst for EFC applications since the strongly

bound flavin cofactor in the redox center of these enzymes obviates the need of supplementing cofactor during the catalytic reactions (Goswami et al., 2013).

Technical developments in the system design may also led to more efficient fuel cell (Minteer et al., 2007) such as, single chambered or membraneless fuel cell and air-breathed systems using compact membrane electrode assemblies (Topcagic and Minteer, 2006). Further, electrode materials need to be more catalytic while maintaining their performance, particularly in the face of problems caused by fouling of the active surfaces and loss of enzyme activity. It is important to study time-dependent performance over practical periods, particularly with a focus on long-term changes in the enzyme activity (Yu and Scott, 2010).

Using alcohols as fuels, the EFC with ADH reached power densities between 32 and 1000 $\mu W\ cm^{-2}$ (Neto et al., 2013; Kim et al., 2013). ADH is the most recurrent enzyme in the literature for alcohol bio-batteries with ethanol or methanol as fuel substrate. In most of the cases, the NADH-dependent ADH is used with few exceptions where PQQ dependent ADH has also been used (Yakushi and Matsushita, 2010). The advantage of the ADH-PQQ is the presence of an exposed heme that allows direct electron transfer, as demonstrated in a hybrid fuel cell with a platinum cathode (Neto et al., 2013). Neto et al., (2011) reported a ethanol/$O_2$ biofuel cell, where enzyme was immobilized by on anode electrostatic layer-by-layer (LBL) technique. The LBL technique was employed for immobilization of dehydrogenase enzymes (ADH and AlDH) and polyamidoamine (PAMAM) dendrimers onto carbon paper support. A gas diffusion membrane (ELAT) composed of platinum (20 %) in C (E-TEK) hot pressed in a nafion membrane was employed as the cathodic material. The cathodic side was kept in direct contact with air. This system generated a power density of 0.12 $mW\ cm^{-2}$. The performances of various alcohol substrate based pure EFC (both anodic and cathodic catalyst is enzyme) are described in table 1.1.

Table 1.1. Performances of different alcohol substrate based pure EFCs.

| Characteristics of the electrodes | | Electrolytes/ Membrane | $P_{max}$ (μw $cm^{-2}$) | OCP (V) | References |
|---|---|---|---|---|---|
| **Anode** | **Cathode** | | | | |
| MDB/AuNPs/ PSSG-CHIT-ADH | AuNPs/PSSG–CHIT-laccase | Ethanol and NADH in 0.10M phosphate solution (pH 6.0 ) | 1780 | 0.68 | Deng et al., (2010) |
| ADH /$NAD^+$ | Bilirubin oxidase | 1.0 mM ethanol in pH 7.15 phosphate buffer | 1670 | 1.1 | Duma and Minteer, (2007) |
| Quino-hemoprotein-ADH adsorbed on graphite electrode | AOx/microperoxidase -8 adsorbed on graphite electrode | 50 mM sodium acetate, 6 pH, 100 mM KCl, 2 mM ethanol | 1.5 | 0.24 | Ramanavicius et al., (2008) |
| Covalently linked SWCNT-$NAD^+$ deposited on glassy carbon. ADH attached to $NAD^+$ | Thioanaline modified bilirubin oxidase copolymerized with thioanaline capped Pt nanoparticles on Au electrode with thioanaline monolayer | 0.1M PBS, 7 pH, 40 mM ethanol | 200 | 0.62 | Yan et al., (2009) |
| CHIT/MWCNT/$NAD^+$/ADH | MWCNT distributed on GDL fused by hydraulic press and laccase was immobilized by physical adsorption | 475 mM ethanol | 25 | 0.618 | Rincon et al., (2011a) |

Abbreviation: MDB, Meldona's blue; PSSG, (3-mercaptopropyl)-trimethoxysilane sol–gel; Pt, Platinum; GDL, Gas diffusion layer, CHIT, Chitosan.

## 2.4. An overview on laccase

Laccase (EC 1.10.3.2), a multicopper redox enzyme, is widely occurring in fungi and less frequently found in higher plants and bacteria (Mayer et al., 2002). The enzyme has been identified as a potential catalyst for the determination of phenolic compounds (Haghighi et al., 2003). Generally, laccase contains four copper atoms classified into type 1 (T1), type 2 (T2), and type 3 (T3), according to their spectroscopic and magnetic properties. T1, the substrate binding site of the enzyme is involved in oxidation of substrate and transfer of electron to T2/T3 cluster, while T3 is responsible for oxygen uptake and as a whole, this T2/T3 site is responsible for the reduction of $O_2$ to water (Li and Trush 1994; Solomon et al., 1996). The copper ions in the active site of the laccase, provide electron transfer mechanism by switching their oxidation states between Cu(II) and Cu(I). The function of the T1 center is to provide the long-range intramolecular electron transfer from the substrate to the T2/T3 redox copper center. The T2/T3 copper center plays a key role in the reduction of oxygen. The fully reduced trinuclear copper center reacts with dioxygen to generate a peroxide level intermediate and finally, molecular oxygen is reduced to water (Ivnitski and Atanassov, 2007). Laccases have wide substrate specificity and great potential for the determination of phenolic compounds (Timur et al., 2004).

### *2.4.1 Laccase based biosensors*

Laccase does not require $H_2O_2$ as co-substrate and any external co-factor for its catalysis and hence the construction of the biosensor becomes simple (Roy et al., 2005). Laccase based biosensor have been developed for the determination of total phenols (Quan et al., 2004).

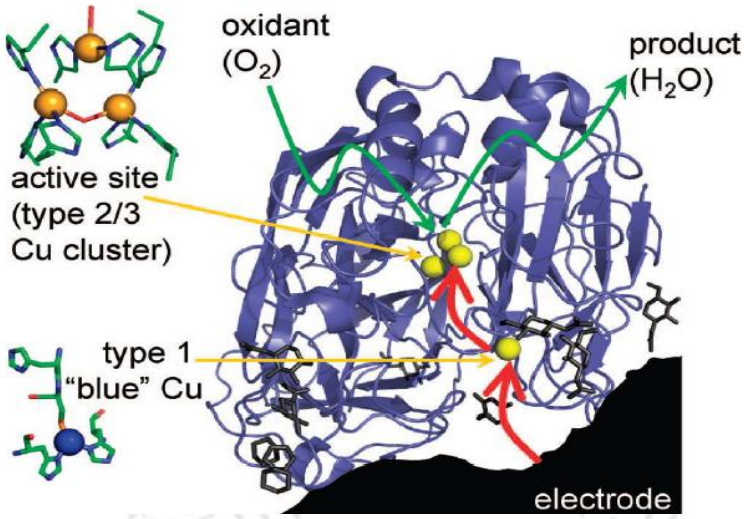


**Scheme 1.5** The structure of laccase showing the protein superstructure in blue and the copper atoms as yellow spheres (Cracknell et al., 2008).

Laccase couples the oxidation of substrate to the four-electron reduction of oxygen. Two general strategies have been employed to attach laccase to electrode surfaces and establish electronic communication. The first utilizes an electron-transfer mediator, typically an osmium complex, to shuttle electrons between the enzyme and the electrode surface. (Mano et al., 2006; Gallaway and Barton, 2008). This method allows thick layers of enzyme to be used, leading to good durability and larger current densities (Blanford et al., 2009). Second strategy based on direct electron transfer between laccase and carbon electrodes which also can be established by utilizing a diazonium coupling reaction to modify the electrode surface with polycyclic aromatic molecules (such as anthracene). These aromatic linkers facilitate binding of laccase to the electrode, apparently in a favorable orientation, and assist in electron transfer to the active site (Lefevre et al., 2002). The performances of various prominent laccase based biosensors are desecribed in table 2.2.

Table 2.2. Performance of laccase based biosensor

| Bioelectrode Characteristics | Substrate | Performance | References |
|---|---|---|---|
| Glutaraldehyde functionalized chitosan-MWCNT/glassy carbon/ Laccase | Catechol | [L]: 0.1-50 µM<br>[DL]: 20 nM | Tan et al., 2009 |
| MB modified MCM-41/ PVA composite film/Au/Laccase | Catechol | [L]: 4.0µM to 87.98 µM<br>[DL]: 0.33 µM<br>[RT]: less than 4 s | Xu et al., 2009 |
| CNT-Chitosan composite film/Laccase | Catechol | [L]: 1.2- 30µM<br>[DL]: 0.66 µM | Liu et al., 2006 |
| Spectrographic graphite electrode/Laccase | Catechol | [L]: 1-10 µM<br>[DL]: 0.23 µM | Haghighi et al., 2003 |
| MBTH/nafion/sol-gel silicate / chitosan Laccase | Catechol | [L]: 0.5-8 mM<br>[DL]: 0.33mM<br>[RT]: 10 min | Abdullah et al., 2007 |
| MTFE/GCE/Laccase | Catechol | $[L]_1$: $0.5X10^{6}$M-<br>$5X\ 10^{-6}$ M<br>$[L]_2$: $2.5X10^{-6}$M<br>$3\times10^{-5}$ M | Kirgoz et al., 2005 |
| GCE/Carbodimide/glutaraldehyde/ Laccase | Chloroguaiacol | [L]:1.0-10.0 µmol $l^{-1}$<br>[DL]: $2.3\times10^{-7}$mol $l^{-1}$ | Freire et al., 2002 |
| GCE/Black Pearl 2000/Laccase | Pyrocatechol | [L]:0.003–5.555 mM<br>[DL]: 0.003 mM | Wang et al., 2012b |

*Cont…….*

| Bioelectrode Characteristics | Substrate | Performance | References |
|---|---|---|---|
| GCE/Chitosan/1-aminopyrene reduced grapheme oxide/Laccase | Hydroquinone | $[L]_1$: 3–2000 µM<br>$[DL]_1$: 2 µM | Zhou et al., 2013 |
| | Catechol | $[L]_2$: 15-700 µM<br>$[DL]_1$: 7 µM | |
| GCE/MWCNTs paste/Laccase | Aminophenol | [L]: $9.90\times10^{-7}$ to $1.15\times10^{-5}$ mol $L^{-1}$<br>[DL]: $1.8\times10^{-7}$ mol $L^{-1}$ | Oliveira et al., 2013 |
| Cu/CNFs/laccase/Nf/GCE | Catechol | [L]: $9.95 \times 10^{-6}$ to $9.76 \times 10^{-3}$ M<br>[DL]: 1.18 µM | Fu et al., 2014 |
| PDA/laccase / NiCNFs | Catechol | [L] :1 µM to 9.1 mM<br>[DL]: 0.69 µM | Li et al., 2014 |
| Laccase/N-OMC/PVA/AuE | Catechol | [L]: 0.39 µM to 8.98 µM<br>[DL]: 0.31 µM | Guo et al., 2014 |

Abbreviation: MCM, Mesoporous silica sieve; PVA, Polyvinyl alcohol; MBTH, 3-methyl-2-benzothiazolinone hydrazone; MTFE, Mercury thin flilm electrode; CNF, Carbon nanofibre; PDA, Polydopamine; N-OMC, Nitrogen-containing ordered mesoporous carbon; DL, Detection limit; L, Linear range.

*2.4.2 Laccase based bioelectrode for EFC applications*

The frequently used cathodic catalysts in EFC are laccase, bilirubin oxidase and peroxidase. The use of oxygenase enzymes such as laccase as $O_2$ reducing catalysts is advantageous over the chemical catalyst platinum (Pt) as the later is expensive and requires high over potential for the reduction (Schaetzle et al., 2009). The potential of laccase as biofuel cell catalyst can also be justified for its high thermal tolerance (Madhavi and Lele, 2009) and substrate turnover rate (Kittl et al., 2012). Among the commonly used cathodic enzymes, laccase from *Trametes versicolor* shows reversible adsorption to carbon (Blanford

et al. 2007; Tarasevich et al., 2001) as well as direct electron transfer with various carbon electrodes (Rubenwolf et al., 2010). Hussein et al., (2011) reported the use of buckypaper, a mechanically stable mat of well dispersed multi-walled carbon nanotubes, as a highly efficient electrode material for mediatorless laccase-catalyzed oxygen reduction cathodes.

Significant efforts have been given on developing a suitable electric connection between electrodes and laccases. There are two main targets for optimizing a laccase cathode: (i) to obtain the highest possible potential for $O_2$ electroreduction and (ii) to produce the most intense current density of the device. The first goal requires an immobilization method that allows the enzyme to transfer the electrons directly (DET) from the electrode to $O_2$ molecules using its biological T1-to- T2/T3 path, thus avoiding a mediated electron transfer (MET) bioelectrocatalysis. When DET is not efficient and a mediator is needed, an undesired decrease in the $O_2$ reduction potential occurs. Maximization of the current output requires dense biocatalyst packing on the electrode surface, oriented in such a way that the DET mechanism is favorable (Pita et al., 2011). Carbon electrodes have shown to be a very suitable electroactive surface for laccase accommodation (Shleev et al., 2005). Pita et al., (2011) reported an efficient laccase cathode where laccase was immobilized on gold surface modified with a mixed monolayer of an aromatic diazonium salt derivative and 6-mercapto-1-hexanol for further use as scaffold for the enzyme's covalent linkage. This strategy offers a variety of advantages such as, high stability of the bioelectrode caused by the laccase-friendly support morphology of the electrode surface. Current density up to 40 $\mu A/cm^2$ were achieved for the electrocatalytic reduction of $O_2$ in the absence of redox mediators. Cardoso et al., (2013) reported a methanol/ $O_2$ biofuel cell using a laccase biocathode where laccase was immobilized with polypyrrole film and PAMAM dendrimers. A gas diffusion membrane (ELAT) consisting of 40 % metal in carbon (Pt 0.66 Ru 0.34, E-TEK commercial mixture)

hot pressed in a nafion® NRE-212 membrane was used as the anode. The maximum power density reported was 25 μW $cm^{-2}$.

### 2.5 Multienzyme cascade based bioanode for EFC application

Most redox enzymes used at the anode catalyze only a single two-electron oxidation per molecule of substrate and leave the remainder of the substrate unreacted, which limits the efficiency and energy density of the biofuel cell (Sokic-Lazic and Minteer, 2009). Many works during the recent years aimed at reaching higher current densities, thus power densities, while increasing the long term stability of the enzymatic bio-electrodes (de Poulpiquet et al., 2014). Attempt has been made to catalyze complete oxidation of substrates through the use of immobilized enzyme cascades. Enzyme cascade-based bioanodes allow deeper substrate oxidation in which multiple pairs of electrons could be extracted from one substrate molecule leading to larger current yield per molecule of the substrate (Hickey et al., 2013). The multi-enzyme cascade showed five times higher NADH production rate than the non-complexed enzyme mixture, due to efficient substrate channeling through the cascade. The amount of NADH produced is proportional to the amount of electrons that can be transferred to the anode. Dehydrogenase enzymes may play an essential role in such cascade pathways, and dependent on the nicotinamide adenine dinucleotide cofactor in its reduced (NADH) and oxidized ($NAD^+$) forms (Rincon et al., 2011b; Sokic-Lazic and Minteer, 2008). The first example of an enzyme cascades employed in a biofuel cell was reported by Palmore et al., (1998) for the oxidation of methanol to carbon dioxide. The reaction mechanism by the multienzyme cascade is as follows:

1. $CH_3OH + NAD \xrightarrow{ADH} HCHO + NADH$

2. $HCHO + NAD + H_2O \xrightarrow{FDH} HCOOH + NADH + 2H^+ + 2e^-$

3. $HCOOH + NAD \xrightarrow{FtDH} CO_2 + NADH + H^+ + 2e^-$

Palmore et al., (1998) also coupled diaphorase with these three enzymes to mediate NADH with benzyl viologen and regenerate NAD. This was the first enzymatic cascade in literature, but the concept holds for oxidation pathways of all biofuels (Sokic-Lazic et al., 2010). However, regeneration of NADH has been a major challenge in practical biotechnology over the past decades. Oxidation of NADH (reductive mediator) at ordinary electrodes like bare glassy carbon or gold requires high overpotentials (Palmore et al., 1998). NADH oxidation on platinum electrodes has poor reaction kinetics and occurs at large overpotentials. Therefore, a polymer-based electrocatalyst was used to regenerate $NAD^+$ and to shuttle electrons from the NADH to the electrode (Sokic-Lazic et al., 2010). The number of multienzyme based EFCs is limited. Among them ADH-FDH-FtDH bioanode based EFC showed power density and OCP 261±7.6 µW/cm² and 1.21 V, respectively (Addo et al., 2010). EFC with ADH-AldDH-FtDH bioanode showed power density and OCP 0.67 $mW/cm^2$ and 0.80 V, respectively (Palmore et al., 1998), while ADH-AldDH-FtDH bioanode reported by Akers et al., (2005) showed power density and OCP 2.04 $mW/cm^2$ and 0.71V, respectively.

**2.6 Electron transport mechanism on enzyme based bioelectrode**

Enzymes used in fuel cells can be categorised into three groups, according to the type of electrical communication (Heller, 1992) or to the nature of their association with the redox cofactors. The first group consists of PQQ-dependent dehydrogenases, e.g. ADH, glucose

dehydrogenase and glycerol dehydrogenase. The second group includes those with a nicotinamide adenine dinucleotide ($NADH/NAD^+$) or nicotinamide adenine dinucleotide phosphate ($NADPH/NADP^+$) as cofactor, e.g. glucose dehydrogenase and ADH. In this case, the redox cofactors areusually loosely bound and may diffuse away. This allows the enzyme to transfer electrons to the electrode by the diffusing center, although the diffusing enzyme site may be lost, especially in continuous flow systems. Covalent linking of such enzymes needs to maintain a flexible link, allowing reversible movement between the protein structure and the electron acceptor. Enzymes in the third category have a tightly bound FAD redox cofactor that is buried deep inside the protein structure, which makes extraction of the electrons difficult. The most commonly used enzyme, glucose oxidase (GOx), belongs to this group. In an aqueous solution, the redox potential of FAD at the enzyme active site is negative, making it ideal for the anode side of a biofuel cell if direct electron transfer (DET) can be achieved. However, the systems employing GOx are typically mediated, although it is possible to achieve DET using nanostructured electrodes (Xiao et al., 2003; Zayats et al., 2005; Cai and Chen, 2004; Patolsky et al., 2004).

The exchange of electrons between electrochemically active redox enzymes and electrode is known to take place through either of the two mechanisms: mediated electron transfer (MET) or DET (Seop et al., 2006; Barton et al., 2004). The MET involves regenerative mediation initiated by some externally supplied electron transfer mediator (ETM). However, there are some drawbacks of using exogenous mediators (e.g. neutral red or methylene blue), such as their toxicity, cost and short life time (Kim et al., 2006). Conversely, in case of DET mechanism the electrons are transferred directly between the active site of the enzyme and the electrode (Barton et al., 2004). Although the trend for developing DET principle based bioelectrodes is quite high in biosensor application, the same

is yet to gain momentum in EFC research (Wu et al., 2009). The major hurdle for developing DET principle based enzyme bioelectrode is the deeply buried redox center in the protein matrix of most of the redox enzymes which hampers the electron hopping between the redox center of the enzyme and the electrode (Yu and Scott, 2010). There is often a large distance between the electrochemically active center of a protein and the electrode surface which has to be crossed by the electrons. If there is no electrochemically active redox mediator in between that can be used by the electrons to overcome the electron transfer (ET) distance by a hopping mechanism, the ET is direct and occurs by a tunnelling process following a super exchange mechanism. This means that the electrons are never vibronically localized at a bridging molecule during ET. When long-range ET occurs by a tunneling mechanism, the ET rate constant decreases exponentially with distance and can be described by the following equation (Marcus and Sutin, 1985).

$$k^{0}_{ET} = \nu \exp[-\beta (d - d_0)] \exp(-\Delta G^*/ RT)$$

Where $\nu$ is the frequency factor, $\beta$ is an electronic tunnelling factor, $d$ is the ET distance, $d_0$ is the nucleus to nucleus ET distance at a donor– acceptor closest approach, and G* is the intrinsic free energy of activation. Even though the ET distance is a crucial parameter governing the ET probability, it also has to be mentioned that for some proteins different ET pathways provided by the peptide matrix exist, and the highest ET rates are not necessarily observed for the ET pathway with the shortest distance (Marcus and Sutin, 1985).

Among the different techniques which have been evolved for establishing DET between the enzyme and electrode, nano-fabrication of electrode surface with highly conductive nanomaterials is emerging as a tool of choice due to its clear effect on establishing DET (Sarma et al., 2009). The nano-fabrication provides high enzyme loading

on the electrode surface due to high surface to volume ratio of the nanomaterials that also increases the extent of electroactive enzyme molecules on the electrode surface due to conducive interaction between the highly conductive nano-particles/tubes with the redox center of the enzymes facilitated by their comparable sizes. In this direction MWCNT has offered a great promise as witnessed from the amperometric enzyme electrodes successfully developed in the field of biosensors research since last decade (Sarma et al., 2009; Gooding, 2005; Vatsyayan et al., 2011).

**2.7 Materials for the fabrication of the bioelectrodes**

A common problem usually encountered in developing various enzyme electrodes is their poor functional stability of the proteins. Protein stability in general, is limited outside their natural environment. Further, during electrochemical studies protein may denatured by the applied potential. Additionally, many proteins may be denatured after their adsorption on bare electrodes (Cernocka et al., 2013). The selection of appropriate combinations of materials, such as, enzyme, electron transport mediator, binding and encapsulating materials, conductive support matrix and solid support, for construction of enzyme-modified electrodes governs the efficiency of the electrodes in terms of electron transfer kinetics, mass transport, stability, and reproducibility (Osman et al., 2011). Recent innovation in conductive electro-active polymers, functionalized polymers, biocompatible composite materials, composites of transition metal-based complexes, organometallic compounds, sol–gel and hydro-gel materials, nanomaterials, other nano-metal composites, and nano-metal oxides has greatly influenced the redox reactions and electron transport kinetics of the enzyme electrodes (Kim et al., 2006). The most crucial step in the fabrication of any enzyme based bioelectrode is the immobilization of the enzyme molecules on the electro-sensing surface. As a consequence, immobilization strategies for biomolecules are of paramount importance in order to preserve

their biological activity. This is done with the help of an immobilizing matrix whose function is to hold the enzyme molecules on the electrode. The properties of the matrix govern the efficiency of the fabricated bioelectrode in terms of sensitivity, selectivity and stability (Sarma et al., 2009). There are various properties of the matrix that are desirable for the successful immobilization of biomolecules on the surface of these electrodes. The support matrix should have good mechanical stability, rigidity and good flow properties for enzyme stability and activity on storage (Park et al., 2010). Also it should be adaptable to different environments like, different pH, temperature, ionic strength and chemical composition of the solvents (Kim et al., 2006). Apart from this, a good support material should be non-degradable and biocompatible without altering the native structure of the enzyme and affecting its biological activity (de Poulpiquet et al., 2014). Different types of matrix materials have been utilized to immobilize enzyme for the construction of AOx based bioelectrode for biosensors developments over the years. Carbon based materials, nanomaterials, electroactive polymers are the most common materials (Kim et al., 2006). Each of the matrix material has its advantages and disadvantages (Ahuja et al., 2007; Nambiar and Yeow, 2011). Major improvements in biological fuel cells over the last ten years have been the result of the development and application of new materials such as nanotubes and graphene, that improve the electron transfer between the biocatalyst and electrode surface, provide improved stability and immobilization of biocatalysts, increase the conductivity and surface area of the electrodes, and facile mass transport on the electrode surface (Minteer et al., 2012).

### *2.7.1 Nanomaterials*

These are attractive electrode support materials because of their unique properties. For example, large surface area, high electrical conductivity, high chemical and thermal

stability are offered by the metallic nanomaterials (Wei et al., 2011). Carbon nanotube (CNT)s with high electrical conductivity have been studied as electrode materials and showed to help in mediating electron transfer reactions (Vatsyayan et al., 2010, Agui et al., 2008). CNTs can also be introduced as efficient molecular-scale"conductive wires" between the electrode surface and redox enzymes (Zhang et al., 2008). In general, enzyme immobilization in nanostructured electrodes extends their lifetime and improves their activity, due to relieved mass transfer limitation of substrates in the nanostructures as compared to macro-scale diffusion, especially when the size of the nanopores is slightly larger than the size of the enzyme (Dominguez-Benetton et al., 2013). Due to high surface area, favorable electronic properties and electrocatalytic effect of nanomaterials, nanomaterials modified electrodes provide a larger electroactive surface area for higher biomolecule loading (Asefa et al., 2009; Kim et al. 2008). Increased flow of electrons between the electrode and the biomolecules is likely to help in decreasing the overpotential, amplifying biorecognition signal and increasing, overall sensitivity of the biosensor. Also, they help in retaining the bioactivity of biomolecules on the electrode surface (Pingarron, 2008).

Nano-metal, oxides (e.g. $Co_3O_4$, $TiO_2$ etc.), silicon nanoparticle, iron (III) hexacyanoferrate, and nanoporous PANIs are used currently for effective electron transfer from enzyme redox centres to the electrode (Prakasam et al., 2007; Chen et al., 2006a,b; Kuswandi et al., 2014). Chen et al., (2006a) reported the use of silicon nanowires (SiNWs) as the supporting matrices for high sensitivity glucose detection. In another report (Chen et al., 2006b), an amperometric $H_2O_2$ biosensor based on the immobilization of HRP on the LBL assembly films of gold colloidal nanoparticles and toluidine blue (TB) was investigated. {TB/Au}n films were used as model film to fabricate a mediated $H_2O_2$ biosensor based on HRP, which responded rapidly to $H_2O_2$ in the linear range from $1.5\times10^{-7}$ to $8.6\times10^{-3}$ mol $L^{-1}$

with a detection limit of $7.0\times10^{-8}$ mol $L^{-1}$. $TiO_2$ nanotube arrays ($TiO_2$ NTAs) have several physical, optical and electrical attributes that draws attention for its use in enzyme electrodes fabrication. The presence of open nanopores with high surface area in $TiO_2$ NTAs, and the micropores for the reactants facilitate the transport of reagents to the active site during catalytic reaction. Besides, chemical stability, non-toxicity and excellent charge transfer properties of $TiO_2$ NTAs make them a potential material for immobilization of bio molecules in enzyme electrode fabrication (Prakasam et al., 2007; Xie et al., 2007; Wu et al., 2008). Saxena et al., (2011a) reported amperometric detection of cholesterol in real samples by covalent immobilization of cholesterol oxidase on self-assembled gold nanoparticles. The fabrication procedure is based on the deposition of gold nanoparticles on the 1,6-hexanedithiol modified gold electrode, functionalization of the surface of deposited gold nanoparticles with carboxyl groups using 11-mercaptoundecanoic acid and then covalent immobilization of cholesterol oxidase on the surface of gold nanoparticle film using the N-ethyl-N′-(3-dimethylaminopropyl carbodimide) and N-hydroxysuccinimide ligand chemistry. The bioelectrode exhibited a linear response to cholesterol in the range of 0.04–0.22 mM with a detection limit of 34.6 μM.

Lu et al., (2007) synthesized, for the first time, layered $Co_3O_4$ nanoflakes with spongy nanostructure. The porous, layered spongy nanostructure of $Co_3O_4$ is advantageous for the immobilization of proteins and enzymes, which were integrated with the ion conducting polymer nafion to form a biocompatible nafion–$Co_3O_4$ organic–inorganic hybrid material. Hemoglobin (Hb) was chosen as a model protein to investigate the nanocomposite. It was reported that Hb entrapped in the composite film could retain its essential secondary structure. These $Co_3O_4$-based hybrid materials are suggested to find wide potential applications in biosensors, biocatalysis, bioelectronics and biomedical devices.

Template synthesis over the electrode is opening a new horizon in biosensor and biofuel cell research. Xian et al., (2007) proposed a strategy to form nanoelectrode arrays by electrochemical deposition of the Prussian Blue (PB) through highly ordered porous anodic alumina membrane. As the highly ordered PB arrays could behave as an ensemble of closely spaced but isolated nanoelectrodes, the nanostructured PB arrays were successfully applied to improve the analytical performances for glucose detection by electrocatalytic reduction of enzymatically liberated $H_2O_2$. The resulting PB-based nanoelectrode arrays showed a wide linear calibration range over three orders of magnitude of glucose concentrations ($5.0 \times 10^{-6}$ to $8.0 \times 10^{-3}$ M) and a low detection limit of 1 μM.

Nanoforest can be obtained when nanomaterials such as CNT are grown on a non-adhesive substrate so that they can be removed from it without losing their ordered structure (Kihara et al., 2011). Ordered structures can also be obtained through the Langmuir–Blodgett method (Sun et al., 2007) or through the LBL self-assembly technique (Szot et al., 2010). Miyake et al., (2011) demonstrate that a CNTs forest dynamically arranges around enzyme molecules in solution due to liquid-induced shrinkage. They described a free-standing film of carbon nanotube forest (CNTF) that can form a hybrid ensemble with enzymes through liquid-induced shrinkage. This provides *in situ* regulation of its inter-CNT pitch to the size of enzymes and eventually serves as a highly active electrode for fuel cell application.

*2.7.2 Mesoporous materials*

Mesoporous materials have attracted much attention for many applications because of their controlled porosity and high surface areas (Schmidt-Winkel et al., 1999; Ying et al., 1999; Lee et al., 2001). Especially, enzyme immobilization has been extensively studied recently using mesoporous materials as the hosts (Diaz and Balkus, 1996; Takahashi et al.,

2000; Wang et al., 2001). One of the most frequently used approaches in immobilizing enzymes into mesoporous materials is a simple adsorption (Diaz and Balkus, 1996; Takahashi et al., 2000). The stability of adsorbed enzymes in mesoporous materials is dependent on many factors, including the pore size of mesoporous materials and charge interaction. The pore size of mesoporous materials affects the adsorption and leaching of enzymes in a more direct way (Diaz and Balkus, 1996; Takahashi et al., 2000).

The pore size of mesoporous materials should be similar to or larger than that of enzymes for successful enzyme adsorption. The size matching between pore size and the molecular diameter of enzymes is important in achieving high stability of adsorbed enzymes (Takahashi et al., 2000). The mesoporous environment can also be fabricated as nanometer-scale reactors for multi-enzyme catalysis with co-immobilized enzymes and cofactors (El-Zahab et al., 2004). Lactate dehydrogenase (LDH), glucose dehydrogenase (GDH), and cofactor (NADH) were covalently co-immobilized in porous silica particles with pore sizes of 30 or 100 nm in diameter. NADH is converted to $NAD^+$ during the LDH-catalyzed reduction of pyruvate to lactate, whereas NADH is regenerated from $NAD^+$ via GDH-catalyzed oxidation of glucose. This approach can be directly applied in the construction of electrodes for biofuel cells.

*2.7.3 Polymers*

In the construction of amperometric enzyme electrodes, it is important to have efficient charge transfer produced by the biochemical reactions to electronic circuit. To some extent, this can be controlled by applying suitable potential. However, some reactions, specifically those which involve biomolecules endure rather slow interfacial electron transfer even with large electrochemical driving forces. This problem can be significantly eliminated by modifying a given electrode with a thin film of an electro-active polymer. These

electroactive polymers have become the materials of choice for the amperometric biosensor fabrication as they can play both as a binding matrix and as an electron transfer mediator for the signal amplification of the biosensors (Ahuja et al., 2007; Nambiar and Yeow, 2011). Other than their conducting nature, the electroactive polymers may have other features like, optical transparency, flexibility in chemical structure, biocompatibility, ion selectivity and ease of handling. The electroactive polymer such as, polyaniline (PANI), polyethyleneimine (PEI), osmium polymer, methylene green (MG), nafion have been utilized for the development of bioelectrode for both biosensor and biofuel cell application. Among different techniques, electrochemical polymerization method is one of the most frequently used methods for fabrication of electrodes that can yield uniform, dense and porous layer (Kowalski and Schmuki, 2010; Lu and Li, 2008).

*2.7.3.1 Polyaniline (PANI), Polypyrrole (PPY)*

PANI is a polymer that changes conductivity and colour with changes in pH or redox reactions as a result of changes in the degree of protonation of the polymer backbone, making it useful as an optical or a visual sensor (Kuswandi et al., 2014). PANI film acts both as a matrix support compatible with biomaterial (e.g., enzyme) and as the indicator, and can be easily be fabricated. It has already been reported as a polymeric matrix in biosensors developments (Xia et al., 2010). In the case of a PANI-based biosensor, most employ oxido reductases, mainly oxidases and dehydrogenases. Myler et al., (2005) reported a sonochemically fabricated AOx enzyme micro-electrode array within PANI. In order to quantify the enzyme modulated resistance and capacitance changes within the polymer, impedance spectra were recorded for AOx/PANI sonochemically fabricated microelectrode arrays across a range of alcohol concentrations. By applying the PANI, impedance could be significantly reduced (Myler et al., 2005).

PPY has been investigated the most among polyheterocyclines. The electrochemical oxidation of pyrrole in aqueous $H_2SO_4$ can be carried out on platinum electrode. The product is a conducting polymer known as 'Pyrrole Black'. Kanazawa et al., (1979) produced coherent films of PPY with a conductivity of 100 $Scm^{-1}$ and exhibited excellent air stability. Ramanathan, (1996) have immobilized glucose oxidase (GOx) on conducting matrices PPY, and have studied the response characteristics, lifetime in detail. They had also studied the changes in the dielectric constant in PPY immobilized GOx. Among the conducting polymers PPY and its derivatives play a leading role due to their versatile applicability and the scope of covalent linking of a wide variety of molecular (redox) species to the pyrrole group (Bidan, 1992).

*2.7.3.2 Polyethyleneimine (PEI)*

It is a polycationic polymer (Rochefort et al., 2008). PEI was used to stabilize the enzyme immobilized on the nano-matrix coated on an Au electrode (Vatsyayan et al., 2010). It has been previously used for other enzymes in combination with MWCNT (Rubianes and Rivas, 2007; Arribas et al., 2007; Jia et al., 2008; Vatsyayan et al., 2010) mostly for its dispersion properties.

*2.7.3.3 Osmium polymer*

The osmium polyvinyl pyridine (OsP4VP) is widely reported for electrical wiring of laccase enzyme (Barton et al., 2001). In case of laccase, one of the Cu-redox center is located in the periphery of the enzyme that promote easy contact between the metal redox moiety of the polymer and the Cu-redox center of the enzyme for the exchange of electrons with the electrode (Yu and Scott, 2010). The redox potential of $Os^{3+/2+}$ redox couple is adjustable and can be optimized to be close to that of the active redox centre of the enzyme by proper

selection of ligands. The most important property of such polymers is the ability of $Os^{3+/2+}$ redox centres to exchange electrons with enzymes. Enzyme leakage is avoided not only by encapsulation of the large enzyme by crosslinked polymer backbones but also by exploiting electrostatic attraction between charged cationic redox groups of polymer and negatively charged protein moieties of the enzyme (Gallaway and Barton, 2008).

*2.7.3.4 Methylene green (MG)*

MG is an electroactive polymer that has been shown to form a stable polymer layer on electrode surfaces when electropolymerized (Zhou et al., 1996). MG is a polymer-based electrocatalyst was used to regenerate $NAD^+$ and to shuttle electrons from the NADH to the electrode (Sokic-Lazic et al., 2010) as oxidation of NADH at ordinary electrodes like bare glassy carbon or gold requires high overpotentials (Palmore et al., 1998). The utilization of MG catalysts for NADH oxidation in biofuel cells has been reported by Minteer and co-workers (Sokic-Lazic and Minteer, 2008; Sokic-Lazic and Minteer, 2009; Blackwell et al., 2009).

*2.7.3.5 Sol–gel materials*

Sol–gel materials provide a versatile way for bioimmobilization due to the presence of inorganic M–O–M or M–OH–M bridges forming a continuous network containing a liquid phase which can then be dried out to form a solid, porous polymeric matrix. In biosensors, this technique could result in the development of novel strategies to generate advanced materials for the immobilization of biological receptors within silica, metal oxide, organosiloxane, and hybrid sol–gel polymers (Wu et al., 1999; Wang, 1999; Gorton, 2005). Lim et al., (2007) fabricated nanostructured electrodes for enzymatic glucose–oxygen biofuel cells. The electrodes were based on enzyme encapsulation in sol–gel $SiO_2$ matrixes and

incorporated CNTs in the matrix to provide enhanced electronic conduction. The sol–gel/organic hybrid composite material based on the crosslinking of the natural polymer chitosan with (3-acryloxypropyl) dimethoxymethylsilane was developed for the fabrication of an amperometric $H_2O_2$ biosensor (Wang et al., 2003b). The composite film was used to immobilize HRP on a gold disk electrode. With the aid of a catechol mediator, the biosensor developed a fast response of less than 2 s with linear range of $5.0\times10^{-9}$ to $1.0\times10^{-7}$ mol $L^{-1}$ and a detection limit of $2\times10^{-9}$ mol $L^{-1}$. The biosensor retained approximately 75 % of its original activity after about 60 days of storage in a phosphate buffer at 4 °C.

*2.7.3.6 Nafion*

It is a sulfonated tetrafluroethylene based fluoropolymer discovered in the late 1960s by Walther Grot of Dupont. The combination of stable Teflon backbone with the acidic sulfonic groups gives nafion highly conductive to cations, making it suitable for many membrane application. Nafion is widely used as supporting matrix to confine biomolecules at the electrode surface in the construction of various biosensors (Fan and Harrison, 1992). It is an extremely suitable material for solubilising MWCNT (Vatsyayan et al., 2010). Nafion polymer also acts as a selective barrier for interferents from non target substances on the electrode surface by electrostatic repulsion (Wang et al., 2003a).

*2.7.4 Self assembled monolayers (SAM)*

SAM is a layer of molecular thickness formed by chemisorption of selected organic molecules on solid metal surfaces (Chaki and Vijayamohanan, 2002). The organic molecules used to generate SAMs are generally bifunctional molecules of different terminal functional groups (sulfides, thiols amines, etc.) which can be tailored using various chemistries making them compatible for desired applications (Arya et al., 2009). Self-assembly technique offers

several interesting perspectives in the field of biosensors. Functionalized SAMs can provide a reproducible and robust method of immobilizing desired biomolecules in the near vicinity of the electrode where some control over the orientation and distribution of the enzyme is afforded (Wink et al., 1997). Saxena et al., (2011a) demonstrated the covalent immobilization of cholesterol oxidase on self-assembled gold nanoparticles for highly sensitive amperometric detection of cholesterol in real samples. Asav and Akyilmaz (2010) develop a bienzymic biosensor, which was based on co-immobilization of AOx and GOx on the same electrode by formation of SAM for selective determination of ethanol and glucose. In this biosensor construction the enzymes and the mediator, tetrathiafulvalene (TTF), were immobilized with cross-linking agents glutaraldehyde and cysteamine by forming a SAM on a gold disc electrode. The sensor showed linear detection range 0.1 to 1.0 mM and 1.0 to 10 mM for glucose and ethanol, respectively.

## 2.8 Design approaches for EFC

### *2.8.1 Membrane less or single chambered fuel cell*

The partitioning or separating membrane between the anode and cathode faces some challenges and drawbacks in developing efficient EFC. In presence of membrane, the water management required in the fuel cell set up adds complexity to the system. In addition, fuel crossover through membrane reduces the cell performance (Neburchilov et al., 2007). Also, swelling and shrinkage of the membrane during water uptake and dehydration deforms the membrane resulting in packaging failure. Further the membrane acts as a barrier for miniaturization of the EFC (Shaegh et al., 2011). Hence, recent focus has been laid on the development of membraneless or single chambered fuel cell (Wen et al., 2014; Topcagic and Minteer 2006). Wu et al., (2009) reported a membraneless fructose/air EFC using

commercially available d-fructose dehydrogenase and bilirubin oxidase adsorbed on the surface of electrodes modified with cellulose–MWCNT matrix. An open circuit voltage of 663 mV and a maximum power density of 126 μW $cm^{-2}$ were obtained. Mano et al., (2004) reported a miniature, membrane-less glucose-$O_2$ biofuel cell built with Os derivatives polymer mediators for glucose and bilirubin oxidase on anode and cathode, respectively. They reported a power density of 4.8 μW $mm^{-2}$ at the voltage of 0.60 V in a physiological buffer at 37.5 °C.

*2.8.2 Three- dimensional electrode architecture*

To achieve maximum power density one can use 3D bioelectrocatalytic electrodes which possess multidimensional and multidirectional pore structures (Minteer et al., 2007). Multidimensionality provides both small pores to support enzyme stabilization and high loading densities, and larger pores to support mass transport of liquid phase fuel. Multidirectionality provides greater surface area and permeability to liquid phase fuel transport, but may eventually decrease structural strength (and surface area). Multidirectionality is also important because it eliminates blind pores and reduces the volume of solid polymer that remains inaccessible and unused (i.e. it increases the porosity of the immobilization support) (Minteer et al., 2007). 3D-structures can also provide suitable immobilization matrices for the enzymes and thus retain their activity for longer time (Ivanov et al., 2010).

*2.8.3 Microfluidic systems*

The intended application of enzymatic biofuel cells as small-scale power devices is inherently associated with the challenging design issues, concerning the miniaturization of such systems. In this context, in parallel with the research on novel bioelectrodes with an

improved performance, there is an emerging research field addressing microfluidic biofuel cells. Tingry and co-workers reported a microfluidic biofuel cell with a Y-shaped channel, based on soluble GOx and potassium ferricyanide for the anodic reaction and laccase and ABTS for the cathodic reaction (Zebda et al., 2009 a; Zebda et al., 2009 b). The pumping power to sustain the necessary flow was compared with the delivered power by the cell and it was found that the ratio of input power to the output power increased from 1.5 % at 100 μL $min^{-1}$ to 76 % at 1000 μL $min^{-1}$ (Zebda et al., 2009 a).

*2.8.4 Air-breathing biocathodes*

A new development in the area of biocathodes is the fabrication of enzymatic biocathodes that can operate using gas-phase $O_2$ (Zloczewska and Jönsson-Niedziolka, 2013). Because the concentration of $O_2$ in air is much higher than in oxygen-saturated water, air-breathing enzymatic biocathodes should be able to produce much more current than biocathodes that utilize dissolved oxygen. One of the first examples of air-breathing cathodes used osmium-based redox polymers to mediate electron transfer between laccase and the electrode, thereby producing current densities up to 1 mA $cm^{-2}$ (Hudak et al., 2009). The biocathodes in this study were used in $H_2$ fuel cells and were fairly unstable due to water loss from the cathode. The next generation of air-breathing biocathodes utilize DET for enzyme/electrode communication. Gellett et al., (2010) immobilized laccase in carbon black with the aid of tetrabutylammonium bromide–modified nafion to create an ink that could be painted onto electrodes and utilized in $H_2$ or direct methanol fuel cell (DMFCs). The laccase/$H_2$ fuel cells produced current densities of up to 38 mA $cm^{-2}$, and the laccase/methanol fuel cells performed even better, producing current densities above 50 mA $cm^{-2}$ and power densities of 10 $mWcm^{-2}$ while maintaining stability for more than 350 h. Gupta et al., (2011a,b) have also developed air-breathing enzymatic biocathodes based on

laccase and bilirubin oxidase by simply drop-casting the enzymes onto the high–surface area carbon black pellet electrodes. These DET air-breathing cathodes produced current densities up to 1 mA $cm^{-2}$ and were stable for up to 30 days.

# Chapter 3

## Fabrication and characterization of alcohol oxidase based bioelectrode for alcohol biosensing application

# Chapter 3

# Fabrication and characterization of alcohol oxidase based bioelectrode for alcohol biosensing application

### 3.1. Overview

The accurate measurement and detection of alcohols with high sensitivity and selectivity are required in many different areas, such as, clinical and forensic analysis, food, beverage, and pulp industries (Azevedo et al., 2005). Many analytical methods have been developed for the determination of ethanol but they are complex, time consuming and require prior separation processes, expensive instrumentation and trained operators. Such disadvantages could be overcome by using biosensor devices incorporating the enzymes as bio-recognition elements (Yildiz and Toppare, 2006). Biosensors for quantitative detection of alcohol are yet to develop properly for commercial applications. Alcohol biosensors described in the literature are largely based on alcohol dehydrogenase (ADH) (Zhang and Gorski, 2011), which normally require the co-factor $NAD^+$ for its activity (Raj and Behera, 2005; Razumiene et al., 2001; Svensson 2005; Lee and Tsai 2009). The major constrain for developing ADH based alcohol biosensor is the need of supplementing the co-factor ($NAD^+$) to the reaction medium (Vijayakumar et al., 1996). Alcohol oxidase (AOx) (EC 1.1.3.13) as bio-recognition element for sensing alcohol has stimulated interest since the last decade (Azevedo et al., 2005). The advantage of AOx is attributed to the avidly bound flavin-based cofactor to the redox center of this enzyme that obviated the need of supplementing the co factor to the reaction medium. AOx catalyzes the oxidation of alcohols using molecular oxygen as the electron acceptor and producing corresponding carbonyl compound and hydrogen peroxide in the reaction medium. The reaction may be followed by measuring $O_2$ or

$H_2O_2$ concentration using optical or electrochemical detections (Azevedo et al., 2005; Vijayakumar et al., 1996). The oxygen-based detection, however, has limitations such as, poor response, low accuracy and reproducibility, and high background signal that may raise the minimum detection level of the substrate alcohol (Bott, 1998). The $H_2O_2$ based biosensor though has the advantages of relatively ease of their manufacturing process and the possibility of constructing them in small sizes, the high potential (~ 600 mV) necessary to oxidize $H_2O_2$ causes electrochemical interference by many compounds present in blood serum samples. On the other hand, suitable electron transport mediator that could shuttle electrons between the redox center of the AOx enzyme and the electrode is not widely known for developing 2$^{nd}$ generation alcohol biosensors.

We report here an amperometric 3$^{rd}$ generation AOx based biosensor that operates on direct electrochemistry principle. The bioelectrode was prepared by using large multimeric AOx from *Pichia pastoris* immobilized in a nano-composite matrix on the surface of gold (Au) electrode.

## 3.2. Experimental approaches

### *3.2.1. Chemicals and reagents*

AOx from *P. pastoris* (21 U/mg protein), multiwalled carbon nanotube (MWCNT, size OD 10–15 nm, ID 2–6 nm, length 0.1–10 μm), Nafion117 (Nf) (5 % w/v in isopropanol), polyethylenimine (PEI) (50 % w/v in water solution), ABTS [2,2′-azino-bis(3 ethylbenzothiazoline-6-sulfonic acid)], and horseradish peroxidase (HRP) were bought from Sigma-Aldrich. Hydrogen peroxide ($H_2O_2$) (50 %) and ethanol (99.9 %) were purchased from Merck. All other chemicals were of analytical grade and used as received without

purification. AOx (1 mg $ml^{-1}$) was freshly prepared in potassium phosphate buffer solution (KPBS) (50 mM, pH 7.5).

*3.2.2. Fabrication of the bioelectrode*

A gold electrode (AuE) (diameter,1 mm) was cleaned first by polishing with alumina slurry, then washed ultrasonically with 70 % ethanol and water separately for 5 min each and finally allowed to dry under clean air at room temperature. A total of 3 mg of MWCNTs were dispersed in 300 µl of 5 % Nf and sonicated for 20 min to obtain a stable homogeneous suspension. Five microliters of the MWCNT-Nf solution was dropped onto the AuE and then allowed to dry under clean air and room temperature. Once dried, 5 µl of AOx solution from the stock solution was dropped above the MWCNT-Nf layer, dried and covered with 5 µl of 10 % (v/v) PEI solution. The fabricated bioelectrode was again dried under clean air at room temperature and stored in KPBS at 4 °C when not in use. The fabrication steps of AuE-MWCNT-Nf-AOx-PEI bioelectrode is depicted in the scheme 3.1.

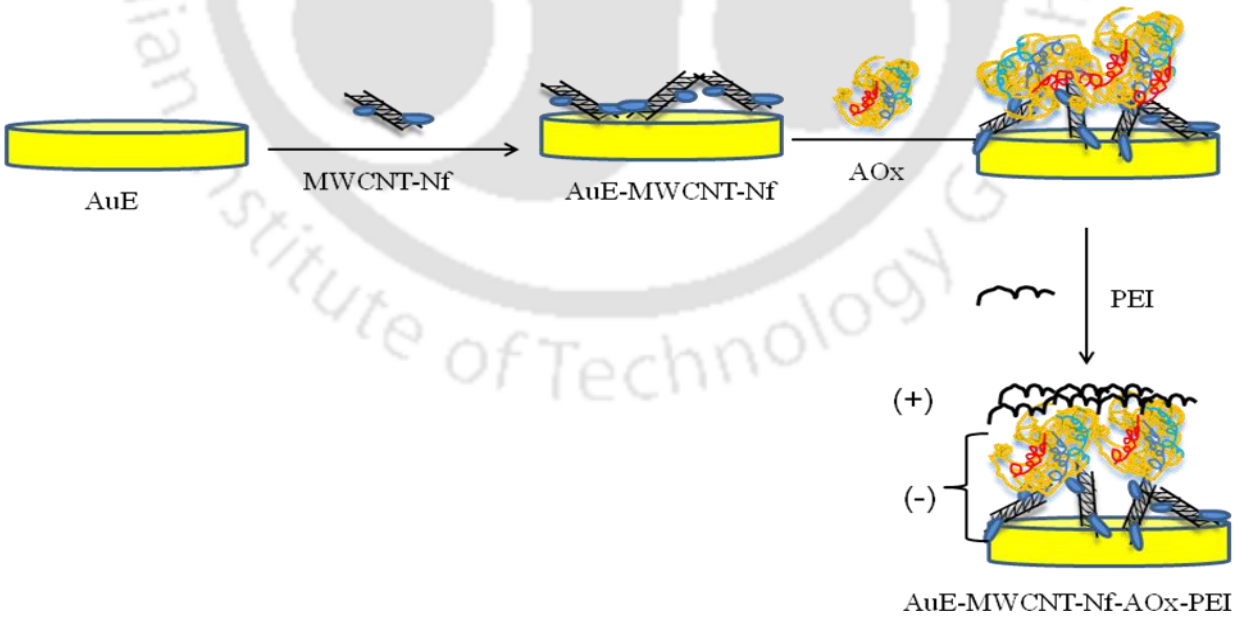


**Scheme 3.1** Fabrication scheme of AuE-MWCNT-Nf-AOx-PEI bioelectrode..

*3.2.3. Apparatus and measurements*

Cyclic voltammetry (CV) was performed with a potentiostat (Autolab PGSTAT 1212, Eco Chemie, Netherland). The measurement was done in a three-electrode system containing platinum rod as counter electrode, Ag/AgCl (saturated KCl) as reference electrode, and AuE or modified AuE as the working electrode. All potentials were measured and reported relative to the Ag/AgCl reference electrode. During the CV measurements, the electrolyte solution was constantly purged with high purity argon gas to maintain an anaerobic environment in the cell during the measurement process. All experiments were performed at room temperature. The images of the morphological characteristics on the bioelectrode were obtained on a field emission scanning electron microscope (FESEM) (Zeiss), with EHT 1.00 kV.

**3.3. Results and discussion**

*3.3.1. Morphological characterization of the bioelectrode*

The surface morphology of bare Au, Au-MWCNT-Nf, Au-MWCNT-Nf-AOx and Au-MWCNT-Nf-AOx-PEI bioelectrodes were investigated using FESEM. As shown in Fig. 3.1, AuE shows homogenous surface (Fig. 3.1A), and the Au-MWCNT-Nf electrode shows uniform distribution of MWCNTs on the electrode surface (Fig. 3.1B) with porous morphology clearly visible from the image taken at higher magnification (inset Fig. 3.1B). When AOx was added on this MWCNT-Nf film, the thread like structure of MWCNT and porosity of the film disappeared (Fig. 3.1C), indicating the immobilization of AOx molecules on the MWCNT-Nf film. Subsequently, when a layer of PEI was applied on the film to fabricate Au-MWCNT-Nf-AOx-PEI bioelectrode, the surface morphology changed to even form with an array of black dots in white patches distributed throughout the surface (Fig.

3.1D). The immobilization of enzymes on the electrode surface occurred under the influence of electrostatic interaction between the negatively charged underneath MWCNT-Nf layer with adsorbed AOx and positively charged overlaying PEI layer. The negative charges on MWCNT and the sulphonated polymer, Nf are well described. The AOx (p*I* 4.3) bears negative charge under the working buffer pH value of 7.5 used in this investigation. The formation of the nearly uniform array of black dots upon encapsulation of the AOx with PEI is interesting. The probable reason being attributed to the reorientation of the negatively charged MWCNTs in the composite matrix to the arrays upon its interaction with the positively charged PEI. However, the role of AOx in the reorientation of the MWCNTs is not clearly known.

*3.3.2. Electrochemical characterization of the bioelectrodes*

CV was carried out to identify the redox potentials of the fabricated working bioelectrodes (Fig. 3.2A) in a solution of argon-saturated KPBS (pH 7.5) at a scan rate of 50 mV $s^{-1}$. No clear redox peaks were observed for the bare AuE-Nf and AuE-MWCNT-Nf suggesting that both the MWCNT and Nf are electro-inactive in this potential window. Following the immobilization of AOx in the MWCNT-Nf film the generated bioelectrode AuE-MWCNT-Nf-AOx displayed a pair of clear redox peaks. However, the bioelectrode AuE-Nf-AOx-PEI (Fig. 3.2B) showed no clear redox peak and the CV response of the MWCNT void bioelectrode was almost similar with Au-Nf, which infers that MWCNTs play an important role in facilitating the electron exchange between the redox center of AOx and AuE. When PEI was layered on the AuE-MWCNT-Nf-AOx electrode the redox peak current of the generated bioelectrode AuE-MWCNT-Nf-AOx-PEI was increased further. The formal potential of the redox couple at the bioelectrode AuE-MWCNT-Nf-AOx-PEI calculated from the average value of anodic and cathodic peak potentials [$(E_{pa} + E_{pc})/2$] was 0.21 V. The

formal potential confirmed from the triplicate studies was 0.21 ± 0.003. The separation of the peak potentials (ΔEp) was 60 mV. The anodic peak current is nearly equal to the cathodic peak current. Therefore, a direct electrochemical reaction of quasi-reversible is ascribed to AOx immobilized on MWCNT-Nf-AOx-PEI. The potential of 0.21 V is attributed to the redox potential of FAD/$FADH_2$ system. Protein-bound flavins exhibit wide range of redox potentials since the redox potential of flavo-oxidases is strongly modulated by the cofactor environment (Fraaije et al., 2009; Munteanu et al., 2008). The redox potential of AOx was further confirmed by the increased current response at the potential with the addition of substrate alcohol. From the above findings it may be suggested that the nanometric MWCNT may be easily accessed to the multimeric AOx protein molecules, as a result of which the distance between the electrode and the redox center of AOx was decreased and promoted the electron exchange between them similar to other enzyme nanomaterial integrated system (Willner et al., 2007). The increase in redox current at 0.21 V of the PEI modified bioelectrode AuE-MWCNT-Nf-AOx-PEI is attributed to the electrostatic effect of PEI on stabilizing the AOx in the electrode, which enhanced the interaction between the electroactive center of the AOx proteins with the MWCNTs. The interaction further facilitated the electron transfer from the redox center of the enzyme to the electrode surface.

The electrochemical behavior of the constructed bioelectrode was characterized by CV at different scan rates (v) (Fig. 3.3A). The anodic ($I_{pa}$) and cathodic ($I_{pc}$) peak currents versus scan rate plots, shown in Fig. 3.3B, exhibit a linear relationship with a correlation coefficient of 0.9734 and 0.9877, respectively which infers that the redox reaction of AOx is a surface-controlled and not a diffusion controlled process. The values of anodic and cathodic peak potentials were plotted against the logarithm of the scan rates as shown in Fig. 3.3(C). The irreversible electrochemistry (i.e., peak separation > 200/n mV taking n = 1) occurred

when the scan rate exceeded 0.7 V $s^{-1}$. The electron transfer coefficient (α) and heterogeneous electron transfer rate constant ($k_s$) for diffusionless thin-layer voltammetry were determined from empirically fitted Laviron equation (Laviron, 1979 a,b). The anodic ($E_{pa}$) and cathodic ($E_{pc}$) peak potential at various scan rates are expressed as Equations (3.1) and (3.2) :

$$E_{pa} = E^{o'} + 2.3RT/(1-\alpha)nF \log v \quad (3.1)$$

$$E_{pc} = E^{o'} - 2.3RT/\alpha nF \log v \quad (3.2)$$

where $E^{o'}$ is the formal potential, and $R$, $T$, $F$, and $n$ have their usual significance. According to equation (1) and (2), the value of $\alpha$ was determined from the relationship of $\Delta E_P$ with log $v$ and found to be 0.52 (taking $n$ = 1). The value of $k_s$ was calculated using Eq. (3) and found to be 1.69 ± 0.15 $s^{-1}$.

$$\log(k_s) = \alpha\log(1-\alpha) + (1-\alpha)\log\alpha - \log RT/nFv - \alpha(1-\alpha)nF\Delta E_P/2.3RT \quad (3.3)$$

The result suggests significant electron transfer between the AOx and the electrode. There is however, no previous report on these kinetic constants from AOx based bioelectrode for comparison in quantitative scale. The surface coverage ($\Gamma$) of AOx on the electrode surface at a scan rate of 50 mV $s^{-1}$ estimated using the equation, $\Gamma$ = Q / $n$FA (Murray, 1984) where Q is the charge obtained by integrating the peak current area, $n$ is the number of electrons involved, F is the Faraday's constant and A is the electrode area, was found to be $2.43 \times 10^{-12}$ mol $cm^{-2}$. The amount of this electroactive protein is nearly 80 % of the total amount of AOx deposited on the electrode surface. This may be suggested that only those proteins with a suitable orientation and close contact with the MWCNTs in the inner layers of the film can exchange electrons with the gold electrode. Theoretically, the maximum possible

electrode surface coverage with a monolayer of the AOx protein calculated from the molecular dimension of AOx (Veenhuis et al., 1981) was $1.25 \times 10^{-4}$ mol $cm^{-2}$. Comparing this theoretical value with the one reported by us it may be inferred that there is a scope for optimizing the concentration of electroactive AOx molecules on the electrode surface by increasing the enzyme loading on the nanomatrix.

*3.3.3 Response characteristics of the bioelectrode*

The response of the bioelectrode was studied at various pH (6–8) values of the KPBS at equal concentration of alcohol (8 μM) and identified pH 7.5 as optimum for the response. It is known that the stability of AOx decreases when the pH is deviated from the physiological pH (Kumar and Goswami, 2006). The optimum pH value for the biocatalytic reaction of the AOx was also 7.5 which conformed to other reports (Suye, 2003). The pH effect on the alcohol biosensor observed here also conformed to other findings (Wen et al., 2007).

We also investigated the cyclic voltammetric response of AOx on the AuE-MWCNT-Nf-AOx-PEI in air saturated condition containing alcohol with increasing concentrations at a scan rate of 50 mV $s^{-1}$ (Fig. 3.4). Similar pair of redox peaks as observed in the presence of argon purged solution was observed. However, as compared to the anodic peak current an increase in cathodic peak current at 0.15 V was observed in the air saturated solution. This is because a fraction of the electrochemically formed $FADH_2$ is invovled in the biocatalytic reduction of dissolved oxygen in the solution resulting in formation of more $FAD^+$ available for its electrocatalytic reduction at 0.15. A parallel increase in broad oxidation peak between + 0.65 V and + 0.7 V occurred due to the electrocatalytic oxidation of $H_2O_2$ produced by the biocatalytic oxidation of alcohol in oxygen containing electrolyte solution. These results infer that the AOx layered on the electrode film retains its bioactivity.

The amperometric response of Au-MWCNT-Nf-AOx-PEI bioelectrode for successive step changes of alcohol concentration in KPBS at the anodic potential of 0.27 V was measured (Fig. 3.5A). The magnitude of the anodic peak current was increased linearly with increasing ethanol concentration with a correlation coefficient of 0.9909 and reached saturation at 42 μM of ethanol (Fig. 3.5B). The response characteristics of the bioelectrode are summarized in Table 3.1.

The detection limit (DL) for the constructed biosensor was determined from the expression DL = 3 × SD / sensitivity (where SD is the estimated standard deviation for the points used to construct the calibration curve and sensitivity its slope). The sensitivity of our constructed bioelectrode with the direct electrochemistry compares favorably with AOx biosensor for hydrogen peroxide-based detection of total content of volatile alcohols (Hammerle et al., 2011).

*3.3.4 Reproducibility, long-term stability and interference study of the bioelectrode*

The operational stability of the fabricated bioelectrodes was investigated from 16 successive measurements with 42 μM alcohol (which was the highest response in the linear range) during a period of 4 h. It was observed that the current response was steady till the last measurement following which the response declined. The results indicate that the activity of the constructed bioelectrode was quite stable during the period. The fabrication reproducibility of the bioelectrode was estimated from the response to various alcohol concentrations at three bioelectrodes prepared by similar procedure. The results showed acceptable reproducibility with a relative SD of ~ 2 % for the bioelectrode. The storage stability of the bioelectrode was checked by carrying out response measurements at a regular interval of three days. It was found that the bioelectrode retains about 90 % of the original response even after four weeks when stored in KPBS (pH 7.5) at 4 °C.

To study the selectivity of the alcohol biosensor to alcohol, the effect of some potential interfering agents present in real samples namely, ascorbic acid, lactic acid, glucose, urea and uric acid, on biosensor response was studied. Biosensor response was examined by exposing it separately to these interferents, each present with 8 μM alcohol solutions in 1:1 ratio. The selectivity coefficient (SC) of the biosensor for each interferent was estimated with respect to the response of the biosensor obtained when it is subjected to only alcohol using the formula, $SC = I_{c+1} / I_c$, where $I_{c+1}$ and $I_c$ (Saxena et al., 2011) are biosensor responses for alcohol (8 μM) in the presence and absence of each interferent, respectively. It was found that the contribution of these compounds to the biosensor response is < 5 % implying no significant interference. The actual level of these interferents in blood serum is usually known to be very low as compared to the concentration used in this study. The optimum selectivity of the bioelectrode towards alcohol may be attributed to two factors. Firstly, the anodic potential chosen was 0.27 V. At such a low potential, the contribution of many interferents towards current response may get substantially minimized. Secondly, nafion polymer acts as a selective barrier for the restricted access of many interferents to the electrode surface by electrostatic repulsion (Wang et al., 2003). This study implies that the biosensor could be used in the physiological conditions without any significant interference from the substances present in the body fluids. The practical usability of the fabricated bioelectrode was evaluated by determining the alcohol content in human serum samples. The alcohol content in the four serum samples supplemented with alcohol was first estimated by measuring the production of $H_2O_2$ using a coupled AOx-peroxidase reaction with ABTS ($\varepsilon_{405} = 36.8\ mM^{-1}\ cm^{-1}$) in KPBS buffer, pH 7.5 (Keesey, 1987). Then, the same samples were analyzed electrochemically with the bioelectrode at 0.27 V after diluting the samples suitably with KPBS buffer to make the concentrations fall in the linear range of the bioelectrode. The data

were compared by using paired t-test (Sigma 12). These results showed a reasonable agreement ($P$ = 0.045) between both methods of analysis.

One of the major focuses of the AOx based biosensor is to prolong the functional activity of this complex multimeric enzyme on the electrode surface. Many AOx based first generation biosensors using hydrogen peroxide or oxygen based detection showed varying operational stability. The operational stability of various AOx based biosensors are described in the table 3.2 While the requirement of high over potential for the operation of first generation biosensors stands a stumbling block for developing interference free detection system, Gouveia-Caridade et al., (2006) developed a $H_2O_2$ detection-based alcohol biosensor in which AOx and BSA were cross linked with glutaraldehyde and attached to the solid MWCNT on the carbon film electrode. The authors have reported significant increase in the sensitivity of the biosensor, while they reported its limitations on the reproducibility and poor operational stability. A comparative analysis as shown in table 3.2, infers that the method of fabrication of the bioelectrode is critical and linked to the stability and response mechanism of the biosensors. The electrostatic interaction principle exploited by us for the adsorption-based physical immobilization of the enzyme on the electrode surface provides the significant operational stability and the reproducibility on the response of the biosensors. Further, the interaction facilitates the electrical communication between the AOx with the electrode as evident from the clear CV response peak at comparatively low over potential of 0.21 V. Although the linear response range obtained by us is comparatively narrow the minimum detection limit in the linear range was superior to other reports mentioned above.

### 3.4. Conclusion

The direct electrochemistry of a multimeric AOx physically immobilized by encapsulating with PEI in a MWCNT-Nf matrix on the gold electrode surface was established for the first time. Direct electron transfer facilitated by the MWCNT between the AOx protein and the electrode was confirmed. The entrapped AOx possesses good bioactivity and electrocatalytic activity at room temperature and physiological pH. The constructed bioelectrode showed linear response at the oxidation potential of 0.27 V for alcohol. The low over potential of the constructed biosensor practically nullifies the interference caused by many common interfering compounds present in the samples. The findings confirmed the potential applications of the constructed bioelectrode as third generation biosensor for detecting alcohol in real samples.

## Figures

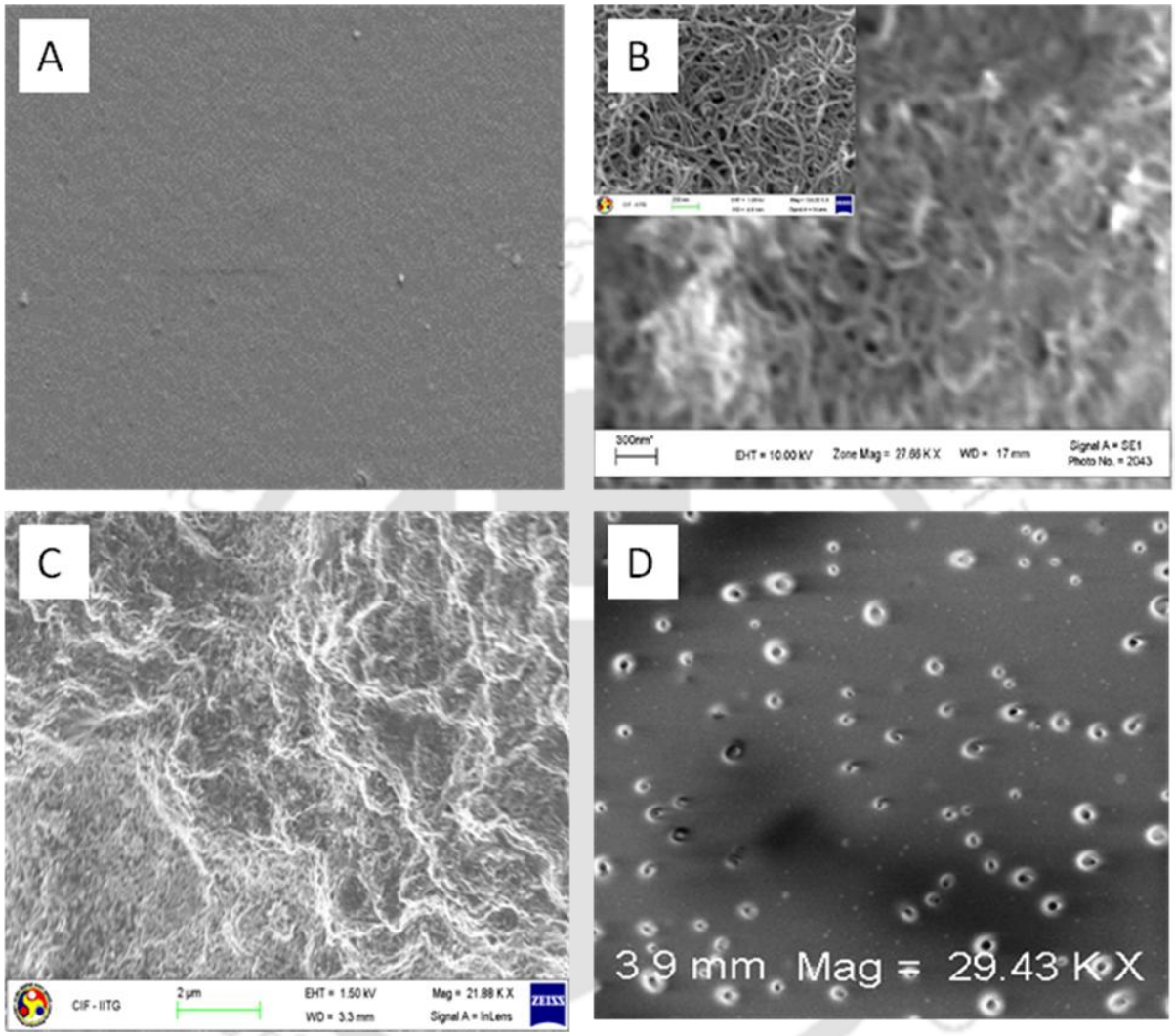


**Figure 3.1** FESEM images of (A) AuE (30 KX), (B) Au-MWCNT-Nf (27.66 KX) with inset at 153 KX, (C) Au-MWCNT-Nf-AOx (21.88 KX) and (D) Au-MWCNT-NF-AOx-PEI (29.43KX) with EHT 1.00 kV.

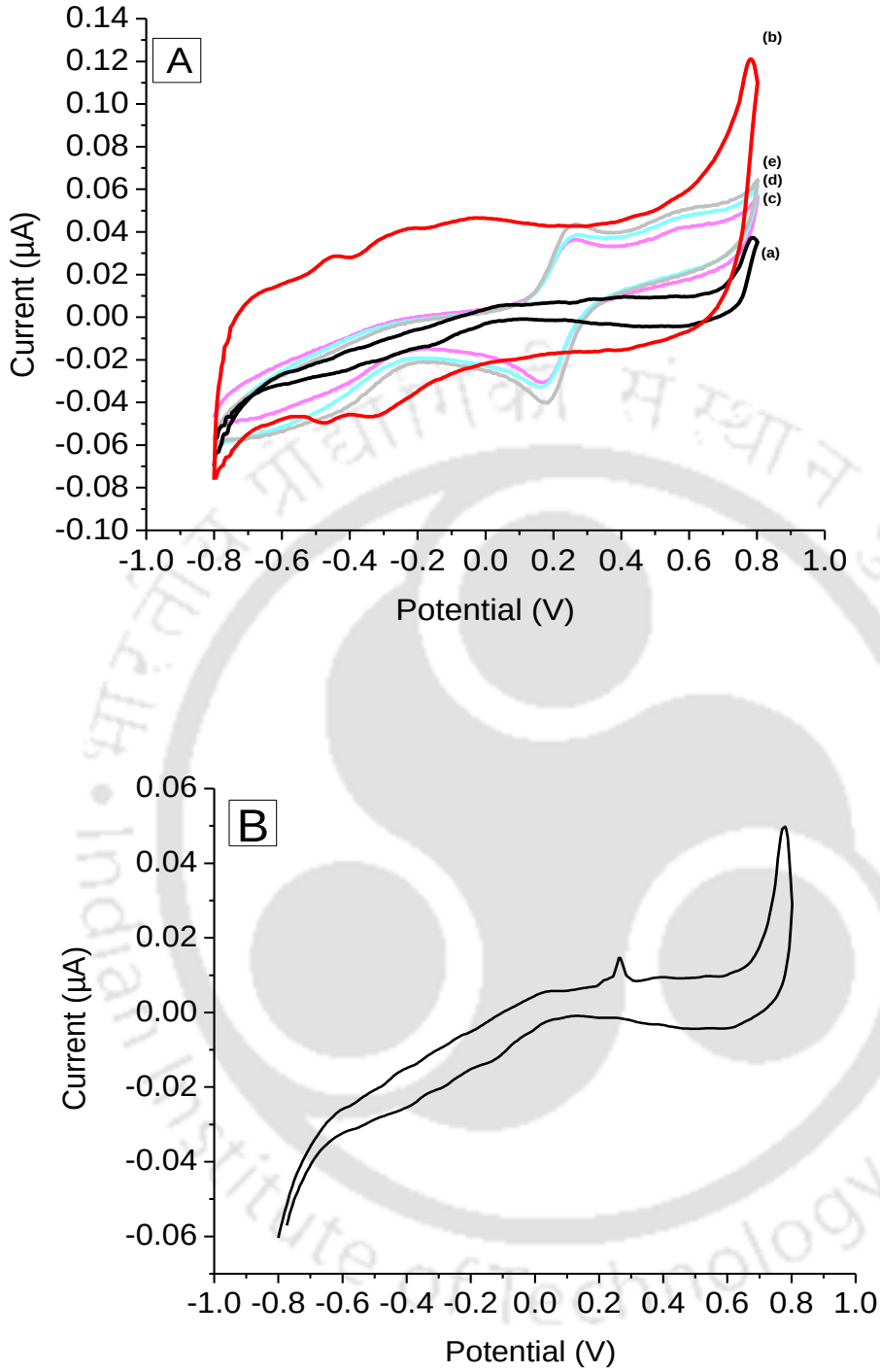


**Figure 3.2** (A) CV of AuE-Nf (a), AuE-MWCNT-Nf (b), AuE-MWCNT-Nf-AOx (c), AuE-MWCNT-Nf-AOx-PEI (d) and AuE-MWCNT-Nf-AOx-PEI (e) with 33 µM ethanol. (B) CV of AuE-Nf-AOx-PEI in an argon gas purged solution of 0.1 M KPBS (pH 7.5) at a scan rate of 50 mV $s^{-1}$.

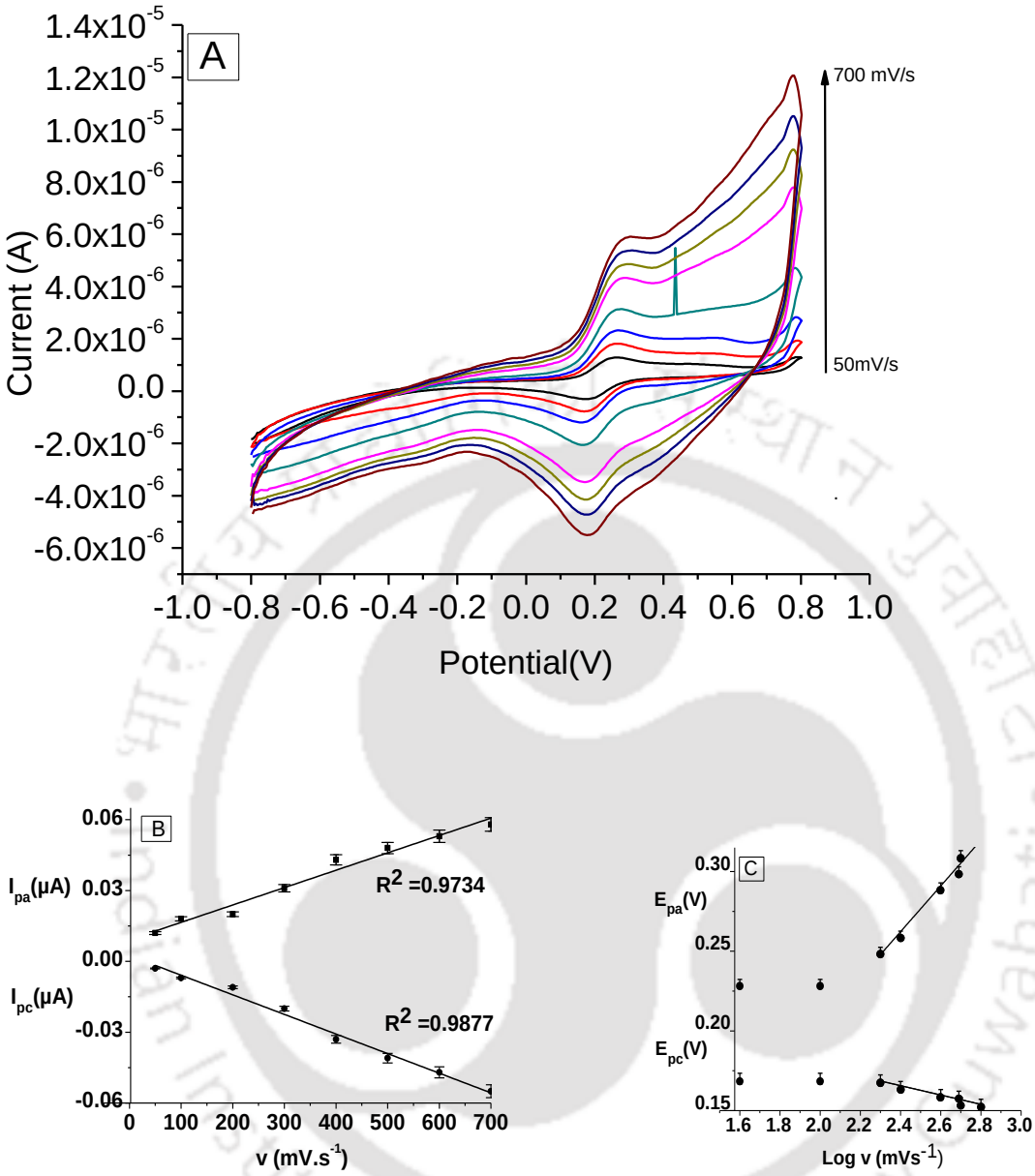


**Figure 3.3** (A) CV of bioelectrode AuE-MWCNT-Nf-AOx-PEI with increasing scan rate (mV $s^{-1}$) (50, 100, 200, 300, 400, 500, 600, 700); (B) anodic ($I_{pa}$ / μA) and cathodic peak current ($I_{pc}$ / μA) versus scan rate (mV $s^{-1}$); (C) peak potential versus log (scan rate, mV $s^{-1}$) in a solution of 0.1 M KPBS, pH 7.5.

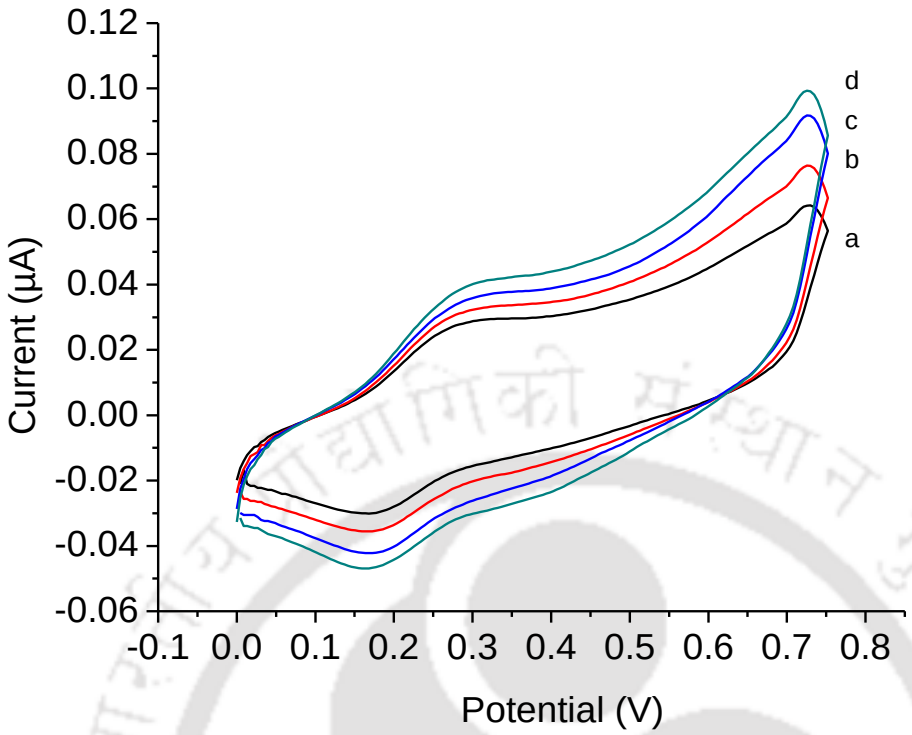


**Figure 3.4.** CV of bioelectrode Au-MWCNT-Nf-AOx-PEI in the presence of oxygen saturated buffer (0.1 M KPBS pH 7.5) with increasing ethanol concentration (µM) (a) 0, (b) 8, (c) 33, and (d) 42 at a scan rate of 50 mV $s^{-1}$.

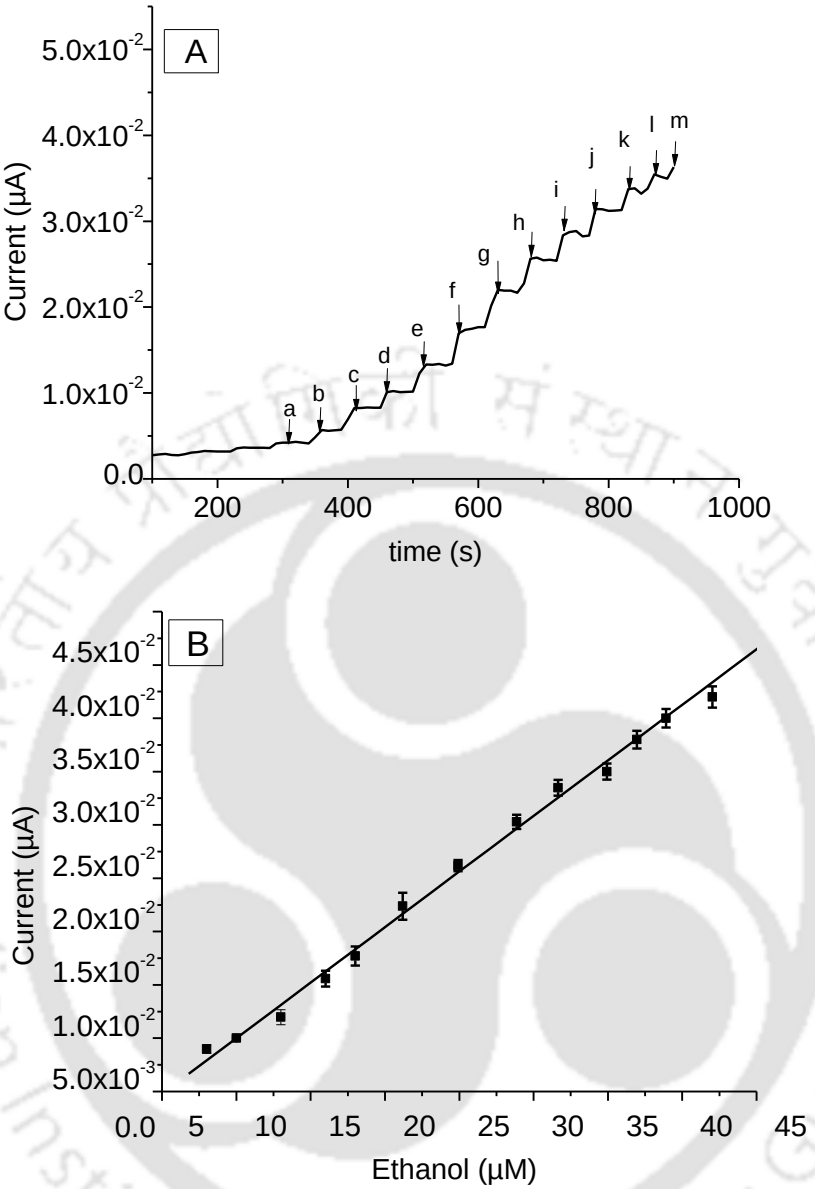


**Figure 3.5 (A)** Chronoamperometric current responses of the AuE-MWCNT-Nf-AOx-PEI bioelectrode for successive addition of alcohol (μM). (a) 8, (b) 10, (c) 13, (d) 16, (e) 18, (f) 21, (g) 25, (h) 28, (i) 31, (j) 35, (k) 37, (l) 39, and (m) 42. (B) The response curve of the bioelectrode with increasing ethanol concentration in argon purged solution of 0.1 M KPBS, pH 7.5. ($R^2$ = 0.9909). The operating potential was 0.27 V (vs. Ag/AgCl electrode).

## Tables

**Table 3.1:** Response characteristics of the bioelectrode

| | |
|---|---|
| Linear range | 8 µM-42 µM |
| DL | 4.94 µM |
| Sensitivity | 3 $\mu AmM^{-1}$ |
| SD limit | $4.94 \times 10^{-3}$ µA |
| Response time | 55 s |

Abbreviation: SD, Standard deviation; DL, Detection limit.

**Table 3.2** Performances of various prominent AOx-based biosensors.

| Biosensor configuration | Detection approach | Operational stability | Linearity (μM) | Reference |
|---|---|---|---|---|
| Carbon Paste Matrix/$AO_x$-HRP-osmium (FIA) | Hydrogen peroxide | 10 % of sensitivity lost after 270 injections carried out in 9 h | 250-2000 | Vijayakumar et al., (1996) |
| Pt/$AO_x$-poly(carbamyl) sulfonate hydrogel (Batch) | Hydrogen peroxide and oxygen. | 32 % of sensitivity lost after 12 measurements carried out in 12 h, and 40 %, sensitivity lost after 18 days | 10-3000 | Patel et al., (2001) |
| Pt/polyvinylferrocenium matrix-$AO_x$ (Batch) | Hydrogen peroxide | 98 % of sensitivity lost after 36 days (132 measurements) | Up to 3000 | Gulce et al., (2002) |
| Carbon paste matrix –(graphite-teflon)/$AO_x$-HRP-feroccene(FIA) | Hydrogen peroxide | No loss after 15 days (3 measurements/ day) | 10-750 | de Prada et al., (2003) |
| Au/$PPY_{ox}$/$AO_x$-glutaraldehyde-BSA(FIA) | Hydrogen peroxide | No loss after 90 injections carried out in 3 h, 5 % of sensitivity lost after 6 h monitoring | Not reported | Carelli et al., (2006) |
| Chitosan/$AO_x$-eggshell membrane (Batch) | Oxygen | No loss after 20 measurements carried out in 8 h, | 60-800 | Wen et al., (2007) |
| Carbon film electrode MWCNT/AOx | Hydrogen peroxide | A decrease of 70 % of the initial sensitivity value after 3 weeks | 1400 | Gouveia-Caridade et al.,(2008) |

*Cont.....*

| | | | | |
|---|---|---|---|---|
| Au/MWCNT/Nf-AOx-PEI | Direct electrochemistry | No loss after 16 measurements carried out in 4h, it retains about 90 % of the original response after 4 weeks | 8-42 | Present work |

# Chapter 4

## Fabrication and characterization of laccase based bioelectrode for biosensor application

# Chapter 4

# Fabrication and characterization of laccase based bioelectrode for biosensor application

## 4.1. Overview

Phenolic compounds are widely used in large scale manufacturing of resins, plastics, pesticides, explosives, detergents and pharmaceutical products. These compounds are frequently leached out during their production and pollute the environment. Besides, certain phenols have been reported as genotoxic, mutagenic, and hepatotoxic (Stob 1983; Castillo and Barcelo, 1997). Amongst these, pyrocatechol or catechol (1,2-dihydroxybenzene) is a potential phenolic compound of concern, as it reacts with different biomolecules, like DNA, protein, membranes and leads to their non repairable damage (Schweigert, 2001; Li and Trush, 1994). Thus, there is an continuously increasing demand for selective and sensitive detection of these phenolic compounds for evaluating their toxicity in environmental samples. Apart from the classical method of Folin–Ciocalteau, many analytical methods based on spectrophotometry (Bosch et al., 1987), chemical, and gas chromatographic principles (Bartak, 2000) have been developed for the detection of pyrocatechol. Although some of these methods are highly sensitive and reliable, they are relatively difficult to perform and often need derivatization and pre-concentration steps. Such disadvantages could be overcome by using biosensor devices for fast, specific, accurate and highly sensitive detection of pyrocatechol in real samples (Yaropolov et al., 1995; Freire, 2002; Kulys, 2003).

Over the past decade, many biosensors have been developed using redox enzymes, such as tyrosinase, peroxidase, laccase as biorecognition elements for the detection of phenolic compounds (Duran and Esposito, 2000). Laccase biosensor has unique merit over

tyrosinase biosensors in having high sensitivity and stability (Wang et al., 2012b). It also has more advantage over peroxidases as biorecognition element, since the background current from hydrogen peroxide limits the sensitivity of peroxidase biosensor (Lindgren, 1997). Laccase (EC 1.10.3.2) a multicopper redox enzyme, widely occurring in fungi (Mayer and Staples, 2002) have been identified as a potential catalyst for the determination of phenolic compounds (Haghighi et al., 2003). The construction of laccase biosensor is simple as laccase does not require $H_2O_2$ as co-substrate and any other external co-factor for its catalysis (Roy et al., 2005). Moreover, thermal tolerance is also a positive feature of laccase for biosensor applications (Kulys and Vidziunaite, 2003). Laccases catalyze the oxidation of various phenolic compounds with concomitant reduction of molecular oxygen to water (Thurston, 1994) without the intermediate formation of toxic $H_2O_2$. Generally, laccase contains four copper atoms classified into type 1 (T1), type 2 (T2), and type 3 (T3). T1, the substrate binding site of the enzyme is involved in oxidation of substrate and transfer of electron to T2/T3 cluster, while T3 is responsible for oxygen uptake and as a whole, this T2/T3 site is responsible for the reduction of $O_2$ to water (Solomon et al., 1996; Morozova et al., 2007).

In the present study, pyrocatechol has been used as the model phenolic compound to be detected in environmental test samples using laccase based amperometric biosensor. The laccase from *Trametes versicolor* was immobilized in a nano-composite matrix including osmium redox polymer on the surface of a GCE. MWCNTs were dispersed on the surface of the electrode using hydrophobic polymer chain of Nafion (Nf) (Wang et al., 2003a). Osmium polymer is known as potential electron transfer mediator between many redox enzymes and electrodes. A detailed account on the characterization of the fabricated laccase electrode and response of the bioelectrode for the substrate pyrocatechol is presented here.

## 4.2 Experimental approaches

### *4.2.1. Chemicals and reagents*

Laccase (p-diphenol: dioxygen oxidoreductase) from *T. versicolor* (0.5 U/mg solid), Nf (5 % w/v in isopropanol), MWCNT with 95 % purity (10–15 nm outer diameter, 2–6 nm inner diameter and 0.1–10 μm length), osmium tetroxide on poly-4(vinyl pyridine) ($OsO_4$ on P4VP) and ethyl benzene were bought from Sigma–Aldrich (India). Tri-sodium citrate from Qualigens (India), monohydrate citric acid from Rankem (India) and pyrocatechol from Spectrochem (India) were purchased. VULCAN XC 72 grade carbon black (CB) was purchased from Cabot India Pvt. Ltd. GCE (3.0 mm diameter) was purchased from Bioanalytical Systems Inc., USA. The stock solution of laccase (10 mg $ml^{-1}$) was freshly prepared in 0.1 M sodium citrate buffer (pH 4.7), prior to being used. 0.1 M sodium citrate buffer solution (pH 4.7) prepared with tri-sodium citrate and monohydrate citric acid was employed as the supporting electrolyte. Again, working solution of pyrocatechol (1 μM) was freshly prepared in 0.1 M sodium citrate buffer (pH 4.7) prior to being used. The entire experiment was performed using Elix Milipore water (with resistivity 15 MΩ cm at 25 °C).

### *4.2.2. Apparatus and measurements*

Electrochemical measurements like CV and differential pulse voltammetry (DPV) were performed with a potentiostat. The measurement was done in a three-electrode system containing platinum rod as counter electrode, Ag/AgCl (saturated KCl) as reference electrode, and GCE or modified GCE as the working electrode. All potentials were measured and reported relative to the Ag/AgCl reference electrode. All experiments were performed at room temperature. The images of the morphological characteristics on the bioelectrode were obtained on a scanning electron microscope (SEM) (Leo 1430vp, Germany).

*4.2.3. Preparation of bioelectrode*

A GCE (diameter, 3 mm) was cleaned first by polishing with alumina slurry, then washed ultrasonically with 70 % ethanol and deionized water separately for 5 min each and finally allowed to dry under clean air at room temperature. A total of 2 mg MWCNTs and 6 mg CB was added in 4 ml Nf and the mixture was sonicated for 30 min to form a homogeneous mixture. 5 µl of the mixture was dropped onto the GCE and then allowed to dry under clean air to make GCE/MWCNT–CB–Nf electrode. Thereafter, 10 mg $OsO_4$P4VP in 1 ml ethyl benzene was sonicated for 1 h and then 1 mg MWCNT was added to it. The mixture was sonicated again for 1 h and then 8 µl of the homogeneous mixture was dropped onto MWCNT–CB–Nf coated GCE to make the GCE/MWCNT–CB–Nf–$OsO_4$P4VP electrode. When the nano-composite mixture on the electrode surface was in semi-dry condition, a total 10 µl of a freshly prepared laccase enzyme stock solution was dropped onto it that resulted in the GCE/MWCNT–CB–Nf–$OsO_4$P4VP–laccase bioelectrode. The fabricated bioelectrode was then dried under clean air in the laminar hood at room temperature. The bioelectrode was immersed in 0.1 M sodium citrate buffer (pH 4.7) for 15 min prior to used. The bioelectrode was stored in 0.1 M sodium citrate buffer (pH 4.7) at 4 °C when not in use.


**Scheme 4.1** Fabrication scheme of GCE/MWCNT-CB-Nf/$OsO_4$P4VP/laccase bioelectrode.

## 4.3. Results and discussions

### *4.3.1. Morphological characterization of the bioelectrode*

The surface morphology of the laccase immobilized GCE/MWCNT–CB–Nf–$OsO_4$P4VP electrode was performed using SEM. Fig.4.1 shows the SEM images of the electrode at different fabrication steps. Blank GCE shows plain homogenous surface (Fig. 4.1A), whereas the GCE/MWCNT–CB–Nf electrode shows porous morphology (Fig. 4.1B), where intertwined thread like structure of MWCNTs is clearly visible in the image with higher magnification (inset, Fig. 4.1B). When solution of $OsO_4$P4VP–MWCNT was added on the surface of GCE/MWCNT–CB–Nf electrode, the surface turned into patchy morphology indicating the $OsO_4$P4VP polymer set in a pattern on the surface of the MWCNT–CB–Nf layer (Fig. 4.1C). Now, when laccase was added to the MWCNT–CB–Nf–$OsO_4$P4VP film, the surface morphology of the generated bioelectrode changed markedly

(Fig. 4.1D). The patchy surface was filled up and small globular structures appeared on the electrode surface. Formation of the globular structures indicates the adsorption of the laccase proteins from the pure laccase solution applied in the supporting nano-composite polymer matrix on the electrode surface. The presence of osmium in the bioelectrode GCE/MWCNT–CB–Nf–$OsO_4$P4VP–laccase was further confirmed by EDX study (Fig 4.1E).

*4.3.2. Electrochemical characterization of the bioelectrode*

CV was carried out in sodium citrate buffer (pH 4.7) separately purged with argon and oxygen gas for bare GCE and different modified GCE at major steps of bioelectrode fabrication to identify the redox potentials of the fabricated working bioelectrodes (Fig. 4.2). No clear redox peaks except at around −0.70 V were observed for bare GCE (Fig. 4.2A, curve a) and GCE/MWCNT–CB–Nf (Fig. 4.2A, curve b), suggesting that both the MWCNT and Nf are electro-inactive in this potential window. The cathodic peak at −0.70 V indicates $O_2$ is electrochemically reduced at the electrode surface. After the adsorption of MWCNT–CB–Nf on the GCE surface, an increase in the background current intensity was observed which is attributed to the increased electroactive surface area of MWCNTs (Fig. 4.2A, curve b). When $OsO_4$P4VP is adsorbed on MWCNT–CB–Nf, the magnitude of the background current decreases with a pair of weak redox peaks appearing at −0.08 V (anodic) and at −0.12 V (cathodic) (Fig. 4.2A, curve c), which are attributed to the redox potential of osmium complex. The laccase enzyme when adsorbed in the nano-composite matrix on the electrode surface, two sharp quasi reversible peaks at 0.34 V (anodic) and at 0.23 V (cathodic) were observed (Fig. 4.2A, curve d). The formal potential of the redox couple calculated from the average value of anodic and cathodic peak potentials [($E_{pa}$ + $E_{pc}$)/2] was 0.28 V. The present value is in agreement with redox potential values previously determined for laccase which fall in the range from 0.23 V to 0.59 V (vs Ag/AgCl) for laccase from different species

(Ivnitski et al., 2010; Shleev et al., 2006). The result implies that at a cathodic potential of about 0.23 V molecular oxygen gets reduced in the redox centre of laccase. The oxidized redox centre of the laccase is regenerated at anodic potential of 0.34 V. The result is supported by the fact that when oxygen was expelled from the buffer solution by purging with argon gas for 15 min, the magnitude of current of the redox pair at 0.34 V and 0.23 V was significantly decreased (Fig. 4.2B, curve a) and the current in the redox pair was regenerated upon passing the oxygen gas through the buffer solution (Fig. 4.2B, curve b). Analysis of the copper centres of multi copper oxidases in the presence of a chelating agent specific for T2 copper centre has shown that a potential area between 0.0 V and +0.4 V (vs Ag/AgCl) belongs to $O_2$ reducing site for the trinuclear copper centre of the enzyme (Ivnitski, et al., 2009).

In absence of oxygen a clear second redox pair at −0.03 V (anodic) and −0.15 V (cathodic) was also observed (Fig. 4.2B, curve a). The result is attributed to the existence of electrical communication of two copper based redox centres in the laccase enzyme with the electrode. When pyrocatechol was added to the buffer, purged with $O_2$, a cathodic current of the bioelectrode in a broad potential range encompassing both the cathodic potentials that obtained in absence of oxygen was recorded (Fig. 4.2B, curve c). Contrary to the high cathodic current, only a negligible increase in anodic current was detected. The result implies that the oxidation of the substrate pyrocatechol on the electrode surface proceeds biocatalytically and reduction proceeds electro-catalytically as shown in Scheme 4.2. The broad reduction potential is ascribed to the cumulative electrocatalytic reduction of the redox centre (~0.23 V) of a fraction of the enzymes and 1,2-benzoquinone (~0.14 V), which is generated by the biocatalytic oxidation of pyrocatechol. The 1,2-benzoquinone generated on the electrode surface thus entered in a redox recycled process between biocatalytic oxidation of pyrocatechol and electrocatalytic reduction of the quinone.

Again, to obtain the various electron transfer parameters of the bioelectrode, CV was carried out with GCE/MWCNT–CB–Nf/$OsO_4$P4VP/laccase bioelectrode in sodium citrate buffer (0.1 M, pH 4.7) at different potential scan rates ($\upsilon$) (30–700 mV/s). At $\upsilon$ = 50 mV/s, the peak separation ($\Delta E_p$) was about 106 mV (Fig. 4.3A), which is more than the peak separation of a reversible process (59 mV), indicating a quasi-reversible redox process (Scott and Lukehart 2007). Moreover, as the scan rate increases, the anodic ($E_{pa}$) and cathodic ($E_{pc}$) peak potentials shift to more positive and more negative values respectively increasing the $\Delta E_p$ further suggesting a quasi-reversible process. Besides this, the magnitude of anodic ($I_{pa}$) and cathodic ($I_{pc}$) peak currents increase linearly with increasing scan rate in the range of 30–700 mV/s (Fig. 4.3B) as expected for a surface confined redox process and indicating a thin layer electrochemical behavior (Scott and Lukehart, 2007). The value of charge transfer coefficient (α) can be determined by using the slopes from linear plots $E_{pa}$ and $E_{pc}$ versus logv (Fig 4.3C). The electron transfer kinetics values of the bioelectrode are calculated by using the similar equation as described in the previous chapter 3, section 3.3.2 and the values are depicted in the table 4.1.

*4.3.3 Electrochemical response of the laccase biosensor to pyrocatechol*

Laccase bioelectrode studies were carried out to evaluate the contribution of each modifier materials employed in developing the biosensor. Fig. 4.4 shows the voltammograms (DPV) obtained using the (a) bare GCE, (b) GCE-laccase, (c) GCE/MWCNT–CB-laccase, (d) GCE/$OsO_4$P4VP-laccase and (e) GCE/MWCNT–CB–Nf–$OsO_4$P4VP–laccase in 16 nM pyrocatechol in 0.1 M sodium citrate buffer solution (pH 4.7) in a potential range for cathodic current. The cathodic current of 1,2-benzoquinone reduction to pyrocatechol was used as the analytical response (cathodic current values are shown in the inset of Fig. 4.4). No current was produced with bare GCE (curve a). However, GCE with immobilized laccase had

produced current ($1.148 \times 10^{-6}$ A) (curve b), indicating laccase oxidizes pyrocatechol to 1,2-benzoquinone, which is electrochemically reduced at the electrode surface. The current was further increased when laccase was immobilized with MWCNT (curve c) or $OsO_4$P4VP (curve d) on GCE, while the magnitude of current with the $OsO_4$P4VP was higher than the bioelectrode containing MWCNT alone. Interestingly, the level of current was highest when laccase was immobilized on GCE/MWCNT–CB–Nf–$OsO_4$P4VP matrix (curve e). Results infer that both MWCNT and osmium polymer provides better electroactive environment for electron exchange between the electrode and the benzoquinone, and their coexistence in the nanocomposite matrix further facilitate the reduction of 1,2-benzoquinone synergistically on the electrode surface.

*4.3.4. Analytical performance of biosensor in pyrocatechol determination*

The response characteristics of the GCE/MWCNT–CB–Nf–$OsO_4$P4VP–laccase sensor towards pyrocatechol was investigated by DPV in the potential range of −0.05 and +0.3 V vs. Ag/AgCl, with step potential 50 mV/s. The GCE/MWCNT–CB–Nf–$OsO_4$P4VP–laccase electrode was subjected to increasing amount of pyrocatechol concentration. It was observed that with the addition of substrate, the current was increasing at +0.14 V, with a negligible shift in peak position (Fig 4.5). It indicates the electrochemical reduction of 1,2-benzoquinone to pyrocatechol was obtained at a potential of +0.14 V (vs. Ag/AgCl). Here the cathodic current of 1,2-benzoquinone reduction to pyrocatechol was used to construct the response curve. The response curve was constructed with current vs concentration of pyrocatechol as shown in the inset of Fig. 4.5. As can be observed, the cathodic current increased with pyrocatechol concentration and the response curve was linear from 3.98 nM to 16.71 nM with the regression coefficient $R^2 = 0.9737$. The response characteristics of the bioelectrode for pyrocatechol are summarized in Table 4.1. The detection limit (DL) for the

constructed biosensor was determined from the expression DL = 3 × SD/sensitivity (where SD is the estimated standard deviation for the points used to construct the calibration curve and sensitivity is its slope). The detection limit obtained with the present fabricated laccase biosensor is lower than aminopyrene reduced graphene oxides/chitosan/GCE hybrid film (Zhou et al., 2013), glutaraldehyde functionalized chitosan–MWCNT/GCE (Tan et al., 2009), MB modified MCM-41/PVA composite film/Au (Xu et al., 2009) and CNT–chitosan composite film (Liu et al., 2006) matrix based laccase biosensor for determination of pyrocatechol. The high sensitivity of the fabricated bioelectrode over other reported laccase biosensors emphasizes the advantage of MWCNT–CB–Nf–$OsO_4$P4VP based electrode for pyrocatechol sensing over other matrices. Based on the CV and DPV studies, the electrocatalytic mechanism of the fabricated bioelectrode in detecting pyrocatechol can be proposed by the schematic diagram 4.2.

*4.3.5. Operational stability, storage stability and reproducibility of the bioelectrode*

The operational stability of the bioelectrode was examined by subjecting a freshly prepared bioelectrode at optimal working conditions to a 15 nM pyrocatechol solution and assessing its response successively for 15 times for a period of 5 h. After each measurement the bioelectrode was kept in sodium citrate buffer (0.1 M, pH 4.7). It was observed that the bioelectrode retained ~94 % of its initial activity at the end of the 15 measurements. This high operational stability indicates that there was negligible enzyme leakage from the bioelectrode. This high operational stability may be due to the biocompatible nanocomposite matrix used for immobilization of the enzyme. The storage stability of the bioelectrode was checked by carrying out response measurements at the regular intervals of three days and it was found that it retained about 81 % of its initial activity even after three weeks when stored in sodium citrate buffer (pH 4.7) at 4 °C. The fabrication reproducibility of the bioelectrode

was estimated from the response to 15 nM pyrocatechol at three bioelectrodes prepared by the same procedure. The results showed an acceptable reproducibility with a relative standard deviation of 2.8 % for the fabricated bioelectrode.

*4.3.6. Interference study*

The effect of some potential interferents present in environment sample such as, sodium fluoride (NaF), sodium azide ($NaN_3$), magnesium sulphate ($MgSO_4$) and zinc sulphate ($ZnSO_4$) on biosensor response was studied (Fig 4.6). The response was examined by separately exposing the sensor in a 4 nM pyrocatechol solutions with the intereferents in 1:1 ratio. Selectivity coefficient (SC) of the biosensor for each interferent was estimated with respect to the response of the biosensor obtained when it is subjected to only pyrocatechol using the formula, $SC = I_{c+i}/I_c$, where $I_{c+i}$ and $I_c$ (Saxena et al., 2011a) are biosensor response for pyrocatechol (4 nM) in the presence and absence of each interferents, respectively. In most of the cases, it was found that the contribution of these compounds to the biosensor response is ≤5 %, implying negligible significant interference. This high sensitivity towards pyrocatechol and less significant interference from other interfering agents may be due to osmium polymer and Nf present in the matrix. The positively charged osmium polymer likely to prevent the positively charged interfering compounds whereas negatively charged Nf known to prevent negatively charged soluble compounds (Saxena et al., 2011b) to penetrate this polymer based enzyme nano-composite matrix. This study implies that the biosensor could be used for pyrocatechol determination without any significant interference from the substances present in the environmental test sample.

### 4.4. Conclusions

A laccase based biosensor for detection of pyrocatechol has been successfully developed by immobilizing the enzyme in a nanocomposite matrix on the electrode surface. The matrix also provides an electroactive surface for facile electron transfer kinetics between the electrode and the redox centre of the laccase that generates the voltametric response of the bioelectrode. The response of the constructed biosensor emanated from the cascade of two reactions, the biocatalyzed oxidation of pyrocatechol and the subsequent electrocatalyzed reduction of the oxidized product 1,2-benzoquinone on the electrode surface. The response characteristics of the constructed biosensors such as, sensitivity, operational stability, minimum detection limit and selectivity are comparable and even superior to many laccase based biosensors reported so far. The linear range of the biosensor for substrate concentration may be further expanded by optimizing the enzyme loading on the nanocomposite matrix based electrode surface. The results validate the potential application of this stable laccase based biosensor for sensitive, quantitative, and selective detection of pyrocatechol in aqueous samples.

## Figures

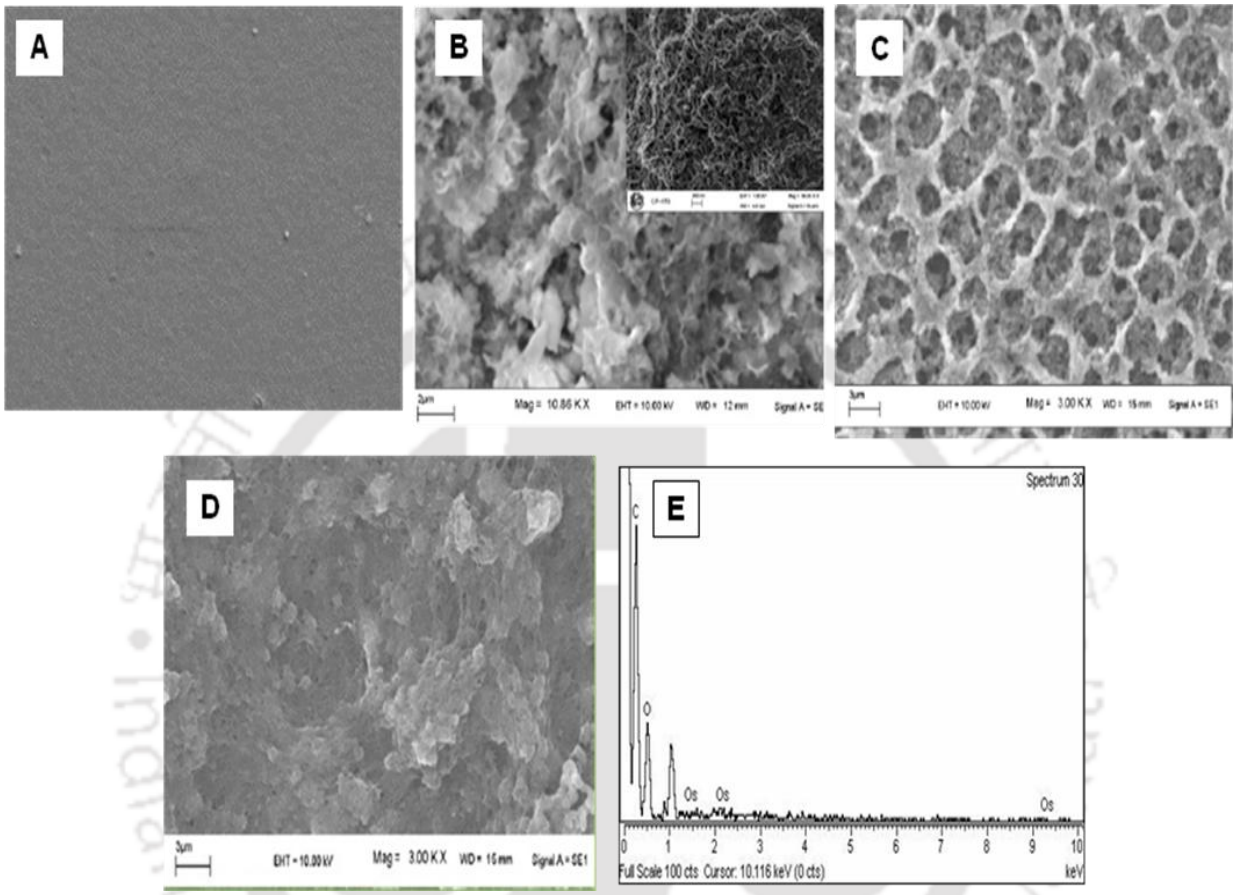


**Figures 4.1.** SEM images of (A) GCE, (B) GCE/MWCNT–CB–Nf, (C) GCE/MWCNT–CB–Nf–$OsO_4$P4VP and (D) GCE/MWCNT–CB–Nf–$OsO_4$P4VP–laccase, (E) EDX of GCE/MWCNT–CB–Nf–$OsO_4$P4VP–laccase.

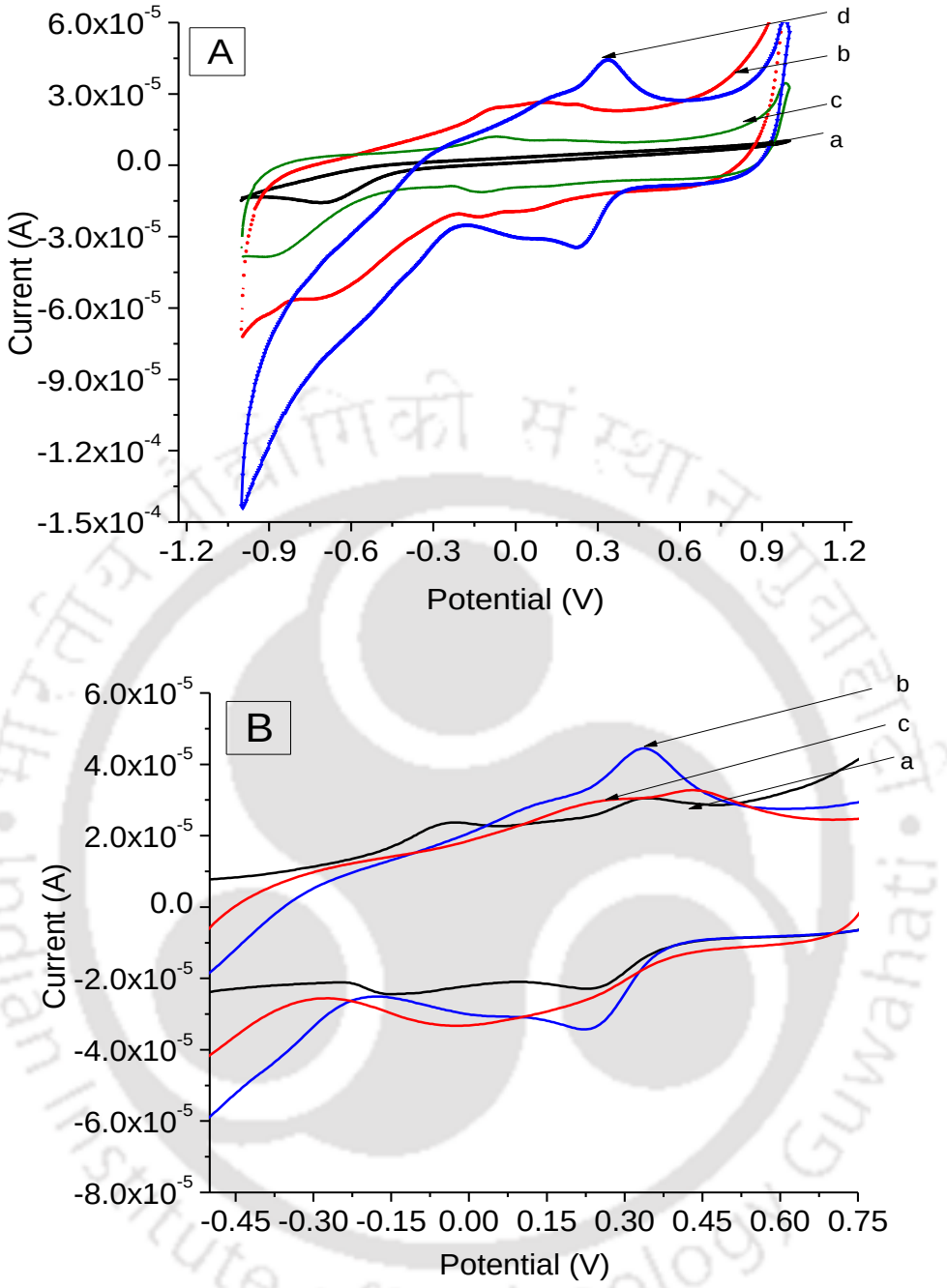


**Figure 4.2.** (A) CV of (a) GCE, (b) GCE/MWCNT–CB–Nf, (c) GCE/MWCNT–CB–Nf–$OsO_4$P4VP, (d) GCE/MWCNT–CB–Nf–$OsO_4$P4VP–laccase, in oxygen gas purged solution of 0.1 M sodium citrate buffer (pH 4.7) at a scan rate of 50 mV/s. (B) CV of GCE/MWCNT–CB–Nf–$OsO_4$P4VP–laccase electrode with (a) argon, (b) oxygen and (c) pyrocatechol in 0.1 M sodium citrate buffer.

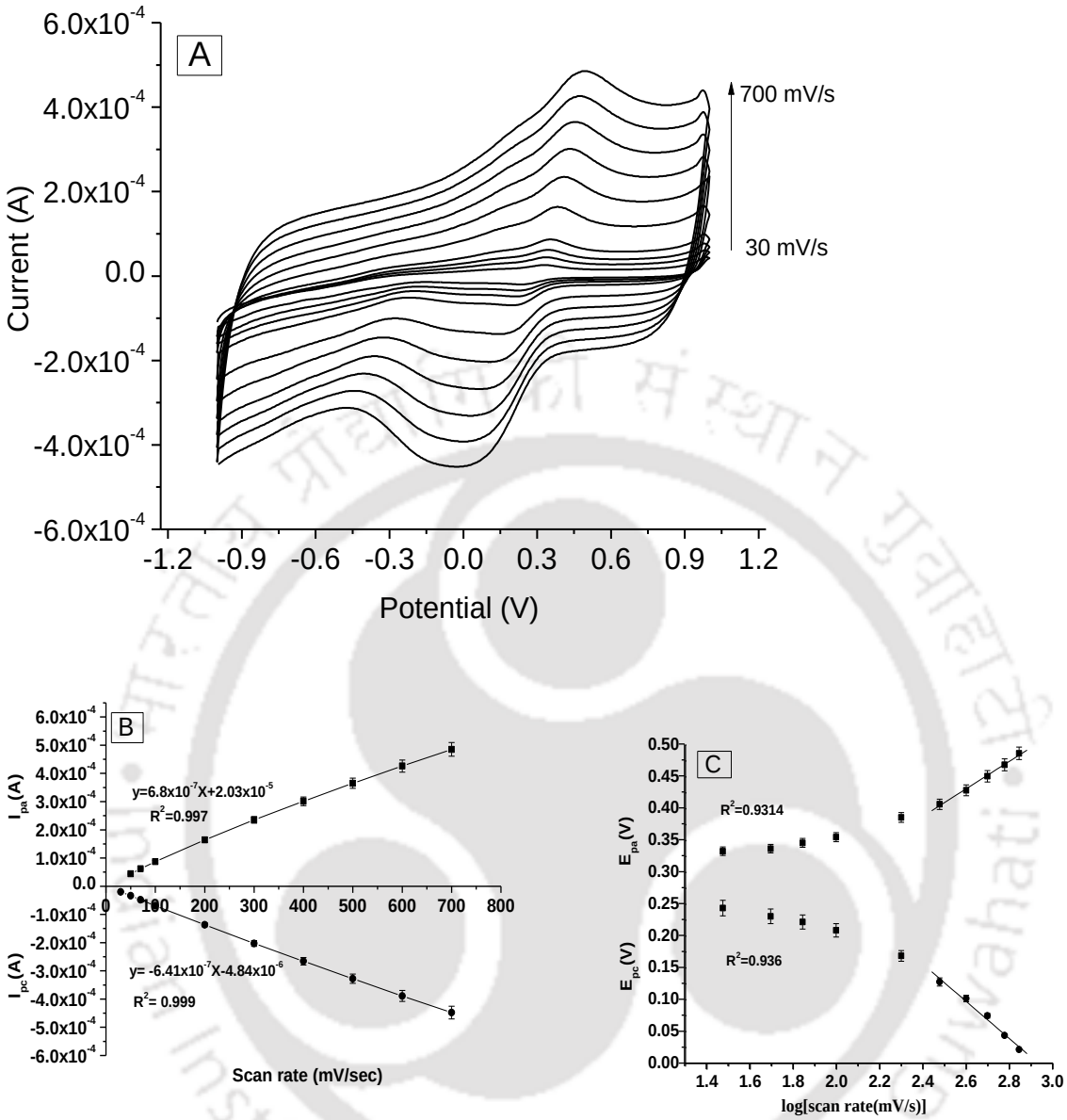


**Figure. 4.3**. (A) CV of laccase electrode with increasing scan rates viz. 30, 50, 70, 100, 200, 300, 400, 500, 600, 700 mV/s in 0.1 M sodium citrate buffer (pH 4.7) purged with $O_2$. (B) Plot of anodic ($I_{pa}$) and cathodic ($I_{pc}$) peak currents vs. scan rate. (C) Plot of anodic ($E_{pa}$) and cathodic ($E_{pc}$) peak potentials vs. log(scan rate).

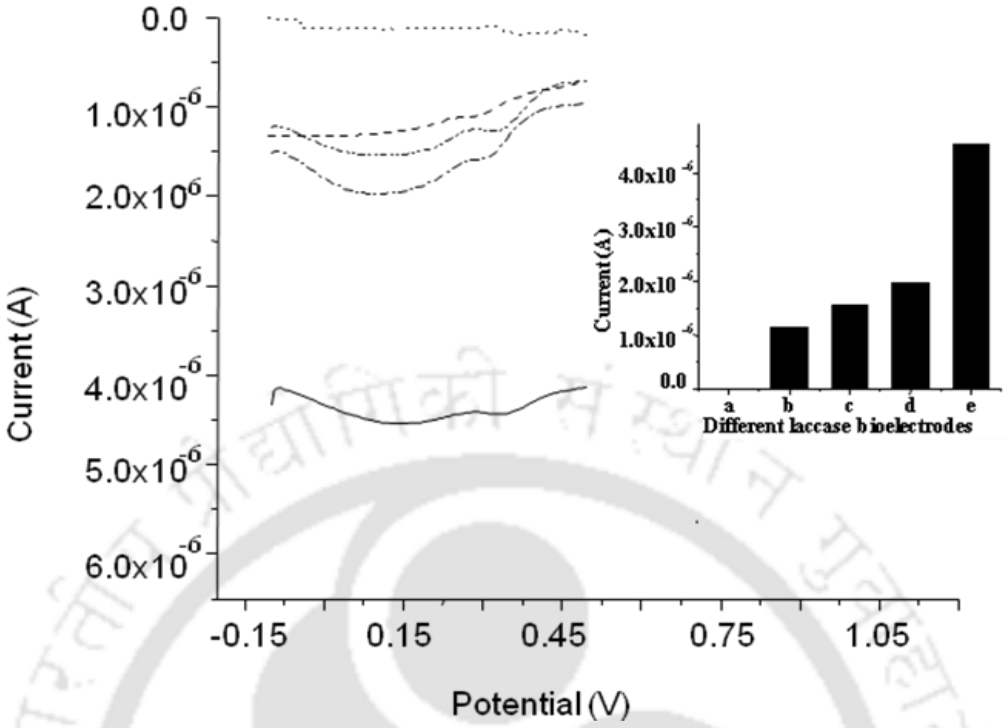


**Figure. 4.4**. DPV of (a) GCE (····), (b) GCE–laccase (- - -), (c) GCE/MWCNT–CB–laccase (–··–··–), (d) GCE/$OsO_4$P4VP–laccase (–·–·–) and (e) GCE/MWCNT–CB–Nf–$OsO_4$P4VP–laccase (—) in 16 nM pyrocatechol in 0.1 M sodium citrate buffer solution (pH 4.7). Inset: cathodic peak current values for bare GCE and different laccase bioelectrodes (b-c) as mentioned above.

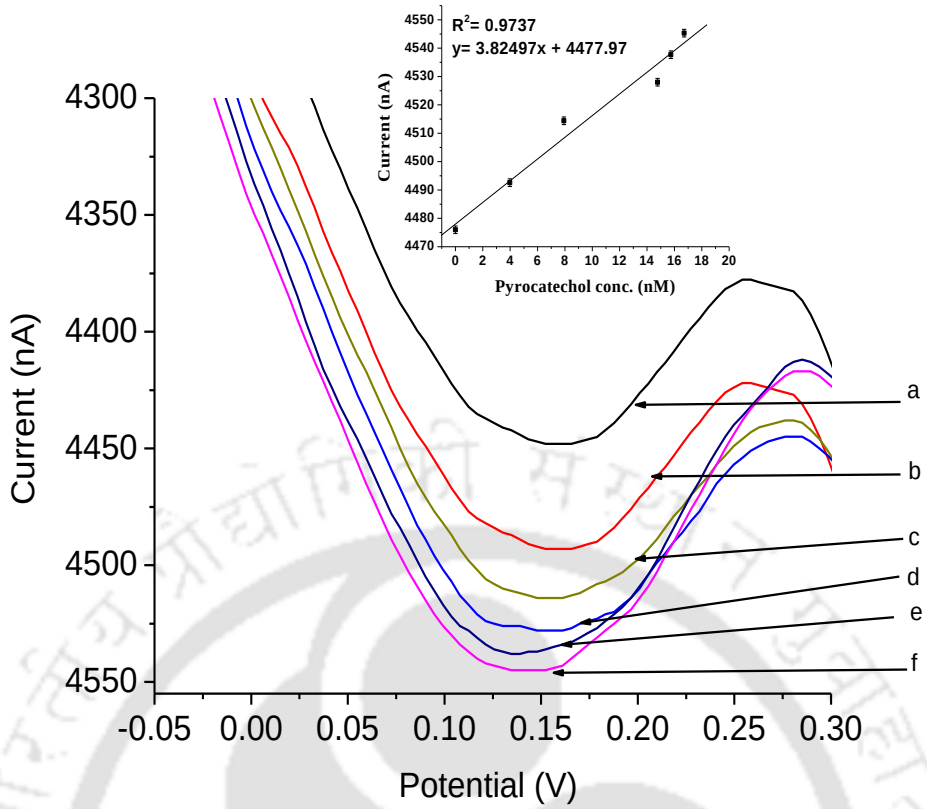


**Figure 4.5.** DPV of laccase biosensor with increasing substrate concentration (nM): (a) 0, (b) 3.98, (c) 7.93, (d) 14.77, (e) 15.74, (f) 16.71. Inset: response curve obtained for laccase biosensor for different concentrations of pyrocatechol in 0.1 M sodium citrate buffer (pH 4.7).

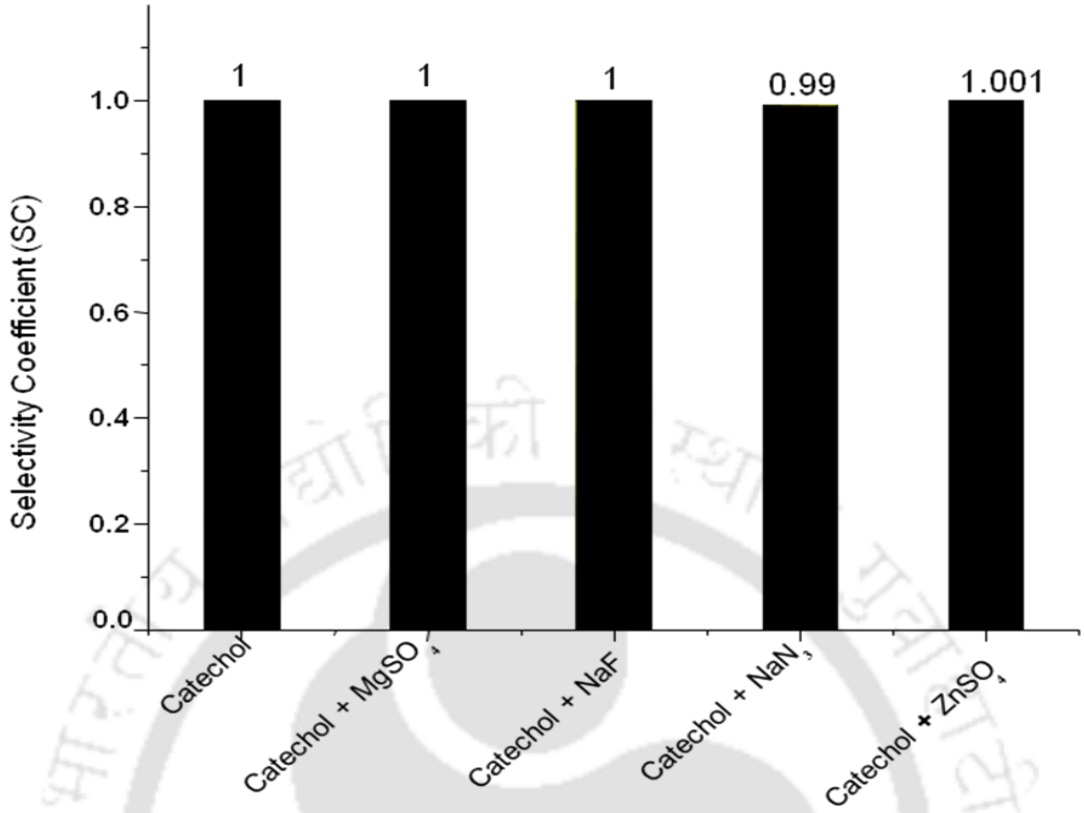


**Figure 4.6.** Effect of potential interferents on the response of laccase based catechol biosensor.

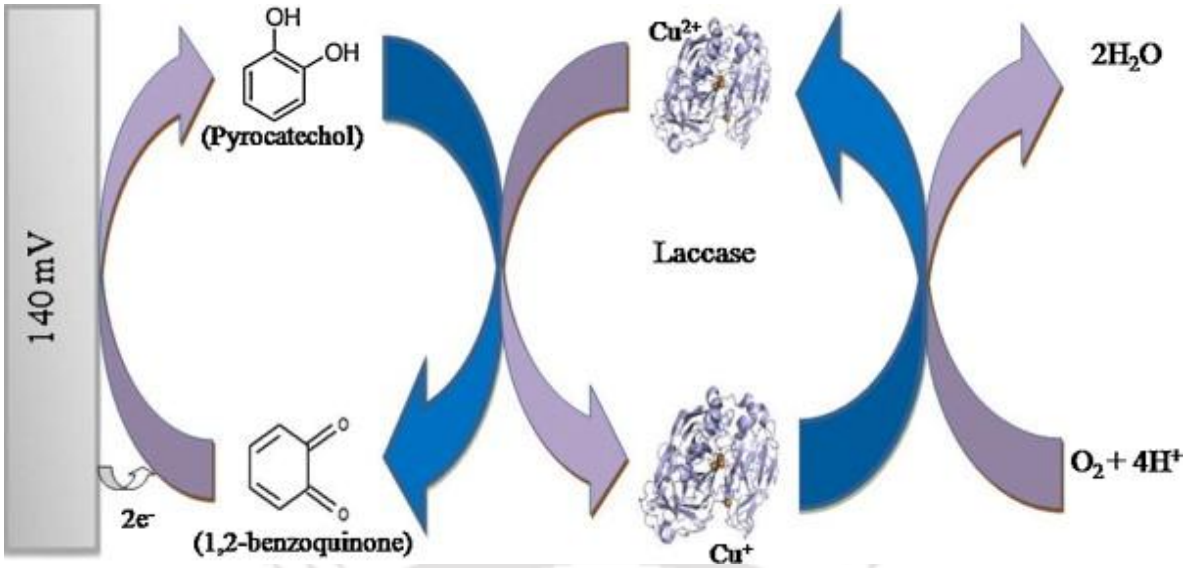


**Scheme 4.2.** Schematic representation of laccase catalyzed oxidation of pyrocatechol with its subsequent electrochemical reduction on the biosensor platform.

## Tables

**Table 4.1.** Electron transfer kinetics and response characteristics of GCE/MWCNT–CB–Nf–MWCNT–$OsO_4$P4VP–laccase bioelectrode

| Parameters | Characteristic data |
|---|---|
| Surface concentration of the ionic species ($\Gamma$) | $1.32 \times 10^{-8}$ mol $cm^{-2}$ |
| Charge transfer coefficient ($\alpha$) | 0.52 |
| No. of electrons transferred ($n$) | 1 |
| Heterogenous electron transfer rate constant ($K_s$) | 0.67 $s^{-1}$ |
| Linear range | 3.98 nM–16.71 nM |
| Detection limit (DL) | 2.82 nM |
| Sensitivity | 3.82 ± 0.31 nA $nM^{-1}$ |
| Standard deviation limit | 3.59 ± $2.57 \times 10^{-4}$ nA |

# Chapter 5

## Development and characterization of alcohol oxidase and laccase based bioelectrodes for biofuel cell application

# Chapter 5

# Development and characterization of alcohol oxidase and laccase based bioelectrodes for biofuel cell application.

## 5.1. Overview

Enzymatic biofuel cell (EFC) is a potential power source for powering micro-scale electronic devices in the field of telecommunications, space, biomedical and environmental research (Cracknell et al., 2008, Minteer et al., 2007). The selection of enzymes for the bioelectrode fabrication is based on the choice of substrate being used to generate the power. Emphasis is usually given on cheap, renewable substrates which do not inhibit the enzymatic function and cause interference in the electrochemical reaction to realize maximum achievable power from the EFCs. From this perspective, alcohol substrates, primarily methanol and ethanol have received increasing attention for developing chemical and biological fuel cells. The other advantages of the alcohols as fuel substrates are their aqueous solubility and wide availability, as these compounds can be readily produced by fermentative or chemical means from cheap renewable substrates. The enzyme commonly used in EFCs for oxidation of the fuel alcohol is $NAD^+$ dependent ADH (Addo et al., 2011) due to its advantages such as low redox potential (Rincon et al., 2011) that support the anode to function at low potential for generating high cell voltage. The challenges commonly encountered in employing ADH for developing operationally stable EFC are the leaching susceptibility of the cofactor $NAD^+$ from the electrode surface (Vijayakumar et al., 1996), and electrode fouling caused by the polymerization of oxidized products on the electrode surface (Cardosi and Liu, 2012) that eventually increase the overvoltage for oxidation of

NADH (Bartlett et al., 2002; Lee and Tsai, 2009). Hence, redox enzymes with strongly bound cofactor in the reactive center may be an alternative choice for developing operationally stable EFC. In this regard, the enzyme alcohol oxidase (AOx) may be projected as potential anodic biocatalyst for EFC applications since the strongly bound flavin cofactor in the redox center of these enzymes obviates the need of supplementing cofactor during the catalytic reactions (Goswami et al., 2013). The exchange of electrons between electrochemically active redox enzymes and electrode is known to take place through either of the two mechanisms: mediated electron transfer (MET) or direct electron transfer (DET). The MET involves by some externally supplied electron transfer mediator (ETM). However, there are some drawbacks of using exogenous mediators (e.g. neutral red or methylene blue), such as their toxicity, cost and short life time (Seop et al., 2006). Conversely, in case of DET mechanism the electrons are transferred directly between the active site of the enzyme and the electrode (Barton et al., 2004). Also DET based electrocatalytic system can reduce the activation overpotential due to facile electron transfer kinetics on the electrode surface. Although the trend for developing DET principle based bioelectrodes is quite high in biosensor application, the same is yet to gain momentum in EFC research (Wu et al., 2009). The major hurdle for developing DET principle based enzyme bioelectrode is however, the deeply buried redox center in the protein. Among the different techniques which have been evolved for establishing DET between the enzyme and electrode, nano-fabrication of electrode surface with highly conductive nanomaterials is emerging as a tool of choice (Sarma et al., 2009). The nano-fabrication provides high enzyme loading on the electrode surface due to high surface to volume ratio of the nanomaterials. In this direction MWCNT has offered a great promise as witnessed from the amperometric enzyme electrodes successfully developed in the field of biosensors research since last decade (Sarma et al., 2009; Gooding, 2005).

We report here an EFC fabricated by using AOx bioanode and laccase biocathode using methanol and air breathed oxygen as the fuel substrates for the respective bioelectrodes. The use of oxygenase enzymes such as laccase as $O_2$ reducing catalysts is advantageous over the chemical catalyst platinum (Pt) as the later is expensive and requires high overpotential for the reduction (Schaetzle et al., 2009). A detailed account on the performance of the EFC fabricated by assembling these two bioelectrodes in a fuel cell membrane electrode assembly (MEA) using methanol as fuel substrate has been described in this chapter.

## 5.2. Experimental approaches

### *5.2.1. Materials and methods*

AOx from *Pichia pastoris* (21 $Umg^{-1}$ protein), laccase from *T. versicolor* (0.66 $Umg^{-1}$ protein dry powder), MWCNT, (size OD 10–15 nm, ID 2–6 nm, length 0.1–10 µm), Nf (5 % w/v in isopropanol), PEI (50 % w/v in water solution), $OsO_4$P4VP, Nafion 117 membrane were procured from Sigma-Aldrich. Methanol (99.9 %), formaldehyde (35 %) and ethyl benzene (99.9 %) were purchased from Merck (India). Toray carbon paper (TCP) (conductivity 0.05 S $m^{-1}$) and carbon powder (CP) were purchased from Electrochem. Inc USA. All other chemicals were of analytical grade and used as received without purification. AOx (1 mg $ml^{-1}$) was freshly prepared in potassium phosphate buffer solution (KPBS) (50 mM, pH 7.5). Laccase solution (10 mg $ml^{-1}$) was prepared in 0.1 M sodium citrate buffer of pH 4.8.

### *5.2.2. Fabrication of bioelectrode for fuel cell study*

A TCP of 9 $cm^2$ working area was used as a support material for bioelectrodes fabrication. A total of 1 mg CP was dispersed in 1000 µl of 5 % Nf and sonicated for 45 min

and in another container 10 mg MWCNT was dispersed in 1000 µl of 5 % Nf and sonicated for 30 min to obtain stable homogeneous suspensions. Both the suspensions, i.e. CP-Nf and MWCNT-Nf were then mixed by sonicating for 1 h to obtain a homogeneous suspension of CP-MWCNT-Nf. A total volume of 1000 µl of CP-MWCNT-Nf was dropped onto the TCP and allowed to dry at room temperature. The hydrophilic microporous layer so obtained on TCP was then further enriched with MWCNT by dropping 10 mg of MWCNT from the initially homogenized suspension of MWCNT-Nf. For bioanode fabrication AOx from the stock solution was layered over the electrode surface to a final concentration of 0.11 mg protein $cm^{-2}$ (2.33 $Ucm^{-2}$) by dropping over the above mentioned microporous nanocomposite layer and then dried in a refrigerator at 4 °C. On the top of the AOx layer, 800 µl of 10 % (v/v) PEI solution was dropped and then allowed to dry under refrigeration at 4 °C. The bioanode was then stored at 4 °C in an airtight container until its use. GCE (diameter, 1 mm) was used instead of TCP as supporting electrode material for CV studies of the bioelectrode fabricated by following the above mentioned steps and material compositions. The GCE was first cleaned by polishing with alumina slurry, then washed ultrasonically with 70 % ethanol and water separately for 5 min each and finally allowed to dry under clean air at room temperature for fabrication of the bioelectrode. For biocathode fabrication, $OsO_4$P4VP-MWCNT-Nf mixture is prepared by the similar method as described in the chapter 4, section 4.2.3. A total volume of 800 µl of $OsO_4$P4VP-MWCNT-Nf was dropped on the hydrophilic microporous layer on TCP and incubated at 140 °C overnight. Once the layer dried and attained room temperature, 1 ml of laccase stock solution was dropped onto the $OsO_4$P4VP-MWCNT-Nf layer to a final laccase concentration of 10 mg protein per 9 $cm^2$ (0.66 U $cm^{-2}$). The biocathode so formed was then air dried and stored at 4 °C.

*5.2.3. Apparatus and measurements*

The fuel cell membrane electrode assembly (MEA) set up from Electrochem Inc. (USA) was used for biofuel cell study. The MEA was fabricated by placing the anode and cathode bioelectrodes on either side of the nafion membrane followed by tightening the fuel cell plates. Methanol (1 M) in KPBS (0.1 M, pH 7.5) was introduced into the anodic chamber with a peristaltic pump (Miclins, India) at a flow rate of 0.2 ml $min^{-1}$ and air or oxygen was purged into the cathodic chamber at a flow rate of 0.7 L $min^{-1}$. A rheostat (Stead electronics Trade, India) was used to apply load between 0 and 60 Ω. Voltage and current were measured with a digital multimeter (Mastech Inc., Hongkong). CV and EIS were performed with an Autolab PGSTAT 1212 (Eco Chemie, Netherlands). EIS measurements were performed in a background solution of 5 mM $K_3Fe(CN)_6/K_4Fe(CN)_6$ (1:1) and 0.1 M KCl in KPBS within the frequency range of 0.05 Hz to 10 kHz. The amplitude of the alternate voltage was 5 mV. All experiments were performed at room temperrature. The images of the morphological characteristics of the bioelectrodes were obtained on a SEM (Leo 1430 vp, Germany) using conditions of 15 KeV EHT, 50 mm aperture.

*5.2.4. Analyses of substrate consumption in EFC*

The substrate consumptions in the anodic half-cell of the EFC were studied by gas chromatographic (GC) analysis (Varian CP 3800). The GC was equipped with a TRMS Wax column (Thermo Scientific, USA) and flame ionization detector. The operating parameters for the GC were carrier gas, $N_2$ at flow rate, 1.5 ml $min^{-1}$; injection port and detector port temperatures, 220 °C and 250 °C, respectively; oven temperature, 250 °C. The sample volume used for injection in the column was 1 µl. The concentrations of the substrate were

estimated by computing the peak area of the injected samples with the corresponding authentic samples of known concentrations in the chromatograms.

## 5.3. Results and Discussion

### *5.3.1. Characterization of bioelectrodes*

SEM was used to capture the images of the critical layers prepared for the fabrication of the bioelectrodes. Fig. 5.1(A–D) and (E and F) shows the SEM images of the layer wise fabrication of the AOx anode and laccase cathode, respectively. The highly porous carbon fibers are distinctly visible in the SEM image of the TCP (Fig. 5.1 A). Fig. 5.1(B) shows the image of the hydrophilic microporous layer of CP-MWCNT-Nf. A thread like structure of the adsorbed MWCNTs is visible from the image (inset Fig. 5.1(B)). The porous nanocomposite structure was considerably filled with the AOx enzyme as revealed from the image of the Fig. 5.1(C). The electrode after application of PEI on the AOx layer further reduced the porosity of the nanocomposite layer (Fig.5.1D). Fig. 5.1(E) shows the image of the electrode after application of $OsO_4$P4VP containing MWCNT-Nf to the hydrophilic nanocomposite layer corresponding to Fig. 5.1(B). The $OsO_4$P4VP layer appears as globular mass distributed well over the hydrophilic layer. Fig. 5.1(F) shows the SEM image after application of the laccase layer, which completely envelope the $OsO_4$P4VP layer in Fig. 5.1(E).

CV was carried out to investigate redox behavior of the fabricated AOx bioelectrode (Fig. 5.2A) in KPBS (pH 7.5) at a scan rate of 50 mV $s^{-1}$. The bioelectrode GCE-CP-MWCNT-Nf-AOx-PEI displayed a pair of clear redox peaks with a formal potential [(Epa+Epc)/2] at 0.1±0.002 V, which is attributed to the redox potential of FAD/$FADH_2$ system. Flavins in protein exhibit wide range of redox potentials since the potential is strongly influenced by the cofactor environment (Fraaije et al., 2003; Munteanu et al., 2008).

MWCNT and CP are electro-inactive in this potential window. The chronoamperometric response (Fig. 5.2B) of the AOx bioelectrode at the anodic potential of 0.35 V was studied to discern the Michaelis–Menten constant ($K_m$) (Fig. 5.2C). The magnitude of the anodic peak current was increased linearly with increasing methanol concentration with a high correlation coefficient $R^2$. From the double reciprocal plot (inset Fig. 5.2(C)) $K_m$ was calculated and found to be 0.126 mM.

EIS was employed to investigate the electrode surface charge behavior during the stepwise assembly of the bioelectrode. The spectra (Fig. 5.2D) are presented in the form of Nyquist plots (where Z′ is the real and Z′′ is the imaginary part of impedance) using FRA software of Autolab systems and are overlaid to pinpoint the differences in electron-transfer resistance ($R_{ct}$) with subsequent modification layers. The value of $R_{ct}$ at the electrode surface can be estimated directly from the diameters of the high frequency semicircle. The spectra of the bare GCE (curve a) consist of a small semicircle ($R_{ct}$: 2450 Ω) with an almost straight tail line. When MWCNT-Nf (curve b) layered on the electrode surface, the $R_{ct}$ was slightly decreased to ~2400 Ω which implies the decreased interfacial resistance due to the assembly of highly conducting MWCNT layer. Addition of AOx (curve c) significantly increased the $R_{ct}$ value (3318 Ω) due to obvious reason of high charge transfer resistant properties of proteins in general. When PEI introduced in the GCE-MWCNT-Nf-AOx (curve d) layer, the $R_{ct}$ was reduced by 261 Ω, which infers that the PEI, which is a polycation, facilitate the diffusion of negative charge on the electrode.

*5.3.2. Fuel cell study*

The AOx bioanode, laccase biocathode and the nafion membrane were assembled in a fuel cell MEA as described in Section 5.2.3. The schematic of the EFC configuration is shown in Scheme 5.3. The open circuit potentials (OCPs) of the EFC were recorded at increasing concentrations of methanol in the anodic chamber. The OCP increased with increasing concentration starting from 0.25 M methanol and the potential was reached to a maximum value of 0.61 V (±0.02) at ~1 M methanol (Fig 5.4(A)), thus showing the Nernstian relation between substrate concentration and generation of potential. 1 M methanol concentration was thus considered for all the electrochemical characterization of the EFC.

The effect of pH change in the anodic half-cell of the EFC on the OCP was studied within pH 6–8. The maximum OCP of 0.61 V (±0.02) was achieved at pH of 7.5 (Fig. 5.4(B)), which conforms to the optimum pH for biocatalytic activity of the AOx.

The short circuit current ($I_{SC}$) of the EFC was found to be 0.329 A. The $I_{SC}$ was calculated by using the Thevenin and Nortan equation (Judd and Chirlian, 1970), $I_{sc}$=OCP/$R_{tn}$, where $R_{tn}$ is the resistance at maximum power density. Fig.5 5(A) shows the power density curve of the EFC operated with 1 M methanol at room temperature. Fig.5.5(B) shows the effect of external load on the power density of the EFC. Power density rose upon increasing the external load resistance and reached maximum value of 46 (±0.002) µW $cm^{-2}$ at 1.85 Ω. With further increase in load resistance, the cell current dropped and reached almost zero at a resistance of 60 Ω. The maximum current density and power density generated in the EFC were 290 µA $cm^{-2}$ (±0.004) and 46 (±0.002) µW $cm^{-2}$, respectively. The coulombic efficiency of the fuel cell was determined by integration of the area under the current–time curve (Liu et al., 2005) and found to be ~59.52 %.

*5.3.3. Operational and storage stability of the EFC*

The operational stability of the EFC was investigated in a 1 M substrate concentration maintained by charging with fresh substrate following each 1 h runtime at a fixed load of 1.85 Ω (Fig. 5.6A). The OCP was steady upto 4th hours of run time followed by gradual decline in OCP as shown in Fig. 5.6A. The stability was further studied with a similar set up and conditions using 1 M methanol as fuel substrate except intermittent recharging with the substrate and found no significant change in operation stability of the EFC. The operational half life ($t_{1/2}$) was found to be 17.22 h. The results imply that the AOx bioelectrode has good tolerance to the methanol being used as substrate for the study.

The storage stability of the assembled bioelectrodes kept at 4 °C was examined by recording OCP of the EFC in room temperature at a regular interval of 7 days. The initial OCP and power density were 0.61 V and 46 μW $cm^{-2}$, respectively. After a period of 3 months, the OCP and power density detected were 0.081 V (±0.03) and 0.8 (±0.002) μW $cm^{-2}$, respectively (Fig. 5.6B), which are 86.72 % and 98.26 % lower than the corresponding initial values. The $t_{1/2}$ of the fuel cell was found to be 52 days.

The application of AOx co-immobilized with microperoxidase as biocatalyst for cathodic reaction in EFC has been reported (Ramanavicius et al., 2008). In that study the $H_2O_2$ formed as a result of the AOx catalyzed aerobic oxidation of alcohol substrate was degraded by the microperoxidase for its associated electrocatalyzed reduction to water. The AOx reported here acts as bioelectrocatalyst in the bioanode where direct electron transfer is involved as the governing principle to generate the OCP. In a comparative scale the OCP or power density generated in the present EFC is though stands in various levels as compared to other prominent alcohol substrate based pure EFC (Deng et al., 2010; Duma and Minteer, 2007, Topcagic and Minteer, 2006; Ramanavicius et al., 2008; Yan et al., 2009; Rincon et al.,

2011; Zhang et al., 2012), the operational stability of this AOx based EFC is significantly higher than ADH-Laccase (Deng et al., 2010) and ADH-bilirubin oxidase (Zhang et al., 2012) based EFC reported during recent past. Conversely, the operational stability of the present methanol substrate based EFC is marginally lower than the ethanol substrate based QH-ADH (anode)-AOx-MP-8(cathode) EFC ($t_{1/2}$ 26 h) reported by Ramanavicius et al., (2008), while the power density of the latter (1.5 μW/cm$^2$) was significantly lower than the one observed in the present EFC. The overall current density of 290 μAcm$^{-2}$ obtained from the EFC is significant. The voltage current relationship observed in this biofuel cell is linear and thus deviated from the ideal rectangular behavior of a chemical fuel cell. This deviation is expressed as the fill factor (*f*) of 0.226 of the biofuel cell calculated by using the following equation (Katz et al., 2003).

$$f = P_{cell} \times I^{-1}_{sc} \times V^{-1}_{oc}$$

where, $f$ = fill factor, $I_{sc}$= short circuit current, and $V_{oc}$= open circuit voltage.

From the slope of the polarization curve, the internal resistance and the activation overpotential have been calculated to be 0.024 μΩ and 0.032 μΩ, respectively (Logan et al., 2006). These low over potentials substantiate the facile conductance of the counter ion through the electrolytes across the membrane from anode to cathode and smooth electron exchange on the electrode surface. The electrode support material TCP used in this investigation though has lower conductivity (0.05 S m$^{-1}$) as compared to gold ($4\times10^7$ S m$^{-1}$), platinum ($9.43\times10^6$ S m$^{-1}$) (Matijasevic and Brandt, 2009), glassy carbon (1.25 to $2\times10^3$ S m$^{-1}$) (Serway, 1998) and graphite (2 to $3\times10^5$ S m$^{-1}$) (Pierson, 1993) electrode materials commonly being used in EFC study, a highly electroactive surface on the TCP for smooth electron exchange could be developed by dispersing MWCNTs in CP medium on its

surface in which CP supports as hydrophilic binder to absorb the enzyme proteins on the hydrophobic electrode surface. The three dimensional nanocomposite matrix, which is evident from Fig. 5.1(B), amplified the surface area for enhanced adsorption of the enzyme. The immobilized AOx (p*I*: 4.3) on the nano-composite matrix was electrostatically stabilized by applying positively charged PEI on top of the enzyme layer under the physiological pH of the electrolyte buffer used in this investigation. The Os polymer (OsP4VP) widely reported for electrical wiring of laccase enzyme (Barton et al., 2001) used for the biocathode fabrication was found to be functionally redundant in AOx bioanode fabrication. The reason is attributed to the lack of interaction of the redox metal moiety of the polymer with the FAD-redox center of AOx located inside the insulating protein matrix. In case of laccase, one of the Cu-redox center is located in the periphery of the laccase enzyme that promote easy contact between the metal redox moiety of the polymer and the Cu-redox center of the enzyme for the exchange of electrons with the electrode (Yu and Scott, 2010).

The coulombic efficiency observed here however, indicates the scope for improvement of the efficiency of the EFC. From the GC analysis the methanol consumption detected was ~0.10 M $min^{-1}$. However, a fraction of the total amount of methanol consumed was aerobically oxidized in the anodic half-cell as evident from the oxidation peak current at around 0.65 V (Fig. 5.2(A)) which is ascribed to the electrocatalytic oxidation of $H_2O_2$ formed as a result of the biocatalytic oxidation of the substrate alcohol by AOx. Additionally, methanol cross over through nafion membrane is also a critical issue in the developing methanol fuel based fuel cells (Neburchilov et al., 2007). Hence, further research may be encouraged to optimize the loading of bioelectrocatalytically active AOx on the anodic surface by improving the effective contact between the nanomaterials and enzyme and thereby shun the natural electron acceptor (oxygen) and thus prevent the wastage of the

substrate electrons from producing $H_2O_2$. A parallel research on the improvement of the half-cells partitioning membrane to reduce the methanol crossover is also urged.

The effect of gas purging on OCP of the fuel cell was investigated. It was observed that both oxygen (99 %) and air (21 % oxygen) gave similar OCP value of 0.61 V under optimum substrate concentrations (1 M methanol). The result indicates that the concentration of $O_2$ in air, which is nearly $1/5^{th}$ of pure oxygen, does not limit the laccase turnover rate and hence maintained the substrate saturation on the biocathode. The OCP was drastically decreased from 0.61 V to 0.289 (±0.03) V after purging argon gas in the cathodic chamber. The reduction of OCP validates the oxygen reductive function of the laccase biocathode. The cause of residual OCP is attributed to the oxygen diffusion to the laccase biocathode across the nafion membrane from the anodic chamber (Zhang et al., 2003).

**5.4 Conclusion**

The potential of AOx as anodic catalyst for generating power from methanol substrate has been demonstrated for the first time. Moreover, the mediator less diffusion free electron transfer on this porous biocompatible nanocomposite based protein thin film electrodes utilized in this investigation has generated the cell potential and operational stability comparable or even superior to many alcohol fuel based pure enzymatic biofuel cell. Overall findings have demonstrated the feasibility of developing EFC using AOx based bioanode and laccase based air-breathed biocathode without applying any toxic free mediator and metal electrode supports for generating power.

## Figures

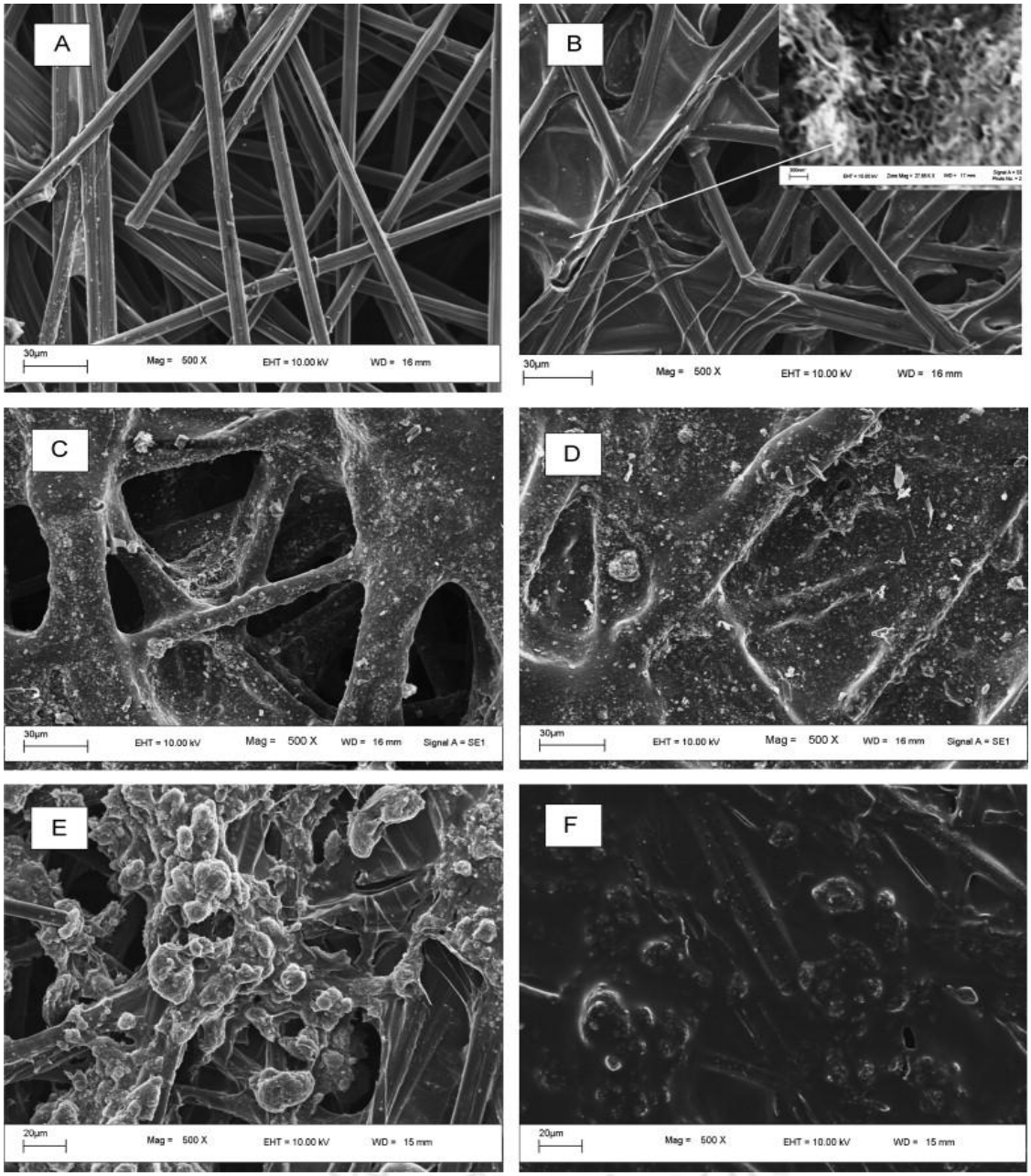


**Figure 5.1**. SEM images of the bioelectrodes at different fabrication stages: (A) bare TCP, (B) TCP/CP-MWCNT-Nf, inset with resolution 27 KX, (C) TCP/CP-MWCNT-Nf-AOx, (D) TCP/CP-MWCNT-Nf-AOx-PEI, (E) TCP/CP-MWCNT-Nf-$OsO_4$P4VP (F) TCP/CP-MWCNT-Nf-$OsO_4$P4VP-Laccase.

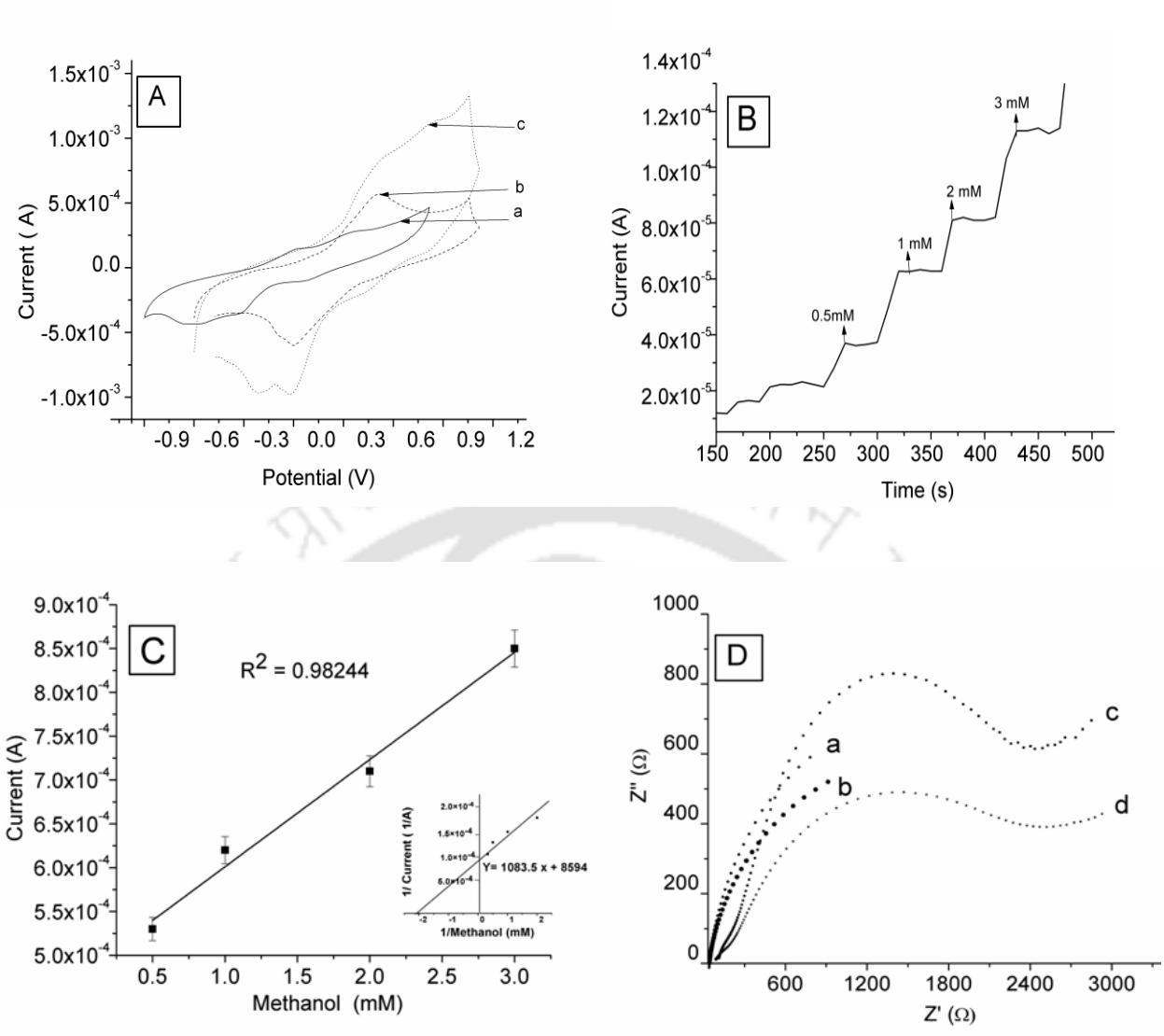


**Figure 5.2.**(A) CV of (a) GCE-Nf (-), (b) GCE-CP-MWCNT-Nf-AOx-PEI (----), (c) GCE-CP-MWCNT-Nf-AOx-PEI with 3 mM methanol (….. ), 0.1 M KPBS, pH 7.5. (B) Chronoamperometric current responses of the against successive addition of methanol in 0.1 M KPBS, pH 7.5. (C) The response curve of the bioelectrode with increasing methanol concentration. Inset figure showing the double reciprocal plot for determination of Michaelis–Menten constant ($K_m$). (D) Electrochemical impedance plots of (a) bare GCE, (b) GCE-CP-MWCNT-Nf, (c) GCE-CP-MWCNT-Nf-AOx and (d) GCE-MWCNT-Nf-AOx-PEI in the presence of 5 mM $K_3Fe(CN)_6/K_4Fe(CN)_6$ (1:1) and 0.1 M KCl in KPBS within the frequency range from 0.05 Hz to 10 kHz.

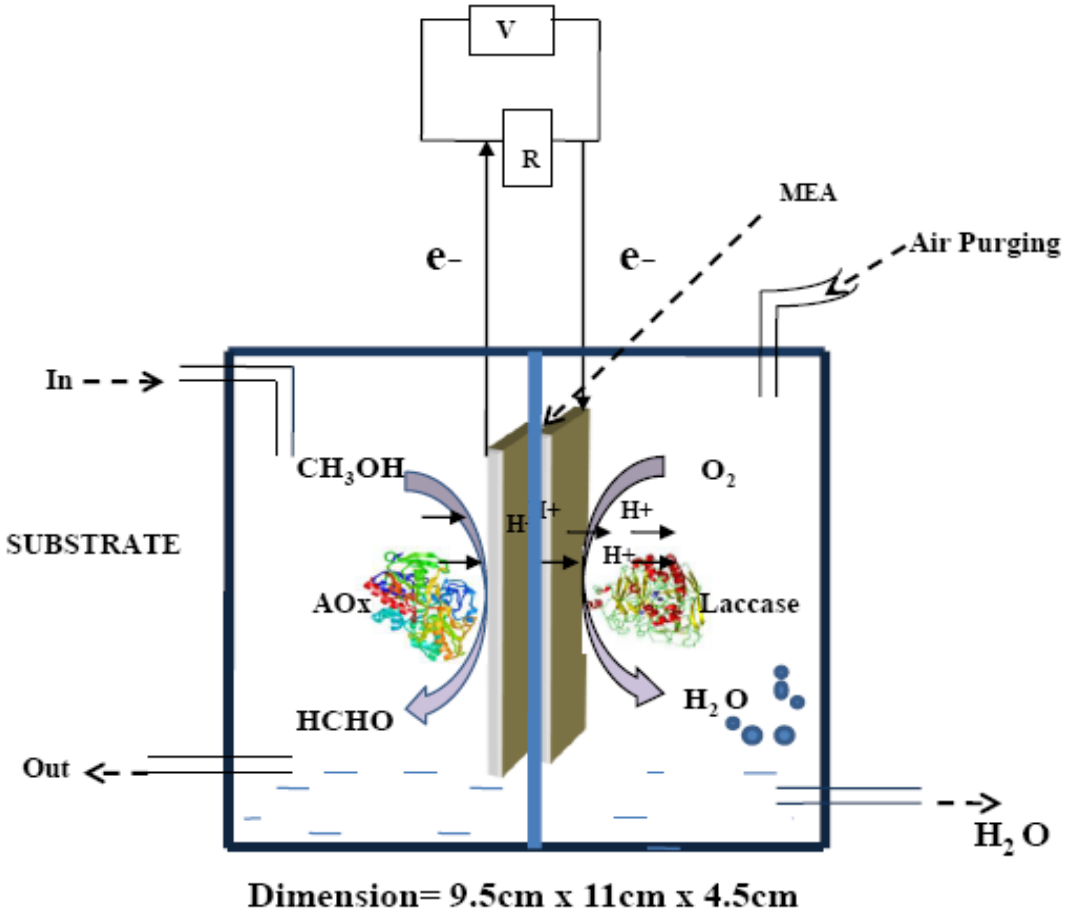


**Scheme 5.3.** Schematic diagram on the operation of AOx and laccase based EFC using methanol as fuel substrate.

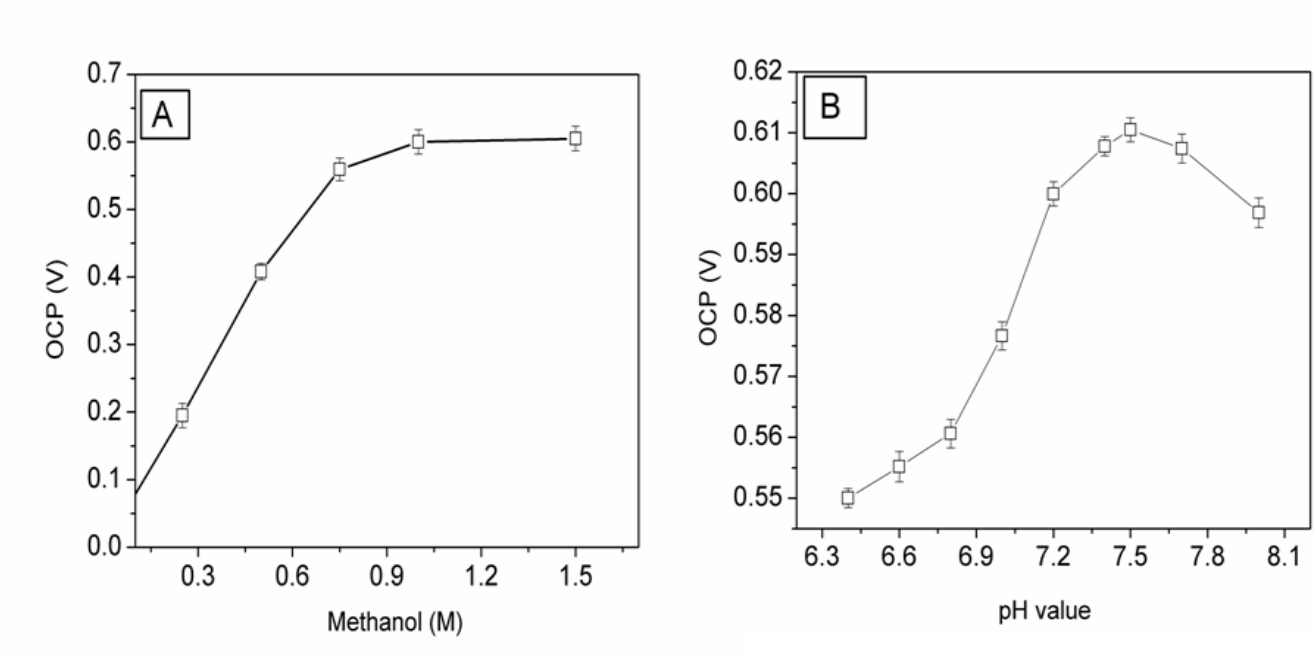


**Figure 5.4**. The effect of methanol concentrations (A) and pH (B) on the OCP of the EFC.

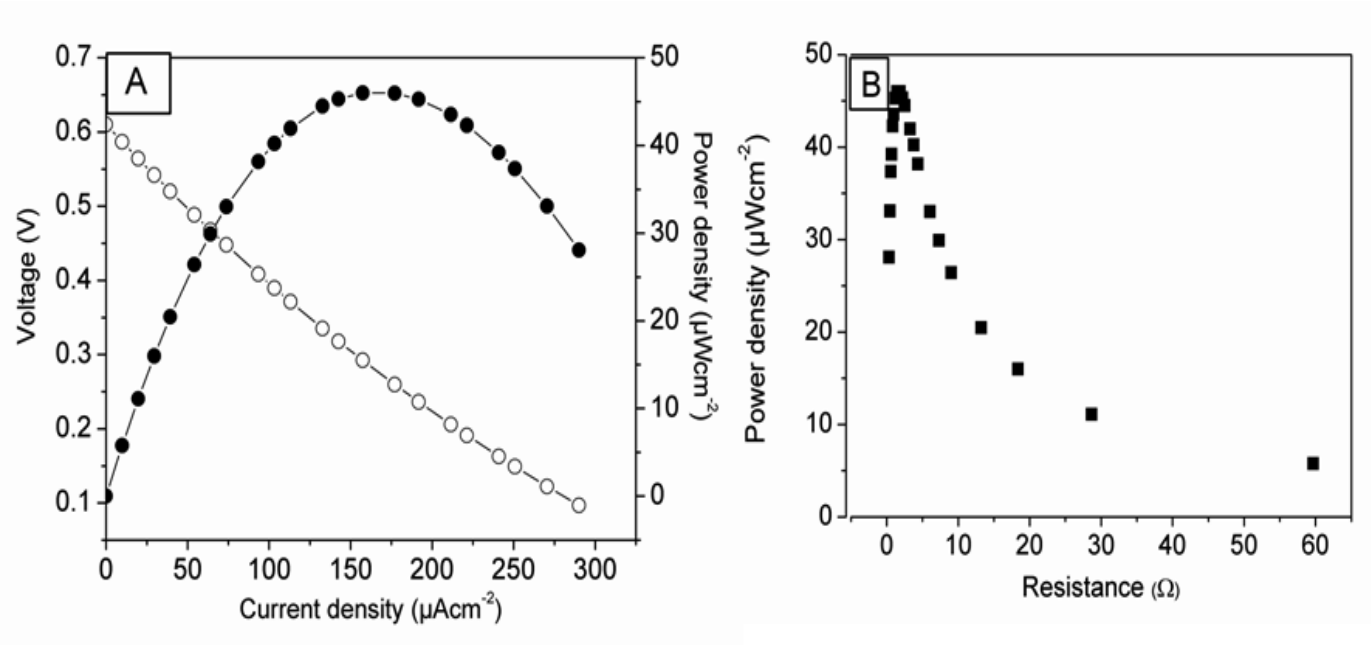


**Figure 5.5**. Performance of the EFC: (A) Power density curve, (B) power density vs. increasing resistance.

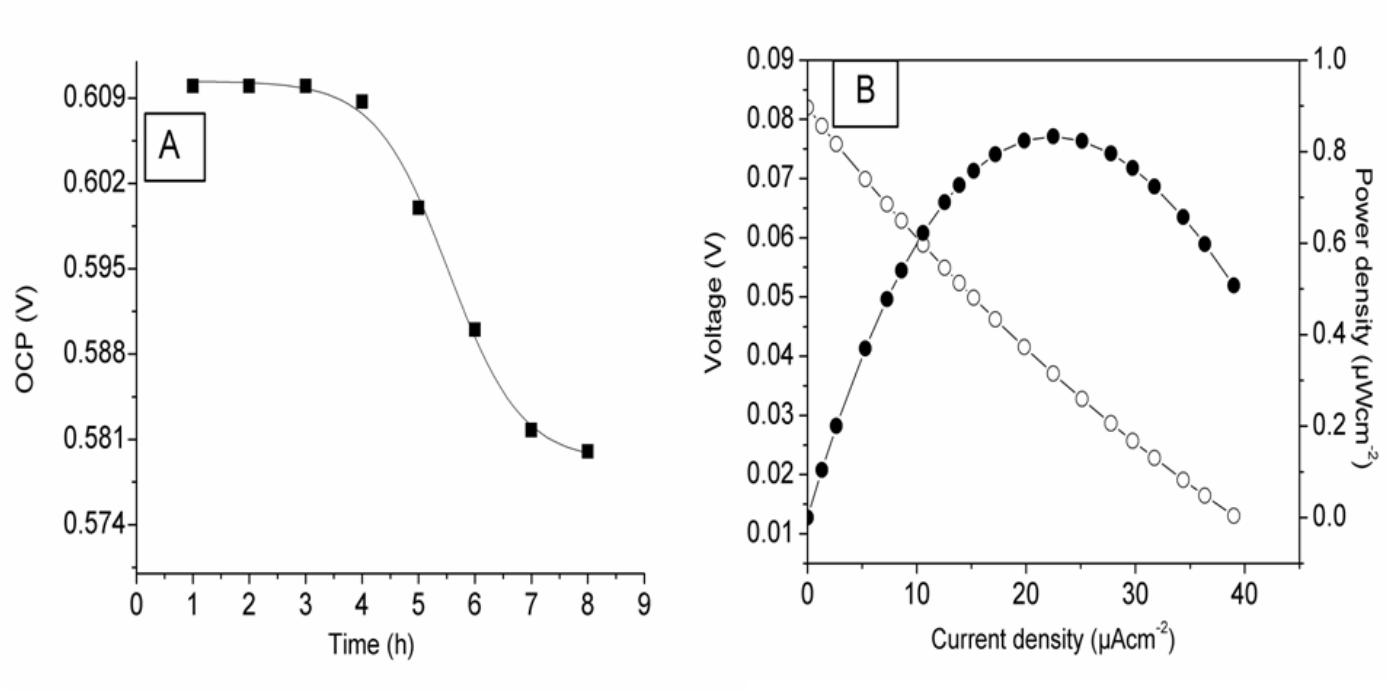


**Figure 5.6.** Stability studies on the EFC: (A) OCP vs time at 1 M methanol; (B) power density curve at 1 M methanol after 3 months of storage at 4 °C.

# Chapter 6

## Alcohol oxidase linked enzyme cascade as anodic biofuel cell catalyst

# Chapter 6

# Alcohol oxidase linked enzyme cascade as anodic biofuel cell catalyst

## 6.1 Overview

The EFC and their potential uses has been accelerated since the beginning of last decade and attracting worldwide attention driven by the demands for clean and renewable energy resources to a viable green technology for powering micro-scale electronic gadgets (Cracknell et al., 2008; Bullen et al., 2006; Cooney et al., 2008). In general, the redox enzymes at the anode catalyze only single step of two-electron oxidation per molecule of substrate that promote continuous accumulation of the product organic compound in the anodic compartment which ultimately may interferes the performance of the EFC due to several reasons. Effort has been made to improve the situation by using cascade of redox enzymes as anodic catalysts that facilitate the deeper oxidation of substrates through which multiple pairs of electrons could be gained from single substrate molecule resulting in increase in power density of the EFC (Hickey et al.,2013; Sokic-Lazic and Minteer, 2008). These enzyme cascades can range from a simple two enzyme system into a cluster of enzymes belonging to complex metabolic system (Sokic-Lazic et al., 2010; Liu et al., 2013).

Among the various substrates studied for EFCs, alcohol has got wide attention. Deep oxidation of alcohol substrates (methanol) for generating power in EFC has been studied with dehydrogenase cascade consisting of the enzymes, ADH, formaldehyde dehydrogenase (FDH) and formate dehydrogenase (FtDH) and the combined action of which converts methanol to carbon dioxide (Kar et al., 2011; Akers et al., 2005). All these enzymes act in the cascade need the cofactor $NAD^+$ to supplement for their function that eventually escalate the

cost and increase technical intricacy related to their function in the enzyme electrode interface. EFC with alcohol as fuel substrate has also been reported with other alcohol oxidizing enzymes namely, PQQ based alcohol oxidases (Ikeda and Kano, 2003). However, the magnitude of power or potential generated by using these single enzyme catalytic systems did not surpass the one yielded by using NAD based dehydrogenase enzyme cascades and one of the reasons attributed to this improved performance of the later system is the deep oxidative led high electrons yield from substrates as discussed above (Rincon et al., 2011). Considering the positive traits of AOx as discussed elsewhere and enzyme cascades for EFC applications, we investigated here an alcohol substrate based EFC where the NAD based ADH present in the dehydrogenase cascade has been replaced by the AOx enzyme for initial oxidation of alcohol to formaldehyde, which is subsequently being oxidized by other dehydrogenases immobilized on the electrode surface along with the enzyme AOx. The performance of the AOx coupled FDH and FtDH bioanode has been evaluated in a half cell studied and subsequently the overall power yield of the EFC with methanol as fuel substrate was investigated in a membrane less EFC using laccase based nanocomposite biocathode for bio-electrocatalytic reduction of molecular oxygen. A detailed account on the findings has been described in this chapter.

## 6.2 Experimental approaches

### *6.2.1 Materials and methods*

AOx from *Pichia pastoris* (21 $Umg^{-1}$ protein), ADH from *Saccharomyces cerevisiae* (300 $Umg^{-1}$ protein), FDH from *Pseudomonas* sp.(1-6 $Umg^{-1}$ solid), formate dehydrogenase (FtDH) from *Candida boidinii* (5-15 $Umg^{-1}$ protein) laccase from *T. versicolor* (0.66 $Umg^{-1}$ protein dry powder), MWCNT, (size OD 10–15 nm, ID 2–6 nm, length 0.1–10 µm), Nf (5 %

w/v in isopropanol), methylene green (MG), nafion 117 membrane, $OsO_4P4VP$, $NAD^+$ were procured from Sigma-Aldrich (USA). Graphite rod electrode (GE) with disc surface area of 0.5 $cm^2$ was procured from Industrial carbon, India. Methanol (99.9 %), formaldehyde (35 %), sodium nitrate, sodium tetraborate and ethyl benzene (99.9 %) were purchased from Merck (India). Carbon powder (CP) was purchased from Electrochem. Inc USA. All other chemicals were of analytical grade and used as received without purification. AOx (1 mg $ml^{-1}$), FDH (1 mg $ml^{-1}$), FtDH (1 mg $ml^{-1}$) were freshly prepared in KPBS (100 mM, pH 7.5). Laccase solution (10 mg $ml^{-1}$) was prepared in 0.1 M sodium citrate buffer of pH 4.8.

*6.2.2 Fabrication of the bioelectrodes*

A graphite electrode was used as a support material for bioelectrode fabrication. At first the electrode was cleaned by sonicating in 70 % ethanol and then in distilled water for half an hour in both the steps. A thin film of MG on the electrode was prepared by performing CV using -0.3 to 1.3 V for 12 sweep segment at a scan rate of 0.05 V/s in a solution containing 0.4 mM MG, 0.1 M sodium nitrate in 10 mM sodium tetraborate. A CP-MWCNT-Nf layer over the electrode was prepared by similar method as described in the chapter 5 section 5.2.2. A total volume of 1000 µl of CP-MWCNT-Nf was dropped into the MG modified graphite electrode. When the nanocomposite mixture in the electrode was in semi dry condition a mixture of enzyme solution containing AOx, FDH, and FtDH from the respective stock solutions was layered over the electrode surface with stepwise loading and drying to a final activities of 42 U $cm^{-2}$, 10 U $cm^{-2}$, and 20 U $cm^{-2}$, respectively, with the total loading of six mg protein per square cm on the electrode surface. The CP included in the electrode fabrication make the layer hydrophilic for better adsoption of enzymes. The layer on the nanocomposite electrode was allowed to dry at room temperature for overnight. Using

same immobilization techniques ADH based multienzyme bioanode was fabricated as control, where ADH was used instead of AOx. The final concentration of ADH, FDH, FtDH in the electrode surface was 600 U cm $^{-2}$, 10 U cm $^{-2}$, 20 U cm $^{-2}$, respectively with the total loading of six mg protein cm$^{-2}$ on the electrode surface. For biocathode fabrication Os $O_4$P4VP - MWCNT-Nf is prepared by similar method as described in the chapter 4, section 4.2.3. A total volume of 1000 µl of $OsO_4$P4VP - MWCNT-Nf was dropped above the hydrophilic microporous layer (CP-MWCNT-Nf) on graphite electrode and incubated at 140 °C overnight. In the semi dry condition, a total 1 ml of laccase stock solution was dropped by stepping method onto the $OsO_4$P4VP- MWCNT-Nf layer to a final concentration of 20 mg protein cm$^{-2}$ (1.32 U cm $^{-2}$) . The biocathode so formed was then air dried and stored at 4° C.

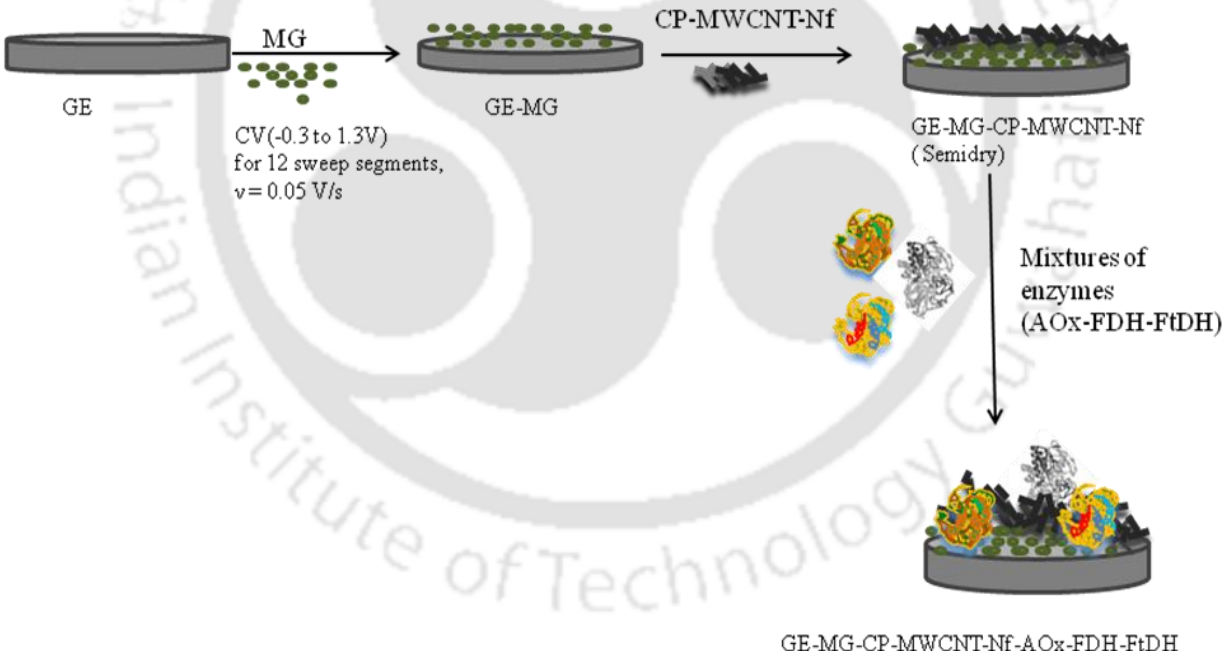


**Scheme 6.1.** Schematic depiction of the GE-MG-MWCNT-Nf-AOx-FDH-FtDH bioanode fabrication process.

### *6.2.3 Apparatus and measurements*

DPV, EIS and polarization curved were performed with a potentiostat. The electrochemical measurement (DPV, EIS) for the each electrode was done in a three-electrode system containing platinum rod as counter electrode, Ag/AgCl (saturated KCl) as reference electrode, and GE or modified GE as the working electrode as describe elsewhere. All potentials were measured and reported relative to the Ag/AgCl reference electrode. EIS measurements were performed in a background solution of 5 mM $K_3Fe(CN)_6/K_4Fe(CN)_6$ (1:1) and 0.1 M KCl in KPBS within the frequency range of 0.05 Hz to 10 kHz. The amplitude of the alternate voltage was 5 mV.

For the fuel cell study, all data were collected and analyzed in the test cell with a potentiostat interfaced to a PC. The bioanode with the AOx based cascade of enzyme was allowed to equilibrate in the 43 mM methanol solution with 0.5 mM $NAD^+$ for 1 h; whereas, the biocathode was allowed to equilibrate in the aerated buffer 100 mM, pH 7.5 for 1 h before the experiment and then open circuit potential was recorded at room temperature. Using the same fuel cell assembly and parameters, the bioanode with ADH based cascade of enzyme was allowed to equilibrate in the 0.1 M methanol fuel solution with 1 mM $NAD^+$ in a 100 mM KPBS, pH 7.5 for 1 h. Both bioanode and biocathode was assembled in a single chambered cell (Scheme 6.2). A rheostat (Stead electronics Trade, India) was used to apply load between 0 and 80 Ω. Linear polarization curves were recorded for each electrode both in the half-cell and full cell assemblies. The data discerned from the polarization curve were used to generate the power curves for both AOx and ADH based cascade bioelectrodes in the fuel cell.

For characterization of the surface morphology, the constructed bioelectrodes were scanned under a SEM (Leo 1430 vp, Germany) using 15 KeV EHT, 50 mm aperture.

## 6.3 Results and discussion

### *6.3.1 Characterization of the bioelectrodes*

The surface morphology of the fabricated bioanodes (Scheme 6.1) was investigated using SEM. GE showed a plane surface (Fig 6.1A). Addition of MG on the GE did not significantly alter the surface morphology on the electrode surface (Fig 6.1B). When MWCNT-CP-Nf was layered on MG surface, the surface transformed to a porous morphology with a thread like structure of the adsorbed MWCNTs visible (Fig.6.1C). When the mixture of enzymes (AOx-FDH-FtDH) was adsorbed on the MG-MWCNT-CP-Nf layer, the surface morphology turned to globular structures indicating the immobilization of the mixtures of the enzymes on the porous CP-MWCNT-Nf film (Fig. 6.1D).

DPV was carried out to investigate redox behavior of the fabricated AOx-FDH-FtDH bioanode (Fig 6.2A) in KPBS (pH 7.5) at a step potential 5 $mVs^{-1}$. The bioanode initiated faradic current response against substrate methanol in the range of 10 - 43 mM with a peak potential at 0.2 V (Fig 6.2A b, c, d). The redox reaction of NADH requires very high potentials (Blaedel and Jenkins, 1975; Karyakin et al., 2004; Cardosi and Liu, 2012). However, the MG modified electrode known to substantially reduce the over potential of NADH oxidation (Dai et al., 2008). In present case no oxidation peak higher than 0.2 V observed. Hence the potential at 0.2 V has been attribute to the oxidation of NADH mediated by MG present in the electrode interfaces. Based on the CV result following reactions at the bioanode in the presence of methanol are proposed:

1. $CH_3OH + O_2 \xrightarrow{AOx} HCHO + H_2O_2$ : Biocatalytic oxidation
2. $CH_3OH \xrightarrow{AOx} HCHO + 2H^+ + 2e^-$ : Direct electrochemical oxidation

3. $HCHO + NAD + H_2O \xrightarrow{FDH} HCOOH + NADH + 2H^+ + 2e^-$

4. $HCOOH + NAD \xrightarrow{FtDH} CO_2 + NADH + H^+ + 2e^-$

5. $NADH + MG^+ \longrightarrow NAD^+ + MGH$

6. $MGH \longrightarrow MG^+ + H^+ + 2e^-$

In the AOx-FDH-FtDH bioanode, the substrate methanol is initially oxidized to formaldehyde by FAD based AOx catalysis. The reaction is likely to follow both catalytically and bioelectrocatalytically [Equation 1 and 2] based on the previous work mentioned in chapter 3. Then the oxidation of the formed formaldehyde takes place by the two NAD based dehydrogenases i.e. FDH and FtDH in aqueous solution in a sequence of reaction [Equation 3 and 4]. The electron transfer in the dehydrogenase enzymes with the electrode takes place via the redox mediator, (MG) through mediated electron transfer (MET) mechanism. NADH reacts with the oxidized form of the mediator ($MG^+$) [Equation 5]. Then the reduced form of the mediator MGH is electrochemically reoxidized [Equation 6]. Preliminary investigation showed that the requirement of NAD in the AOx-FDH-FtDH based bioanode (apprx. 0.5 mM NAD) is significantly lower than the ADH-FDH-FtDH based bioanode (1mM NAD) and previously reported ADH-FDH-FtDH based bioanode (Karyakin et al., 1994; Addo et al., 2010).

EIS was employed to investigate the electrode surface charge transfer behavior during the stepwise assembly of the bioelectrode. The spectra (Fig.6.2B) are presented in the form of Nyquist plots (where $Z'$ is the real and Z" is the imaginary part of impedance) using FRA software of Autolab system and are overlaid to pinpoint the differences in electron-transfer resistance ($R_{ct}$) with subsequent modification of layers. The spectrum of the GE-MG (curve

a) is almost straight line. When CP-MWCNT-Nf layered on the electrode surface, semicircle with resistance of 165 Ω (curve b) was found, which is due to low electronic conductivity of nafion. When mixtures of enzymes AOx/FDH/FtDH (curve d) (i.e. without MWCNT) layered on the CP-Nf electrode surface, the $R_{ct}$ was increased to 951Ω which implies the increased interfacial resistance due to presence of poor conducting enzyme molecules and absence of electroactive MWCNT layer on the electrode. When the mixture of enzymes AOx/FDH/FtDH was layered on the CP-MWCNT-Nf electrode surface (curve c), the semi circle diameter decreased to 363 Ω due to obvious reason of highly electroactive properties of MWCNT that decreased the interfacial charge transfer resistance.

The fabricated AOx-FDH-FtDH bioanode and laccase biocathode were assembled in a fuel cell setup as shown in Scheme 6.2. The OCPs of the EFC were recorded at increasing concentrations of methanol. The OCP increased with increasing methanol concentration starting from 10 mM methanol and the potential was reached to a maximum value of 0.901 V at 43 mM methanol (Fig 6.3), thus showing the nernstian relation between substrate concentration and generation of potential. A methanol concentration of 43 mM was thus considered for all the electrochemical characterization of the EFC. The half cell characterization with the reference electrode (Ag/AgCl) was investigated and the anodic OCP was found to be 0.69 V. From the OCP values of the cell and anodic half cell, the OCP of the cathodic half cell has been discerned as 0.21V. Figure 6.4A shows the power density curve of the EFC operated with 43 mM methanol at room temperature 25 °C. Fig. 6.5 shows the effect of external load on the power density of the EFC. Power density rose upon increasing the external load resistance and reached maximum value of 2.5 $mWcm^{-2}$ at 8 Ω. Further increase in load resistance, the cell current dropped and reached almost zero at a resistance of 80 Ω. The maximum power density generated in the EFC was 2.5 $mWcm^{-2}$ (Fig 6.4 A). The power density of ADH-FDH-FtDH based multienzyme fuel cell (Fig 6.4B) was 4.6 $mWcm^{-2}$. One of

reasons for lower power density may be due to the biocatalytic instead of bioelectrocatalytic function of some of the immobilized AOx. From our previous studies (Chapter 3 section 3.3.3) it has been observed that not all AOx immobilized on the electrode surface participated DET due their inappropriate orientation on the electrode surface that likely to prevent the electron exchange between the redox centre of the enzyme and electrode. As a result majority of the AOx molecules involve in biocatalytic reactions producing the co-substrate $H_2O_2$ by exchanging the substrate derived electrons with the molecular oxygen bypassing the electrode. The other reason attributed to the lower power density for AOx coupled bioanode based EFC is the lower AOx enzyme loading (42 $Ucm^{-2}$) on the electrode than the corresponding loading (600 $Ucm^{-2}$) of ADH on the bioanode. Nevertheless, the power density of the present AOx couple dehydrogenase fuel cell is comparable (Sokic-Lazic and Minteer 2008; Addo et al., 2010; Hickey et al., 2013) and even higher than the previously reported methanol fuel based multienzymatic fuel cell (261± 7.6 µW $cm^{-2}$ by Addo et al., 2010; 0.67 $mWcm^{-2}$ by Palmore et al., 1998, 2.04 $mWcm^{-2}$ by Akers et al., 2005). We also observed that the power density of the present AOx based multienzyme fuel cell is higher than our previously reported single enzyme (i.e. AOx) based fuel cell (Chapter 5 section 5.3.2) due to obvious reason of the involvement of additional two redox enzymes (FDH and FtDH) operated through bioelectrocatalytic mechanism which contributed higher current density in the fuel cell.

The operational stability of the bioanode was investigated from several successive measurements, each cycle of 1h duration with fresh methanol substrate of 43 mM concentration at a fixed load of 8 Ω (Fig. 6.6). The OCP response was steady from 1$^{st}$ to 4$^{th}$ cycle. This indicates that there was no leaching and denaturation of the enzymes in the fabricated bioelectrodes till 4$^{th}$ cycle of operation. The functional stability implies proper nanofabrication approach followed here for immobilization of the enzymnes on the electrode

surface. The MG based mediated electron exchange was facilitated by the highly conductive MWCNT present in the naocomposite matrix (Sarma et al., 2009). The nanofabrication also provides high enzyme loading on the electrode surface and tailored increase electroactive enzyme molecules on the electrode surface.

### 6.4 Conclusion

Enzymatic biofuel cell fabricated by assembling AOx coupled multienzyme based bioanode and laccase based biocathode has been developed for generating power from methanol substrate. The fuel cell generated higher power density than the single redox enzyme based methanol fuel cell reported previously and the reason is attributed to the extraction of more electrons from the substrate methanol by its mineralization through a cascade of oxidative reaction electrocatalyzed by the NAD based dehydrogenase enzymes coupled to the FAD based AOx enzyme on the anodic electrode surface. The dehydrogenase based bioelectrocatalytic reactions on the anodic surface were mediated by MG that significantly reduce the oxidation potential of the NADH and thereby contributed to the increase potential of the NADH.

## Figures

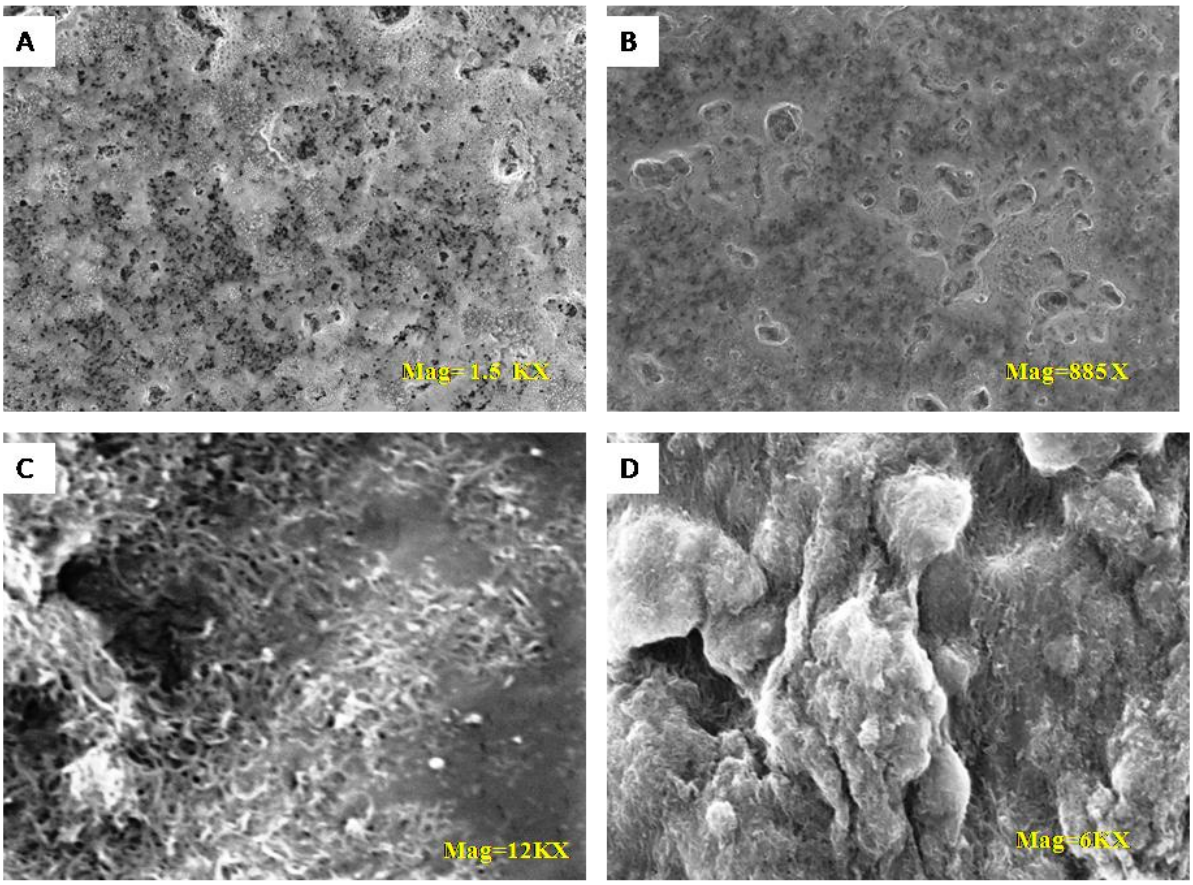


**Figure 6.1**. SEM images of the bioelectrodes at different fabrication stages: A. Bare GE, B. GE- MG. C. GE-MG-CP-Nf-MWCNT, D. GE-MG-CP-Nf-MWCNT- Mixtures of Enzymes (AOx-FDH-FtDH).

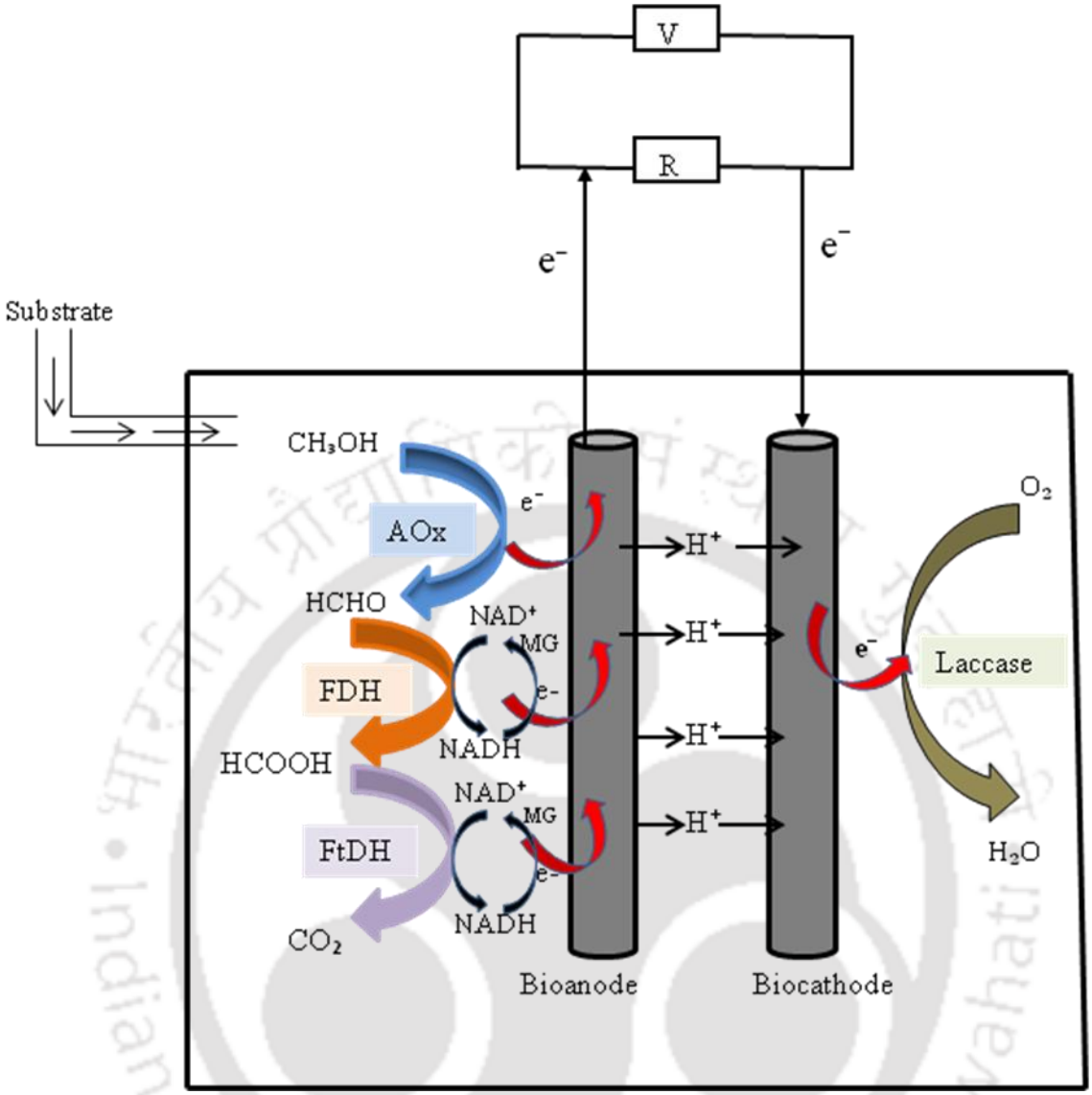


**Scheme 6.2** Schematic diagram on the operation of AOx-FDH-FtDH and laccase based EFC using methanol as fuel substrate.

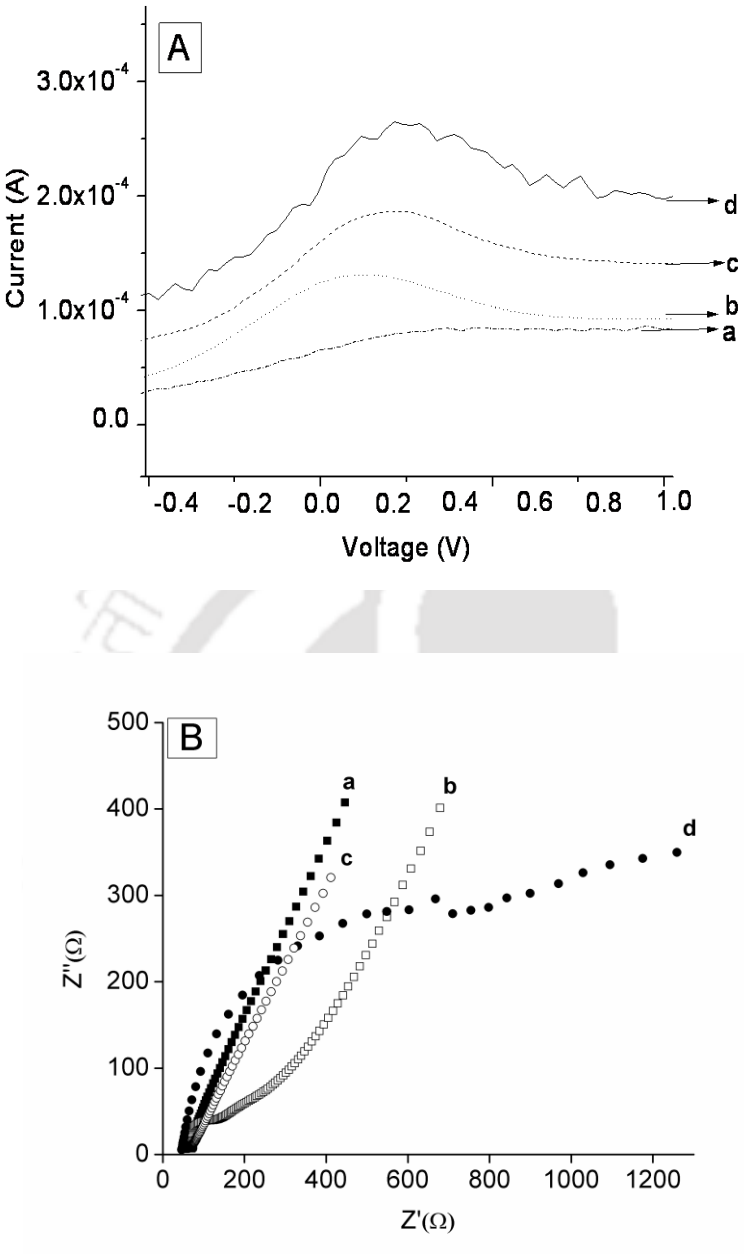


**Figure 6.2**.(A) DPV of GE-MG-CP-MWCNT-Nf-AOx/FDH/FtDH electrode at 100 mM KPBS, pH 7.5 with increasing methanol concentration (mM), (a) 0, (b) 10, (c) 21, (d) 43 at a scan rate of 50mVs$^{-1}$**.** (B) EIS of (a) GE-MG, (b) GE-MG-CP-MWCNT-Nf, (c) GE-MG-CP-MWCNT-Nf-AOx/FDH/FtDH (d) GE-MG-CP-Nf-AOx/FDH/FtDH in presence of 5 mM $K_3Fe(CN)_6/K_4Fe(CN)_6$ (1:1) and 0.1M KCl in KPBS within the frequency range from 0.05 Hz to 10 kHz.

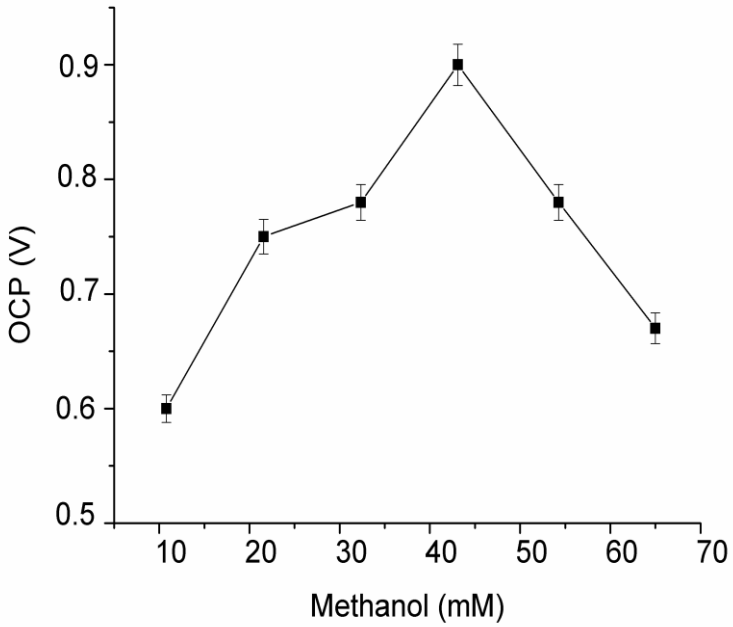


**Figure 6.3** Effect of methanol concentration on the OCP of the EFC.

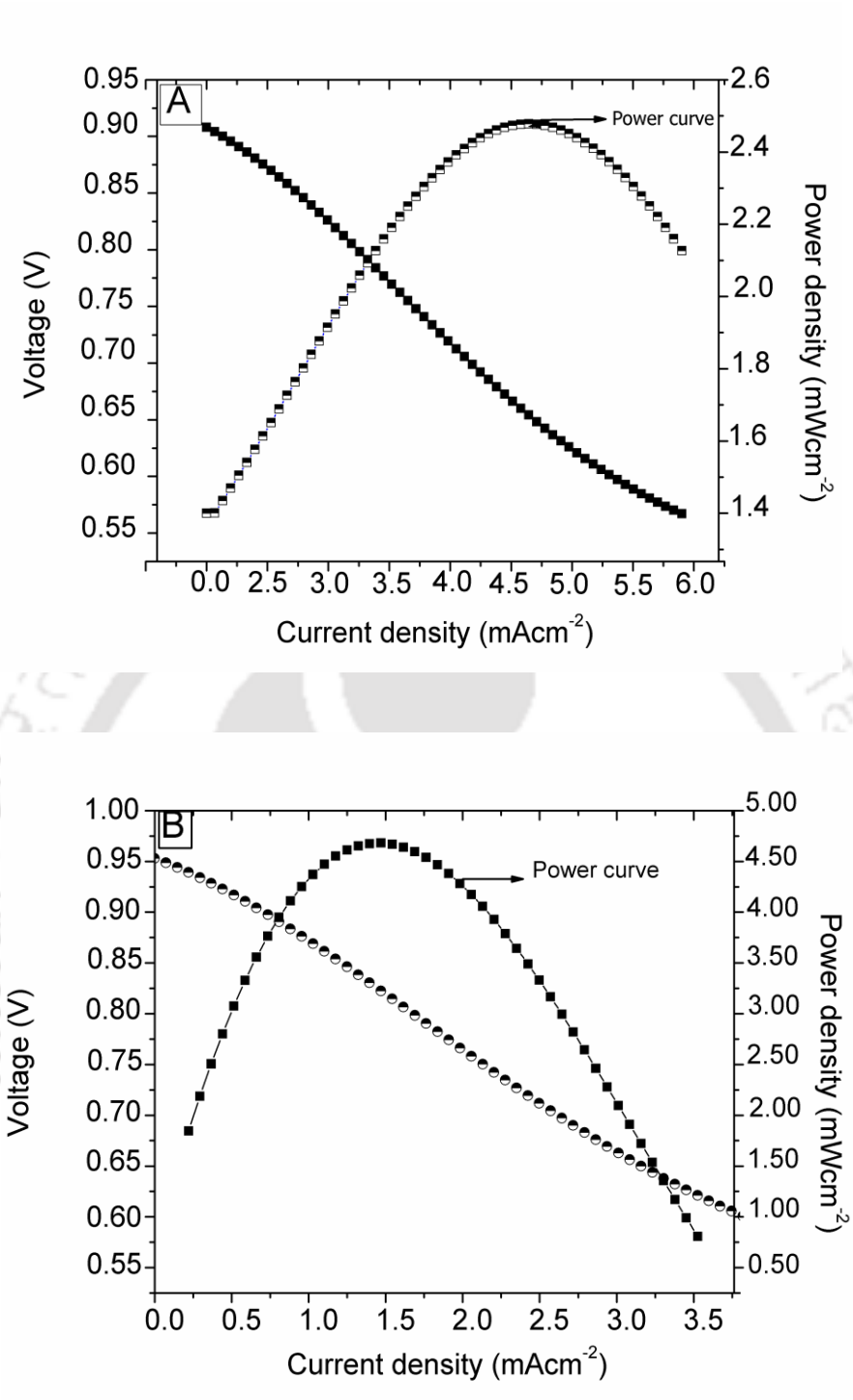


**Figure 6.4** Power density curve of the (A) AOx-FDH-FtDH and (B) ADH-FDH-FtDH fuel cell cascade based EFC using laccase as biocathode.

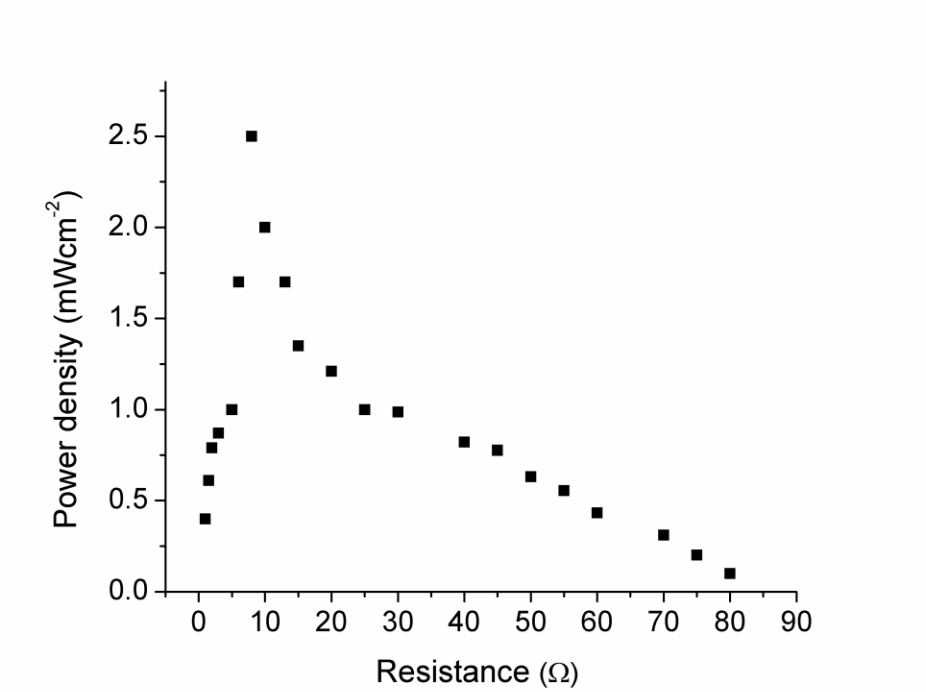


**Figure 6.5.** Effect of the resistance on the power density of the EFC fabricated by AOx-FDH-FtDH bioanode and laccase based biocathode.

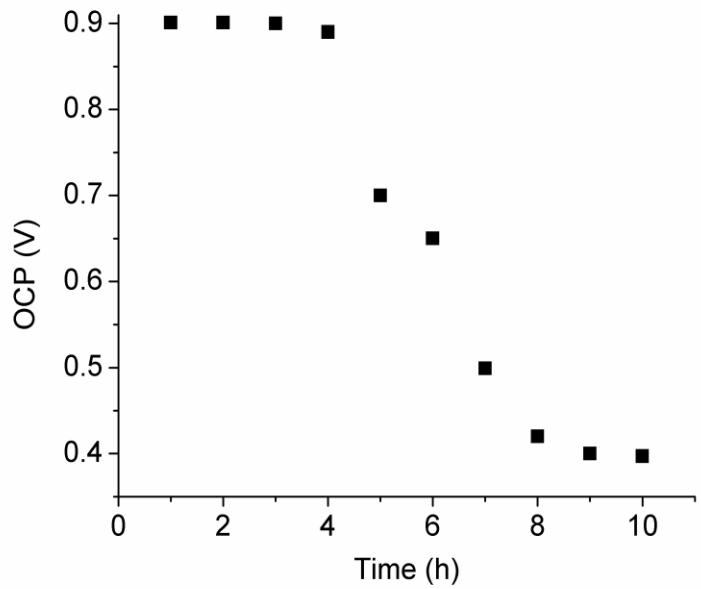


**Figure 6.6**. Stability studies of the EFC fabricated by AOx-FDH-FtDH based bioanode and laccase based biocathode in an operating condition of 43 mM methanol, 25° C temperature, 8 Ω load within 10 h duration which is maintained by charging with fresh substate (methanol 43 mM ) following each 1 h runtime.

# CONCLUSIONS AND SCOPE FOR FUTURE WORK

# Conclusions and Scope for Future Work

## Conclusion

The direct electrochemistry of the massive multimeric AOx protein from *Pichia pastoris* immobilized on gold electrode by encapsulating with PEI in a MWCNT-Nf matrix was established for the first time. The entrapped AOx possesses good bioactivity and electrocatalytic activity at room temperature and physiological pH condition. The constructed bioelectrode showed response at considerably low oxidation potential for alcohol thus obviate the electrochemical interference caused by the common interfering compounds present in the blood serum. The values on operational and storage stability and lower detection limit in the linear response range obtained by using the constructed bioelectrode towards the substrate alcohol were comparable to or even superior to many reports on alcohol biosensors. In another work, a laccase based biosensor for detection of pyrocatechol was successfully developed. An osmium polymer supported MWCNT based nanocomposite matrix utilized to immobilize laccase had provided an electroactive surface for facile electron transfer kinetics between the electrode and the redox centre of the enzyme. The response of the constructed biosensor was generated from the cascade of two reactions, the biocatalyzed oxidation of pyrocatechol and the subsequent electrocatalyzed reduction of the oxidized product 1,2-benzoquinone on the electrode surface. The aforementioned fabrication protocols for AOx and laccase based bioelectrodes were reproduced on toray carbon paper with suitable modification as supporting electrode material and assembled the as prepared bioelectrodes in a fuel cell setup. The cell potential and operational stability of the constructed mediator less biofuel cell were comparable or even superior to many alcohol fuel based pure enzymatic biofuel cells. To improve the power density of the biofuel cell, the AOx enzyme in the bianode was coupled with formaldehyde dehydrogenase and formate dehydrogenase.

Methylene green was used as an electron transfer mediator for the dehydrogenase enzymes on the bioelectrode. The power density of the biofuel cell achieved by using the multienzyme cascade based bioanode and laccase based biocathode was significantly higher than the corresponding single enzyme based bioanode system. It is thus concluded that the AOx and laccase based bioelectrodes developed through this investigation have the potential for developing biosensor and biofuelcell of practical applications. Further, it is established that the FAD based AOx enzyme can cohesively functions with the dehydrgenase enzymes for deep oxidation of substrate methanol on the electrode surface and thus, increasing the power density in the methanol substrate based biofuel cell.

# Scope for future work

Following points have been identified as major gap areas emanated from the current studies that warrant further investigations for augmenting the concept and technology to a realistic height.

- Further technical improvement of membrane electrode assembly for installing the AOx and laccase based bioelectrodes in a suitably designed fuel cell setup is expected to reduce the ohmic overpotential for generating an efficient methanol substrate based EFC with enhanced power density for practical application.
- Miniaturization of the alcohol and pyrocatechol based biosensors by using screen printed electrodes in a micro fluidic platform may be investigated as these require small sample volume and make the system cost-effective and easy for transportation.

- Optimization of nano-enzyme interaction by immobilizing the enzyme on efficient electroactive nanocomposite matrix on the electrode surface may help to achieve better electrokinetics for the performance of the constructed bioelectrodes for the bioelectronic devices.
- Selection of the biocompatible matrix to provide a promising platform for immobilization of the enzyme by considering their unique inert, thermal and electrical properties which prevent enzyme denaturation or leaching and stabilize the enzymes on the electrode surface by retaining enzyme activity may increase the operational stability of the enzymatic fuel cell.
- Porous three dimensional electrode design may be investigated to increase the enzyme loading and effective mass transport for increasing the power density of the enzymatic fuel cell.
- In order to enhance the EFC power density of the AOx linked enzyme cascade based bioanode further investigation is warranted on the nanocomposite electrode material and enzyme loading on the electrode surface. Notebly, the loading capacity of the studied nanocomposite bioelectrode support for AOx protein is far less than the corresponding ADH proteins probably due to bulky nature of the multimeric AOx ($M_w$ ~675 kDa) as compared to ADH ($M_w$ ~141-151 kDa). The electroactive nanocomposite support material should also alter suitable microenvironment for enhancing electrocatalytically active AOx enzyme for accelerating electron exchange through DET principle.

# BIBLIOGRAPHY

# Bibliography


Abdullah J, Ahmad M, Heng LY, Karuppiah N, Sidek H (2007) An optical biosensor based on immobilization of laccase and MBTH in stacked films for the detection of catechol. Sensors 7:2238-2250.

Addo PK, Arechederra RL, Minteer SD (2011) Towards a rechargeable alcohol biobattery. Journal of Power Sources 196:3448-3451.

Addo PK, Arechederra RL, Minteer SD (2010) Evaluating enzyme cascades for methanol/air biofuel cells based on $NAD^+$-Dependent Enzymes. Electroanalysis 22:807-812.

Agui L, Yanez-Sedeno P, Pingarron JM (2008) Role of carbon nanotubes in electroanalytical chemistry: A review. Analytica Chimica Acta 622:11–47.

Ahuja T, Mir IA, Kumar D, Rajesh (2007) Biomolecular immobilization on conducting polymers for biosensing applications. Biomaterials 28:791-805.

Akers NL, Moore CM, Minteer SD (2005) Development of alcohol/$O_2$ biofuel cells usig salt-extracted tetrabutylammonium bromide/Nafion membranes to immobilize dehydrogenase enzymes. Electrochimca Acta 50:2521- 2525.

Akyilmaz E, Dinckaya E (2000) A mushroom (*Agaricus bisporus*) tissue homogenate based alcohol oxidase electrode for alcohol determinationin serum. Talanta 53:505–509.

Akyilmaz E, Dinckaya E (2005) An amperometric microbial biosensor development based on *Candida tropicalis* yeast cells for sensitive determination of ethanol. Biosensors and Bioelectronics 20:1163-1269.

Alpeeva IS, Vilkanauskyte A, Ngounou B, Csoregi E, Sakharov IY, Gonchar M, Schuhmann W (2005) Bi-enzyme alcohol biosensors based on genetically engineered alcohol oxidase and different peroxidases. Microchimica Acta 152:21–27.

Apers S, Meenen E V, Pieters L, Vlietinck A (2003) Quality control of liquid herbal drug preparations: ethanol content and test on methanol and 2-propanol. Journal of Pharmaceutical and Biomedical Analysis 33: 529–537.

Arribas S, Bermejo E, Chicharro M, Zapardiel A, Luque GL, Ferreyra NF, Rivas GA (2007) Analytical applications of glassy carbon electrodes modified with multi-wall carbon nanotubes dispersed in polyethylenimine as detectors in flow systems. Analytica Chimica Acta 596: 183-194.

Arya SK, Solanki PR, Datta M, Malhotra BD (2009) Recent advances in self-assembled monolayers based biomolecular electronic devices. Biosensors and Bioelectronics 24: 2810-2817.

Asav E, Akyilmaz E (2010) Preparation and optimization of a bienzymic biosensor based on self-assembled monolayer modified gold electrode for alcohol and glucose detection. Biosensors and Bioelectronics 25:1014–1018.

Asefa T, Duncan CT, Sharma KK (2009) Recent advances in nanostructured chemosensors and biosensors. Analyst 134:1980-90.

Azevedo AM, Prazeres DMF, Cabral JMS, Fonseca LP (2005) Ethanol biosensors based on alcohol oxidase. Biosensors and Bioelectronics 21:235–247.

Barriere F, Kavanagh P, Leech D (2006) A laccase–glucose oxidase biofuel cell prototype operating in a physiological buffer. Electrochima Acta 51:5187–5192.

Barton SC, Gallaway J, Atanassov P (2004) Enzymatic biofuel cells for implantable and microscale devices. A review. Chemical Reviews 104:4867- 4886.

Barton SC, Kim HH, Binyamin G, Zhang Y, Heller A (2001) Electroreduction of $O_2$ to water on the “wired” laccase cathode. Journal of Physical Chemistry B 105:11917-11921.

Bartak P, Frnkova P, Cap L (2000) Determination of phenols using simultaneous steam distillation–extraction. Journal of Chromatography A 867:281-287.

Bartlett PN, Simon E, Toh CS (2002) Modified electrodes for NADH oxidation and dehydrogenase based biosensors. Bioelectrochemistry 56 :117-122.

Bidan G (1992) Electroconducting conjugated polymers. New sensitive matrices to build up chemical or electrochemical sensors: a review. Sensors and Actuators B Chemical 6: 45-56.

Blackwell AE, Moehlenbrock MJ, Worsham JR, Minteer SD (2009) Comparison of electropolymerized thiazine dyes as an electrocatalyst in enzymatic biofuel cells and self powered sensors. Journal of Nanoscience Nanotechnology 9:1714-1721.

Blaedel WJ, Jenkins, RA (1975) Study of the electrochemical oxidation of reduced nicotinamide adenine dinucleotide. Analytical Chemistry 47:1337- 1343.

Blanford CF, Foster CE, Heath RS, Armstrong FA (2009) Efficient electrocatalytic oxygen reduction by the 'Blue' copper oxidase, laccase, directly attached to chemically modified carbons. Faraday Discuss 140:319-335.

Blanford CF, Heath RS, Armstrong FA (2007) A stable electrode for high-potential, electrocatalytic $O_2$ reduction based on rational attachment of a blue copper oxidase to a graphite surface. Chemical Communication 17:1710-1712.

Bosch F, Font G, Manes J (1987) Ultraviolet spectrophotometric determination of phenols in natural and waste waters with iodine monobromide. Analyst 112:1335-1337.

Bott AW (1998) Electrochemical methods for the determination of glucose. Current Seperation 17:25–31.

Bullen RA, Arnot TC, Lakeman JB, Walsh FC (2006) Biofuel cells and their development. Biosensors and Bioelectronics 21:2015-2045.

Cai C, Chen J (2004) Direct electron transfer of glucose oxidase promoted by carbon nanotubes. Analytical Biochemistry 332:75-83.

Cardosi M, Liu Z (2012) Amperometric glucose sensors for whole blood measurement based on dehydrogenase enzymes. In Dehydrogenases; Canuto RA. Eds.; InTech. 319-348.

Cardoso FP, Neto SA, Fenga PG, Ciancaglini P, De Andrade AR (2013) Electrochemical characterization of methanol/$O_2$ biofuel cell: Use of laccase biocathode immobilized with polypyrrole film and PAMAM dendrimers. Electrochimica Acta 90:90-94.

Carelli D, Centonze D, Giglio AD, Quinto M, Zambonin PG (2006) An interference-free first generation alcohol biosensor based on a gold electrode modified by an overoxidised non-conducting polypyrrole film. Analytica Chimica Acta 565: 27–35.

Castillo M, Barcelo D (1997) Analysis of industrial effluents to determine endocrine-disrupting chemicals. Trends in Analytical Chemistry 16:574-583.

Cernocka H, Ostatna V, Palecek E (2013) Enzymatic activity and catalytic hydrogen evolution in reduced and oxidized urease at mercury surfaces. Analytica Chimica Acta 789: 41- 46.

Chaki NK, Vijayamohanan K (2002) Self-assembled monolayers as a tunable platform for biosensor applications. Biosensors and Bioelectronics 17:1-12.

Chen S, Yuan R, Chai Y, Xu, L,Wang N, Li X, Zhang L (2006b) Amperometric hydrogen peroxide biosensor based on the immobilization of horseradish peroxidase (HRP) on the layer-by-layer assembly films of gold colloidal nanoparticles and toluidine blue. Electroanalysis 18: 471-477.

Chen W, Yao H, Tzang CH, Zhu J, Yang M, Lee ST (2006a) Silicon nanowires (SiNWs) as the supporting matrixes for high sensitivity glucose detection. Applied Physical Letters 88:213104/1-213104/2.

Clark Jr LC, Wolf R, Granger D, Taylor Z (1953) Continuous recording of blood oxygen tensions by polarography. Journal of applied physiology 6: 189-193.

Clauwaert P, Aelterman P, Pham TH, De Schamphelaire L, Carballa M, Rabaey K, Verstraete W (2008) Minimizing losses in bio-electrochemical systems: The road to applications. A review. Applied Microbiology and Biotechnology 79:901-913.

Cooney MJ, Svoboda V, Lau C, Martin G, Minteer SD (2008) Enzyme catalysed biofuel cells. Energy and Environmental Science 1:320-337.

Couderc R, Baratti J (1980) Oxidation of methanol by the yeast *Pichia pastoris*: purification and properties of alcohol oxidase. Agricultural and Biological Chemistry 44:2279 -89.

Cracknell JA, Vincent KA, Armstrong FA (2008) Enzymes as working or inspirational electrocatalysts for fuel Cells and electrolysis. Chemical Reviews 108:2439-2461.

Dai ZH, Liu FX, Lu GF, Bao JC (2008) Electrocatalytic detection of NADH and ethanol at glassy carbon electrode modified with electropolymerized films from methylene green. Journal of Solid State Electrochemistry 12:175-180.

Davis G, Hill HAO, Aston WJ, Higgins IJ, Turner APF (1983) Bioelectrochemical fuel cell and sensor based on a quinoprotein, alcohol dehydrogenase. Enzyme and Microbial Technology 5:383-388.

Deng L, Shang L, Wen D, Zhai J, Dong S (2010) A membraneless biofuel cell powered by ethanol and alcoholic beverage. Biosensors and Bioelectronics 26:70–73.

de Poulpiquet A, Ciaccafava A, Lojou E (2014) New trends in enzyme immobilization at nanostructured interfaces for efficient electrocatalysis in biofuel cells. Electrochimica Acta 126:104-114.

de Prada AGV, Pena N, Mena ML, Reviejo AJ, Pingarron JM (2003) Graphite/Teflon composite bienzyme amperometric biosensors for monitoring of alcohols. Biosensors and Bioelectronics 18:1279-1288.

Diaz JF, Balkus Jr KJ (1996) Enzyme immobilization in MCM-41 molecular sieve. Journal of Molecular Catalalysis B Enzymatic 2:115-26.

Dominguez-Benetton X, Srikanth S, Satyawali Y, Vanbroekhoven K, Pant D (2013) Enzymatic Electrosynthesis: An overview on the progress in enzyme-electrodes for the production of electricity, fuels and chemicals, Article. Journal of Microbial and Biochemical Technology S6: 1-20.

Duma R, Minteer SD (2007) Bilirubin oxidase biocathodes for ethanol biofuel cells. ECS Transactions 5:117-127.

Duran N, Esposito E (2000) Potential applications of oxidative enzymes and phenoloxidase-like compounds in wastewater and soil treatment: a review. Applied Catalysis B 28: 83-99.

El-Zahab B, Jia H, Wang P (2004) Enabling multienzyme biocatalysis using nanoporous materials. Biotechnology and Bioenggineering 87:178-183.

Fan Z, Harrison DJ (1992) Permeability of glucose and other neutral species through recast perfluorosulfonated ionomer films. Analytical Chemistry 64:1304-1311.

Fraaije MW, van den Heuvel RHH, Mattevi A, van Berkel WJH (2003) Covalent flavinylation enhances the oxidative power of vanillyl-alcohol oxidase. Journal of Molecular Catalysis B Enzymatic 21:43-46.

Freire RS, Duran N, Kubota LT (2002) Development of a laccase-based flow injection electrochemical biosensor for the determination of phenolic compounds and its application for monitoring remediation of Kraft E1 paper mill effluent. Analytica Chimica Acta 463:229-238.

Freire RS, Pessoa CA, Mello LD, Kubota LT (2003) Direct Electron Transfer: An Approach for Electrochemical Biosensors with Higher Selectivity and Sensitivity. Journal of Brazilian Chemical Society 14:2230-2430.

Fu J, Qiao H, Li D, Luo L, Chen K, Wei Q (2014) Laccase biosensor based on electrospun copper/carbon composite nanofibers for catechol detection. Sensors (Basel) 14:3543-3556.

Gallaway JW, Barton SAC (2008) Kinetics of Redox Polymer-Mediated Enzyme Electrodes. Journal of American Chemical Society 130:8527-8536.

Geissler J, Hemmerich P (1981) Yeast methanol oxidases: an unusual type of flavoprotein. FEBS. Letter. 126:152-156.

Gellett W, Schumacher J, Kesmez M, Le D, Minteer SD (2010) High current density air-breathing laccase biocathode. Journal of Electrochemical Society 157:B 557-562.

Gomez C, Shipovskov S, Ferapontova EE (2010) Peroxidase biocathodes for a biofuel cell development. Renewable and sustainable energy reviews 2:013103-1-013103-12.

Gooding JJ (2005) Nanostructuring electrodes with carbon nanotubes: a review on electrochemistry and applications for sensing. Electrochimica Acta 50:3049-3060.

Gorton L (2005) Comprehensive Analytical Chemistry Volume XLIV: Biosensors and Modern Biospecific Analytical Techniques. Elsevier Science 285-327.

Goswami P, Chinnadayyala SSR, Chakraborty M., Kumar AK, Kakoti A (2013) An overview on alcohol oxidases and their potential applications. Applied Microbiology and Biotechnology. Applied Microbiology and Biotechnology 97:4259-4275.

Gouveia- Caridade C, Pauliukaite R, Brett CMA (2008) Development of electrochemical oxidase biosensors based on carbon nanotube-modified carbon film electrodes for glucose and ethanol. Electrochimica Acta 53:6732-6739.

Guo M, Wang H, Huang D, Han Z, Li Q, Wang X, Chen J (2014) Amperometric catechol biosensor based on laccase immobilized on nitrogen-doped ordered mesoporous carbon (N-OMC)/PVA matrix. Science and Technology of Advanced Materials 15:035005.

Gulce H, Gulce A, Kavanoz M, Coskun H, Yildiz A (2002) A new amperometric enzyme electrode for alcohol determination. Biosensors and Bioelectronics 17:517-521.

Gupta G, Lau C, Branch B, Rajendran V, Ivnitski D, Atanassov P (2011b) Direct bioelectrocatalysis by multi-copper oxidases: gas-diffusion laccase-catalyzed cathodes for biofuel cells. Electrochimica Acta 56:10767-10771.

Gupta G, Lau C, Rajendran V, Colon F, Branch B, Ivnitski D, Atanassov P (2011a) Direct electron transfer catalyzed by bilirubin oxidase for air breathing gas-diffusion electrodes. Electrochemistry Communication 13:247-249.

Hack JB, Early J, Brewer KL (2007) An alcohol oxidase dipstick rapidly detects methanol in the serum of mice. Academic Emergency Medicine 14:1130-1134.

Haghighi B, Gorton L, Ruzgas T, Jonsson LJ (2003) Characterization of graphite electrodes modified with laccase from *Trametes versicolor* and their use for bio-electrochemical monitoring of phenolic compounds in flow injection analysis. Analytica Chimica Acta 487: 3-14.

Hammerle M, Hilgert K, Horn MA, Moos R (2011) Analysis of volatile alcohols in apple juices by an electrochemical biosensor measuring in the headspace above the liquid Sensors and Actuators B: Chemical 158:313-318.

Heller A (1992) Electrical connection of enzyme redox centers to electrodes. Journal of Physical Chemistry 96:3579-3587.

Heller A (2004) Miniature biofuel cells. Physical chemistry chemical Physics 6: 209-216.

Hickey DP, Giroud F, Schmidtke DW, Glatzhofer DT, Minteer SD (2013) Enzyme cascade for catalyzing sucrose oxidation in a biofuel cell. ACS Catalysis 3:2729-2737.

Huang CJ, Damasceno LM, Anderson KA, Zhang S, Old LJ, Batt CA (2011) A proteomic analysis of the *Pichia pastoris* secretome in methanol-induced cultures. Applied Microbiology and Biotechnology 90:235-247.

Hudak NS, Gallaway JW, Barton SC (2009) Mediated biocatalytic cathodes operating on gas phase air and oxygen in fuel cells. Journal of Electrochemical Society 156:B 9-15.

Hussein L, Rubenwolf S, von Stetten F, Urban G, Zengerle R, Krueger M, Kerzenmacher S (2011) A highly efficient buckypaper-based electrode material for mediatorless laccase-catalyzed dioxygen reduction**.** Biosensors and Bioelectronics 26:4133-4138.

Iannello RM, Iacynych AM (1981) Immobilised enzyme chemically modified electrode as an amperometric sensor. Analytical Chemistry 53:2090-2095.

Ikeda T, Kano K (2003) Bioelectrocatalysis-based application of quinoproteins and quinoprotein-containing bacterial cells in biosensors and biofuel cells. Biochima Biophysica Acta 1647:121-126.

Ivanov I, Vidakovic-Koch T, Sundmacher Kai (2010) Recent advances in enzymatic fuel cells: experiments and modeling. Energies 3: 803-846.

Ivnitski D, Artyushkovab K, Khripin C, Luckariftc H, Ramasamy R, Johnsonc G, Atanassov P (2009) Surface characterization and direct electrochemistry of multi-copper oxidases. in: Proceedings 216th ECS Meeting 2969.

Ivnitski D, Atanassov P (2007) Electrochemical studies of intramolecular electron transfer in laccase from *Trametes versicolor*. Electroanalysis 19:2307-2313.

Ivnitski D, Branch, B, Atanassov P, Apblett C (2006) Glucose oxidase anode for biofuel cell based on direct electron transfer. Electrochemistry Communication 8:1204-1210.

Ivnitski DM, Khripina C, Luckarift HR, Johnson GR Atanassova P (2010) Surface characterization and direct bioelectrocatalysis of multicopper oxidases. Electrochimica Acta 55:7385-7393.

Jia F, Shan C, Li F, Niu L (2008) Carbon nanotube/gold nanoparticles/polyethylenimine-functionalized ionic liquid thin film composites for glucose. Biosensors and Bioelectronics 24:945-950.

Judd FF, Chirlian PM (1970) The application of the compensation theorem in the proof of Thevenin's and Norton's theorems. IEEE Transaction on Education 13:87-88.

Kar P, Wen H, Li H, Minteer SD Barton SC (2011) Simulation of multistep enzyme-catalyzed methanol oxidation in biofuel cells. Journal of Electrochemical Society 158:B 580-B586.

Karyakin AA, Ivanova YN, Revunova KV, Karyakina EE (2004) Electropolymerized flavin adenine dinucleotide as an advanced NADH transducer. Analytical Chemistry 76:2004-2009.

Karyakin AA, Karyakina EE, Schuhmann W, Schmidt HL, Varfolomeyev SD (1994) A new amperometric dehydrogenase electrodes based on electrocatalytic NADH-oxidation at poly(methylene blue)-modified electrodes. Electroanalysis 6:821-829.

Katz E, Shipway N, Willner I, Vielstich W, Gasteiger HA, Lamma A (2003) Biochemical fuel cells. In Handbook of Fuel Cells – Fundamentals, Technology and Applications; Vielstich W, Gasteiger HA, Lamm A, Eds.; John Wiley Sons Ltd., 1-26.

Katz E, Willner I, Kotlyar AB (1999) A non-compartmentalized glucose/$O_2$ biofuel cell by bioengineered electrode surfaces. Journal of Electroanalytical Chemistry 479:64-68.

Kanazawa KK, Diaz AF, Geiss RH, Gill WD, Kwak JF, Logan JA, Rabolt JF, Street GB (1979) 'Organic Metals': polypyrrole, a stable synthetic 'metallic' polymer Journal of the Chemical Society, Chemical Communications 19:854-855.

Kemp GD, Dickinson FM, Ratledge C (1988) Inducible long chain alcohol oxidase from alkane-grown *Candida tropicalis*. Applied Microbiology and Biotechnology 29:370-374.

Keesey J (1987) Biochemica Information, in: Boehringer Mannheim Biochemicals, Indianapolis, IN1st edition 58.

Kihara T, Liu XY, Nakamura C, Park KM, Han SW, Qian DJ, Kawasaki K, Zorin NA, Yasuda S, Hata K, Wakayama T, Miyake J (2011) Direct electron transfer to hydrogenase for catalytic hydrogen production using a single-walled carbon nanotube forest. International Journal of Hydrogen Energy 36:7523-7529.

Kim J, Grate JW, Wang P (2008) Nanobiocatalysis and its potential applications. Trends in Biotechnology 26:639-646.

Kim J, Jia H, Wang P (2006) Challenges in biocatalysis for enzyme-based biofuel cells. Biotechnology Advances 24:296- 308.

Kim YH, Campbell E, Yu J, Minteer SD, Banta S (2013) Complete oxidation of methanol in biobattery devices using a hydrogel created from three modified dehydrogenases. Angewandte Chemie International Edition 52:1437-1440.

Kirgoz UA, Tural H, Timur S, Pazarlioglu N, Telefoncu A, Pilloton R (2005) Laccase biosensors based on mercury thin film electrode. Artifical Cells Blood Substitute and Immobilization Biotechnology 33:447-56.

Kittl R, Mueangtoom K, Gonaus C, Khazaneh ST, Sygmund C, Haltrich D, Ludwig R (2012) A chloride tolerant laccase from the plant pathogen ascomycete *Botrytis aclada* expressed at high levels in *Pichia pastoris*. Journal of Biotechnology 157:304-314.

Kowalski D, Schmuki P (2010) Polypyrrole self-organized nanopore arrays formed by controlled electropolymerization in $TiO_2$ nanotube template. Chemical Communication (Camb) 46:8585-8587.

Kulys J, Vidziunaite R (2003) Amperometric biosensors based on recombinant laccases for phenols determination. Biosensors and Bioelectronics 18:319-325.

Kumar AK, Goswami P (2006) Functional characterization of alcohol oxidases from *Aspergillus terreus* MTCC 6324. Applied Microbiology and Biotechnology 72:906-911.

Kunnecke W, Schmid RD (1990) Gas-diffusion dilution flow-injection method for the determination of ethanol in beverages without sample pretreatment. Analytica Chimica Acta 234:213-220.

Kuswandi B, Irmawati T, Hidayat MA, Jayus, Ahmad M (2014) A simple visual ethanol biosensor based on alcohol oxidase immobilized onto polyaniline film for halal verification of fermented beverage samples. Sensors 14:2135-2149.

Laviron E (1979a) General expression of the linear potential sweep voltammogram in the case of diffusionless electrochemical system. Journal of Electroanalytical Chemistry 101:19-28.

Laviron E (1979b) The use of linear potential sweep voltammetry and of a.c. voltammetry for the study of the surface electrochemical reaction of strongly adsorbed systems and of redox modified electrodes. Journal of Electroanalytical Chemistry 100:263-270.

Lee CA, Tsai YC (2009) Preparation of multiwalled carbon nanotube-chitosan alcohol dehydrogenase nanobiocomposite for amperometric detection of ethanol. Sensors and Actuators B Chemical 138:518-523.

Lee J, Sohn K, Hyeon T (2001) Fabrication of novel mesocellular carbon foams with uniform ultralarge mesopores. Journal of American Chemical Society 123:5146-5147.

Lefevre M, Dodelet JP, Bertrand P (2002) Molecular oxygen reduction in PEM fuel cells: Evidence for the simultaneous presence of two active sites in Fe based catalysts. Journal of Physical Chemistry B 106:8705-8713.

Li D, Luo L, Pang Z, Ding L, Wang Q, Ke H, Huang F, Wei Q (2014) Novel phenolic biosensor based on a magnetic polydopamine-laccase-nickel nanoparticle loaded carbon nanofiber composite. ACS Applied Materials and Interfaces. 9:5144-5151.

Lim J, Malati P, Bonet F, Dunn B (2007) Nanostructured sol-gel electrodes for biofuel cells Journal of Electrochemical Society 154:A140-A145.

Lindgren A, Emneus J, Ruzgas T, Gorton L, Marko-Varga G (1997) Amperometric detection of phenols using peroxidase-modified graphite electrode. Analytica Chimica Acta 347:51–62.

Liu F, Banta S, Chen W (2013) Functional assembly of a multi-enzyme methanol oxidation cascade on a surface-displayed trifunctional scaffold for enhanced NADH production. Chemical Communications 49:3766-3768.

Liu H, Cheng S, Logan BE (2005) Power generation in fed-batch microbial fuel cells as a function of ionic strength, temperature, and reactor configuration. Environmental Science and Technology 39:658-662.

Liu Y, Qu X, Guo H, Chen H, Liu B, Dong S (2006) Facile preparation of amperometric laccase biosensor with multifunction based on the matrix of carbon nanotubes–chitosan composite. Biosensors and Bioelectronics 21:2195-2201.

Li Y, Trush MA (1994) Reactive oxygen-dependent DNA damage resulting from the oxidation of phenolic compounds by a copper-redox cycle mechanism. Cancer Research 54:1895-1898.

Logan BE, Hamelers B, Rozendal R, Schroder U, Keller J, Freguia S, Aelterman P, Verstraete W, Rabaey K (2006) Microbial fuel cells: methodology and technology. Environmental Science and Technology 40:5181-5192.

Lu Q, Li CM (2008) One-step co-electropolymerized conducting polymer-protein composite film for direct electrochemistry-based biosensors. Biosensors and Bioelectronics 24:773-778.

Lu X, Zou G, Li J (2007) Hemoglobin entrapped within a layered spongy $Co_3O_4$ based nanocomposite featuring direct electron transfer and peroxidase activity. Journal of Materials Chemistry 17:1427-1432.

Madhavi V, Lele SS (2009) Laccase: properties and applications. BioResources 4:1694-1717.

Mano N (2008) A 280 μW $cm^{-2}$ biofuel cell operating at low glucose concentration. Chemical Communication 19:2221-2223.

Mano N, Mao F, Heller A (2004) A miniature membrane-less biofuel cell operating at +0.60 V under physiological conditions. Chembiochemistry 5:1703-1705.

Mano N, Soukharev V, Heller A (2006) A laccase-wiring redox hydrogel for efficient catalysis of $O_2$ electroreduction. The Journal of Physical Chemistry B 110:11180-11187.

Marcus RA, Sutin N (1985) Electron transfers in chemistry and biology. Biochimica et Biophysica Acta (BBA) - Bioenergetics 811:265-322.

Mataix E, de Castro MDL (2000) Simultaneous determination of ethanol and glycerol in wines by a flow injection-pervaporation approach with in parallel photometric and fluorimetric detection. Talanta 51:489-496.

Matijasevic G, Brandt L (2009) Conductive materials, wires and cables. In Electrical Engineerin; Wong KP Eds. 17-40.

Mayer AM, Staples RC (2002) Laccase: new functions for an old enzyme. Phytochemistry 60:551-565.

Mendes LS, Oliveira FCC, Suarez PAZ, Rubim JC (2003) Determination of ethanol in fuel ethanol and beverages by fourier transform (FT)-near infrared and FT-Raman spectrometries. Analytica Chimica Acta 493:219-231.

Meredith MT, Minteer SD (2012) Biofuel cells: enhanced enzymatic bioelectrocatalysis. Annual Review of Analytical Chemistry 5:157-179.

Minteer SD, Atanassov P, Luckarift HR, Johnson GR (2012) New materials for biological fuel cells. Materials today 15:166-173.

Minteer SD, Liaw BY, MJ Cooney (2007) Enzyme-based biofuel cells. Current Opinion in Biotechnology 18:228- 234.

Mitsubayashi K, Kon T, Hashimoto Y (2003) Optical bio-sniffer for ethanol vapor using an oxygen-sensitive optical fiber. Biosensors and Bioelectronics 19:193-198.

Miyake T, Yoshino S, Yamada T, Hata K, Nishizawa M (2011) Self-regulating enzyme-nanotube ensemble films and their application as flexible electrodes for biofuel cells Journal of the American Chemical Society 133:5129-5134.

Moiroux J, Elving PJ (1980) Mechanistic aspects of the electrochemical oxidation of dihydronicotinamide adenine dinucleotide (NADH). Journal of American Chemical Society 102: 6533-6538.

Morozova OV, Shumakovich GP, Gorbacheva MA, Shleev SV, Yaropolov AI (2007) "Blue" laccases. Biochemistry (Mosc.) 72:1136-1150.

Munteanu FD, Ferreira P, Ruiz-Duenas FJ, Martinez AT, Cavaco-Paulo A (2008) Bioelectrochemical investigations of aryl-alcohol oxidase from *Pleurotus eryngii*. Journal of Electroanalytical Chemistry 618:83-86.

Murata K, Suzuki M, Kajiya K, Nakamura N, Ohno H (2009) High performance bioanode based on direct electron transfer of fructose dehydrogenase at gold nanoparticle-modified electrodes. Electrochemistry Communication 11:668-671.

Murray RW (1984) in: A.J. Bard (Ed.), Electroanalytical Chemistry, 7 Marcel Dekker, New York 191–368.

Myler S, Collye SD, Davis F, Gornall DD, Higson SPJ (2005) Sonochemically fabricated microelectrode arrays for biosensors: Part III. AC impedimetric study of aerobic and anaerobic response of alcohol oxidase within polyaniline. Biosensors and Bioelectronics 21:666-671.

Nambiar S, Yeow JT (2011) Conductive polymer-based sensors for biomedical applications. Biosensors and Bioelectronics 26:1825-32.

Neburchilov V, Martin J, Wang H, Zhang J (2007) A review of polymer electrolyte membranes for direct methanol fuel cells. Journal of Power Sources 169:221-238.

Neto SA, Forti JC, Zucolotto V, Ciancaglini P, de Andrade AR (2011) Development of nanostructured bioanodes containing dendrimers and dehydrogenases enzymes for application in ethanol biofuel cells. Biosensors and Bioelectronics 26:2922-2926.

Neto SA, Suda EL, Xu S, Meredith MT, De Andrade AR, Minteer SD (2013) Direct electron transfer-based bioanodes for ethanol biofuel cells using PQQ-dependent alcohol and aldehyde dehydrogenases. Electrochimica. Acta 87:323-329.

Oliveira TMBF, Fatma BM, Morais S, de Lima-Neto P, Correia AN, Oliveira MBPP, Delerue-Matos C (2013). Biosensor based on multiwalled carbon nanotubes paste electrode modified with laccase for pirimicarb pestcide quantifcaton. Talanta 106:137-143.

Osman MH, Shah AA, Walsh FC (2011) Recent progress and continuing challenges in bio-fuel cells. Part I: Enzymatic cells. Biosensors and Bioelectronics 26:3087-3102.

Ozimek P, Veenhuis M, van der Klei IJ (2005) Alcohol oxidase: a complex peroxisomal, oligomeric flavoprotein. FEMS Yeast Research 5:975-983.

Palmore GTR, Bertschy H, Bergens SH, Whitesides GMA (1998) A methanol/dioxygen biofuel cell that uses $NAD^+$-dependent dehydrogenases as catalysts: application of an electro-enzymatic method to regenerate nicotinamide adenine dinucleotide at low overpotentials. Journal of Electroanalytical Chemistry 443:155-161.

Park BW, Yoon DY, Kim DS (2010) Recent progress in bio-sensing techniques with encapsulated enzymes. Biosensors and Bioelectronics 26:1-10.

Patel NG, Meier S, Cammann K., Chemnitius GC (2001) Screen-printed biosensors using different alcohol oxidases. Sensors and Actuators B:Chemical 75:101-110.

Patolsky F, Weizmann Y, Willner I (2004) Long-range electrical contacting of redox enzymes by SWCNT connectors. Angewandte Chemie-International Edition 43:2113-2117.

Pierson, HO (1993) Handbook of carbon, graphite, diamond, and fullerenes: properties, processing, and applications; William Andrew.

Pingarron JM, Yanez-Sedeno P, Gonzalez-Cortes A (2008) Gold nanoparticle-based electrochemical biosensors. Electrochimica Acta 53:5848-5866.

Pita M, Gutierrez-Sanchez Cristina, Olea D, Velez M, Garcia-Diego C, Shleev S, Fernandez V M, De Lacey AL (2011) High redox potential cathode based on laccase covalently attached to gold electrode. Journal of Physical Chemistry C 115:13420- 13428.

Prakasam HE, Shankar K, Paulose M, Varghese OK, Grimes CA (2007) A new benchmark for $TiO_2$ nanotube array growth by anodization. Journal of Physical Chemistry C111: 7235-7241.

Quan D, Kim Y, Shin W (2004) Characterization of an amperometric laccase electrode covalently immobilized on platinum surface. Journal of Electroanalytical Chemistry 561:181-189.

Quaranta M, Borisov SM, Klimant I (2012) Indicators for optical oxygen sensors. Bioanalytical Reviews 4:115-157.

Raj CR, Behera S (2005) Mediatorless voltammetric oxidation of NADH and sensing of ethanol. Biosensors and Bioelectronics 21:949-956.

Ramanathan K, Ram MK, Verghese MM, Malhotra BD (1996) Dielectric spectroscopic studies on polypyrrole glucose oxidase films. Journal of Applied Polymer Science 60:2309-2316.

Ramanavicius A, Kausaite A, Ramanaviciene A (2008) Enzymatic biofuel cell based on anode and cathode powered by ethanol. Biosensors and Bioelectronics 24:761-766.

Ramanavicius A, Ramanaviciene A (2009) Hemoproteins in design of biofuel cells. Fuel Cells 9:25-36.

Razumiene J, Gureviciene V, Laurinavicius V, Grazulevicius JV (2001) Amperometric detection of glucose and ethanol in beverages using flow cell and immobilised on screen printed carbon electrode PQQ-dependent glucose or alcohol dehydrogenasers. Sensors and Actuators B: Chemical, 78:243-248.

Rigla M, Hernando ME, Gomez EJ, Brugues E, Garcia-Saez G, Capel I, Pons B, de Leiva A (2008) Real-time continuous glucose monitoring together with telemedical assistance improves glycemic control and glucose stability in pump-treated patients. Diabetes Technology and Therapeutics 10:194-199.

Rincon RA, Lau C, Garcia KE, Atanassov P (2011b) Flow-through 3D biofuel cell anode for $NAD^+$-dependent enzymes. Electrochima Acta 56:2503-2509.

Rincon, RA, Lau C, Luckarift HR, Garcia KE, Adkins E, Johnson GR, Atanassov P (2011a) Enzymatic fuel cells: Integrating flow-through anode and air-breathing cathode into a membrane-less biofuel cell design. Biosensors and Bioelectronics 27:132- 136.

Rochefort D, Kouisni L, Gendron K (2008) Physical immobilization of laccase on an electrode by means of poly(ethyleneimine) microcapsules. Journal of Electroanalytical Chemistry 617:53-63.

Roy JJ, Abraham TE, Abhijith KS, Sujith Kumar PV, Thakur MS (2005) Biosensor forthe determination of phenols based on Cross-Linked Enzyme Crystals (CLEC) of laccase. Biosensors and Bioelectronics 21:206-211.

Rubenwolf S, Strohmeier O, Kloke A, Kerzenmacher S, Zengerle R, von Stetten F (2010) Carbon electrodes for direct electron transfer type laccase cathodes investigated by current density–cathode potential behavior. Biosensors and Bioelectronics 26:841-845.

Rubianes MD, Rivas GA (2007) Dispersion of multi-wall carbon nanotubes in polyethylenimine: a new alternative for preparing electrochemical sensors. Electrochemistry Communication 9:480-484.

Sakai H, Nakagawa T, Tokita Y, Hatazawa T, Ikeda T, Tsujimura S, Kano K (2009) A high-power glucose/oxygen biofuel cell operating under quiescent conditions. Energy and Environmental Science 2:133-138.

Sarma AK, Vatsyayan P, Goswami P, Minteer SD (2009) Recent advances in material science for developing enzyme electrodes. Biosensors and Bioelectronics 24:2313-2322.

Saxena U, Chakraborty M, Goswami P (2011a) Covalent immobilization of cholesterol oxidaseon self-assembled gold nanoparticles for highly sensitive amperometric detection of cholesterol in real samples. Biosensors and Bioelectronics 26: 3037-3043.

Saxena U, Das M, Ahmed S, Barbora L, Borthakur M, Verma A, Bora U, Goswami P (2011b) Multiwalled carbon nanotube-based bi-enzyme electrode for total cholesterol estimation in human serum. Journal of Experimental Nanoscience 6:84–95

Schaetzle O, Barriere F, Schroder U (2009) An improved microbial fuel cell with laccase as the oxygen reduction catalyst. Energy and Environmental Science 2:96-99.

Schmidt-Winkel P, Lukens WW, Zhao DY, Yang PD, Chmelka BF, Stucky GD (1999) Mesocellular siliceous foams with uniformly sized cells and windows. Journal of American Chemical Society 121:254-255.

Schweigert N, Zehnder AJB, Eggen RIL (2001) Chemical properties of catechols and their molecular modes of toxic action in cells, from microorganisms to mammals. Environmental Microbiology 3:81-91.

Scott RA, Lukehart CM (2007) Applications of Physical Methods to Inorganic and Bioinorganic Chemistry, tenth ed., Wiley, Hoboken, NJ. 25.

Seop CI, Moon H, Bretschger O, Jang JK, Park HI, Nealson KH, Kim BH (2006) Electrochemically active bacteria (EAB) and mediator-less microbial fuel cells. Journal of Microbiology and Biotechnology 16:163-177.

Serway RA (1998) Principles of Physics; 2nd, ed.; Fort Worth, Saunders College Pub: London.

Shaegh SAM, Nguyen NT, Chan SH (2011) A review on membraneless laminar flow-based fuel cells. International Journal of Hydrogen Energy 36:5675-5694.

Shleev S, Jarosz Wilkolazka A, Khalunina A, Morozova O, Yaropolov A, Ruzgas T, Gorton L (2005) Direct electron transfer reactions of laccases from different origins on carbon electrodes. Bioelectrochemistry.67:115-124.

Shleev S, Pita M, Yaropolov A I, Ruzgas T, Gorton L (2006) Direct heterogeneous electron transfer reactions of *Trametes hirsute* laccase at bare and thiol-modified gold electrodes. Electroanalysis 18:1901-1908.

Shkotova LV, Soldatkin AP, Gonchar MV, Schuhmann W, Dzyadevych SV (2006) Amperometric biosensor for ethanol detection based on alcohol oxidase immobilised

within electrochemically deposited Resydrol film. Materials Science and Engineering: C 26:411-414.

Smutok O, Ngounou B, Pavlishko H, Gayda G, Gonchar M, Schuhmann W (2006) A reagentless bienzyme amperometric biosensor based on alcohol oxidase/peroxidase and an Os-complex modified electrodeposition paint. Sensors and Actuators B Chemical 113:590-598.

Sokic-Lazic D, Arechederra RL, Treu BL, Minteer SD (2010) Oxidation of biofuels: fuel diversity and effectiveness of fuel oxidation through multiple enzyme cascades. Electroanalysis 22:757-764.

Sokic-Lazic D, Minteer SD (2008) Citric acid cycle biomimic on a carbon electrode. Biosensors and Bioelectronics 24:939-944.

Sokic-Lazic D, Minteer SD (2009) Pyruvate/air enzymatic biofuel cell capable of complete oxidation. Electrochemical and Solid-State Letters 12: F26-F28.

Solomon EI, Sundaram UM, Machonkin TE (1996) Multicopper oxidases and oxygenases. Chemical Reviews 96:2563-2605.

Solomon S, Pavani T, Sarma PN, Venkata Mohan S (2011) Synergistic interaction of biocatalyst with bio-anode as a function of electrode materials. International Journal of Hydrogen Energy 36:2271-2280.

Stob M (1983) Naturally occurring food toxicants: estrogens, in: M. Rechnig Jr. (Ed.), Handbook of Naturally Occurring Food Toxicants, CRC Press, Boca Raton, FL, 81–100.

Sun Q, Zorin NA, Chen D, Chen M, Liu TX, Miyake J, Qian DJ (2010) Langmuir-blodgett films of pyridyldithio-modified multiwalled carbon nanotubes as a support to immobilize hydrogenase. Langmuir, 26:10259-10265.

Suye S (2003) Purification and properties of alcohol oxidase from *Candida methanosorbosa*

M-2003. Current Microbiology 34:374-377.

Svensson K, Bulow L, Kriz D, Krook M (2005) Investigation and evaluation of a method for determination of ethanol with the SIRE® Biosensor P100, using alcohol dehydrogenase as recognition element. Biosensors and Bioelectronics 21:705-711.

Szot K, Watkins JD, Bull SD, Marken F, Opallo M (2010) Three dimensional film electrode prepared from oppositely charged carbon nanoparticles as efficient enzyme host, Electrochemistry Communications 12:737-739.

Takahashi H, Li B, Sasaki T, Miyazaki C, Kajino T, Inagaki S (2000) Catalytic activity in organic solvents and stability of immobilized enzymes depend on the pore size and surface characteristics of mesoporous silica. Chemistry of Materials 12:3301-3305.

Tan Y, Deng W, Ge B , Xie Q, Huang J, Yao S (2009) Biofuel cell and phenolic biosensor based on acid-resistant laccase–glutaraldehyde functionalized chitosan–multiwalled carbon nanotubes nanocomposite film. Biosensors and Bioelectronics 24:2225-2231.

Tarasevich MR, Bogdanovskaya VA, Kuznetsova LN (2001) Bioelectrocatalytic reduction of oxygen in the presence of laccase adsorbed on carbon electrodes. Russian Journal of Electrochemistry 37:833-837.

Thevenot DR, Toth K, Durst RA, Wilson GS (1999) Electrochemical Biosensors: Recommended Definitions and Classification. Pure and Applied Chemistry 7:2333-2348.

Thurston CF (1994) The structure and function of fungal laccases. Microbiology 140:19-26.

Timur S, Pazarlioglu N, Pilloton R, Telefoncu A (2004) Thick film sensors based on laccases from different sources immobilized in polyaniline matrix. Sensors and Actuators B: Chemical 97:132-136.

Togo M, Takamura A, Asai T, Kaji H, Nishizawa M (2007) An enzyme-based microfluidic biofuel cell using vitamin $K_3$-mediated glucose oxidation. Electrochimica Acta 52:4669-4674.

Topcagic S, Minteer SD (2006) Development of a membraneless ethanol/oxygen biofuel cell. Electrochimica Acta 51:2168-2172.

Vatsyayan P, Bordoloi S, Goswami P (2010) Large catalase based bioelectrode for biosensor application. Biophysical Chemistry 153:36-42.

Vatsyayan P, Chakraborty M, Bordoloi S, Goswami P (2011) Electrochemical investigations of fungal cytochrome P 450. Journal of Electroanalytical Chemistry 662:312-316.

Veenhuis M, Harder W, van Dijken JP, Mayer F (1981) Substructure of crystalline peroxisomesin methanol-grown *Hansenula polymorpha*: evidence for an in vivo crystal of alcohol oxidase. Molecular and Cellular Biology 1:949-957.

Vijayakumar AR, Csoregi E, Heller A, Gorton L (1996) Alcohol biosensors based on coupled oxidase-peroxidase system. Analytica Chimica Acta 327:223-234.

Wang G, Xu JJ, Chen HY, Lu ZH (2003b) Amperometric hydrogen peroxide biosensor with sol gel/chitosan network-like film as immobilization matrix. Biosensors and Bioelectronics 18:335-343.

Wang J, Musameh M, Lin Y (2003a) Solubilization of carbon nanotubes by nafion toward the preparation of amperometric biosensors. Journal of American Chemical Society 125:2408-2409.

Wang J (1999) Sol–gel materials for electrochemical biosensors. Analytica Chimica Acta 399: 21-27.

Wang J (2001) Glucose biosensors: 40 Years of advances and challenges. Electroanalysis 13:983-988.

Wang JY, Nien PC, Chen CH, Chen LC, Ho KC (2012a) A glucose bio-battery prototype based on a GDH/poly(methylene blue) bioanode and a graphite cathode with an iodide/tri-iodide redox couple. Bioresource Technology 116:502-506.

Wang K, Tang J, Zhang Z, Gao Y, Chen G (2012b) Laccase on Black Pearl 2000 modified glassy carbon electrode: characterization of direct electron transfer and biological sensing properties for pyrocatechol. Electrochimica Acta 70:112-117.

Wei J, Liang P, Huang X (2011) Recent progress in electrodes for microbial fuel cells. Bioresourse technology 102:9335-9344.

Wen D, Liu W, Herrmann AK, Eychmuller A (2014) A membraneless glucose/$O_2$ biofuel cell based on Pd aerogels chemistry - A European Journal 20: 4380-4385.

Wen G , Zhang Y, Shuang S, Dong C, Choi MMF (2007) Application of a biosensor for monitoring of ethanol. Biosensors and Bioelectronics 23:121-129.

Willner I (2009) Biofuel cells: harnessing biomass or body fluids for the generation of electrical power. Fuel Cells 9:5.

Willner I, Arad G, Katz E (1998) A biofuel cell based on pyrroloquinoline quinone and microperoxidase-11 monolayer-functionalized electrodes. Bioelectrochemistry and Bioenergetics 44:209-214.

Willner I, Baron R, Willner B (2007) Integrated nanoparticle-biomolecule systems for biosensing and bioelectronics. Biosensors and Bioelectronics 22:1841-1852.

Willner I, Willner B (2001) Biomaterials integrated with electronic elements: en route to Bioelectronics. Trends in Biotechnology 19:222-230.

Willner I, Willner B, Katz E (2002) Functional biosensor systems *via* surface-nanoengineering of electronic elements. Reviews in Molecular Biotechnology 82:325-355.

Wink T, van Zuilen SJ, Bult A, van Bennkom WP (1997) Self-assembled monolayers for

biosensors. Analyst 122:43R-50R.

Wu F, Xu J, Tian Y, Hu Z, Wang L, Xian Y, Jin L (2008) Direct electrochemistry of horseradish peroxidase on $TiO_2$ nanotube arrays via seeded-growth synthesis. Biosensors and Bioelectronics 24:198-203.

Wu J, Suls J, Sansen W (1999) Amperometric glucose sensor with enzyme covalently immobilized by sol gel technology. Analytical Sciences 15:1029-1032.

Wu X, Zhao F, Varcoe JR, Thumser AE, Avignone-Rossa C, Slade RCT (2009) A one-compartment fructose/air biological fuel cell based on direct electron transfer. Biosensors and Bioelectronics 25:326-331.

Xia L, Wei Z, Wan M (2010) Conducting polymer nanostructures and their application in biosensors. Journal of Colloid and Interface Science 341:1-11.

Xian Y, Hu Y, Liu F, Xian Y, Feng L, Jin L (2007) Template synthesis of highly ordered Prussian blue array and its application to the glucose biosensing. Biosensors and Bioelectronics 22:2827-2833.

Xiao Y, Patolsky F, Katz E, Hainfeld JF, Willner I (2003) Plugging into enzymes: Nanowiring of redox enzymes by a gold nanoparticle. Science 299:1877-1881.

Xie X, Suleiman AA, Guilbault GG, Yang ZM, Sun ZA (1992) Flow injection determination of ethanol by fiber-optic chemiluminescence measurement. Analytica Chimica Acta. 266:325-329.

Xie YB, Zhou LM, Huang HT (2007) Bioelectrocatalytic application of titania nanotube array for molecule detection. Biosensors and Bioelectronics 22:2812-2818.

Xu X, Lu P, Zhou Y, Zhao Z, Guo M (2009) Laccase immobilized on methylene blue modified mesoporous silica MCM-41/PVA. Materials Science and Engineering C 29:2160-2164.

Yahiro AT, Lee SM, Kimble DO (1964) Bioelectrochemistry. I. enzyme utilizing bio-fuel cell studies. Biochimica Biophysica Acta—Specialized Section on Biophysical Subjects 88:375-383.

Yakushi T, Matsushita K (2010) Alcohol dehydrogenase of acetic acid bacteria: structure, mode of action, and applications in biotechnology. Applied Microbiology and Biotechnology 86:1257-1265.

Yan YM, Baravik I, Tel-Vered R, Willner I (2009**)** An ethanol/$O_2$ biofuel cell based on an electropolymerized bilirubin oxidase/Pt nanoparticle bioelectrocatalytic $O_2$-reduction cathode. Advance Materials 21:4275-4279.

Yaropolov AI, Kharybin AN, Emneus J, Marko-Varga G, Gorton L (1995) Flow injection analysis of phenols at a graphite electrode modified with co-immobilised laccase and tyrosinase. Analytica Chimica Acta 308:137-144.

Yildiz HB, Toppare L (2006) Biosensing approach for alcohol determination using immobilized alcohol oxidase. Biosensors and Bioelectronics 21:2306-2310.

Ying JY, Mehnert CP, Wong MS (1999) Synthesis and applications of supramolecular-templated mesoporous materials. Angewandte Chemie International Edition 38:56-77.

Yu EH, Scott K (2010) Enzymatic biofuel cells-fabrication of enzyme electrodes. Energies 3:23-42.

Zayats M, Katz E, Baron R, Willner I (2005) Reconstitution of apo-glucose dehydrogenase on pyrroloquinoline quinone-functionalized Au nanoparticles yields an electrically contacted biocatalyst. Journal of the American Chemical Society 127:12400-12406.

Zebda A, Renaud L, Cretin M, Pichot F, Innocent C, Ferrigno R, Tingry S (2009a) A microfluidic glucose biofuel cell to generate micropower from enzymes at ambient temperature. Electrochemistry Communication 11:592-595.

Zebda A, Renaud L, Cretin M, Innocent C, Pichot F, Ferrigno R, Tingry S (2009b) Electrochemical performance of a glucose/oxygen microfluidic biofuel cell. Journal of Power Sources 193: 602-606.

Zhang J, Kuznetsov AM, Medvedev IG, Chi Q, Albrecht T, Jensen PS, Ulstrup J (2008) Single molecule electron transfer in electrochemical environments. Chemical Reviews 108:2737-2791.

Zhang L, Ma C, Mukerjee S (2003) Oxygen permeation studies on alternative proton exchange membranes designed for elevated temperature operation. Electrochimica Acta 4:1845-1859.

Zhang L, Zhou M, Dong S (2012) A self-powered acetaldehyde sensor based on biofuel cell. Analytical Chemistry 84:10345-1034.

Zhang M, Gorski W (2011) Amperometric ethanol biosensors based on chitosan-$NAD^{+}$-alcohol dehydrogenase film. Electroanalytical 23:1856-1862.

Zhang W, Li G (2004) Third-generation biosensors based on the direct electron transfer of proteins. Analytical Sciences 20:603-609.

Zhou D, Fang HQ, Chen H, Ju H, Wang Y (1996) The electrochemical polymerization of methylene green and its electrocatalysis for the oxidation of NADH. Analytica Chimica Acta 329:41-48.

Zhou X, Liu L, Bai X, Shi H (2013) A reduced graphene oxide based biosensor for high-sensitive detection of phenols in water samples. Sensors and Actuators B:Chemical 181:661-667.

Zloczewska A, Jönsson-Niedziolka M (2013) Efficient air-breathing biocathodes for zinc/oxygen batteries. Journal of Power Sources 228:104-111.

# List of Publication

**Publication in Referred Journals**

1. **Madhuri Das**, Lepakshi Barbora, Priyanki Das, Pranab Goswami (2014) Biofuel cell for generating power from methanol substrate using alcohol oxidase bioanode and air-breathed laccase biocathode..Biosensors and Bioelectronics 59:184-191.
2. Priyanki Das, Lepakshi Barbora, **Madhuri Das**, Pranab Goswami (2014) Highly sensitive and stable laccase based amperometric biosensor developed on nano-composite based matrix for detecting pyrocatechol in environmental samples. Sensors and Actuators B: Chemical 192 :737-744.
3. **Madhuri Das**, Pranab Goswami (2013) Direct electrochemistry of alcohol oxidase using multiwalled carbon nanotube as electroactive matrix for biosensor application. Bioelectrochemistry 89:19-25. **[Research highlight in Nature India.com: doi:10.1038/nindia.2012.142; Published online 26 September 2012].**
4. Urmila Saxena, **Madhuri Das**, Seraj Ahmad, Lepakshi Barbora, Mala Borthakur, Anil Verma, Utpal Bora, Pranab Goswami (2011) Multiwalled carbon nanotube-based enzyme electrode for total cholesterol estimation in human serum. Journal of Experimental Nanoscience 6:84–95.

**Abstract Published in Conferences**

1. **Madhuri Das,** Pranab Goswami, Development of bioanode for biofuel cell application, organized by Reflux 1.0, Annual Technical Festival of Dept of Chemical Engineering, IIT Guwahati during 6$^{th}$ to7$^{th}$ April 2013.

2. **Madhuri Das**, Priyanki Das, Lepakshi Barbora, Pranab Goswami, Electroactive nanomaterials based alcohol oxidase bioanode and laccase biocathode for biofuel cell development, Indo-US workshop on Electrocatalytic Materials for Fuel and Biofuel Cells ( Indo-US ECM 2013), jointly organised by Indo-US science and technology forum and Banaras Hindu University (BHU) February 25-28, 2013 Abstarct no PP-58.
3. **Madhuri Das**, Pranab Goswami, Development of nanocomposite based enzymatic bioanode and biocathode for biofuel cell, Indo German workshop on "Advanced materials for Future Energy requirements."(WAMFER 2012)" jointly organized by Max Planck Institute for Polymer Research, Mainz, Germany and University of Delhi, India, 29th november-1st December 2012. (Oral)
4. **Madhuri Das,** Pranab Goswami, Fabrication of alcohol oxidase based bioanode for biofuel cell application. Secone 2012, (Synergy for Energy, Challenges and opportunities in North East India), NEDFi convention centre. Guwahati 28$^{th}$ April 2012.
5. **Madhuri Das,** Pranab Goswami, Advances in the biofuel cell research, potential energy generating devices for biomedical application, National seminar on New and renewable sources of energy, organised by Environmental Watch and Management Institute, sponsored by Ministry of New and Renewable Energy, India ,MD trade centre Guwahati. March 21-22, 2012. (Oral)
6. **Madhuri Das**, Leepakshi Barbora, Priyanki Das, Pranab Goswami, Development of laccase based biocathode for biofuel cell application, The 18$^{th}$ International Conference (POST ISCBC-2012) IASST Guwahati, Assam, India, January 28-30, 2012.
7. **Madhuri Das,** Pranab Goswami, Carbon nanotube as electroactive matrix for immobilization of alcohol oxidase on gold electrode for biosensor and biofuel cell application, ICANN 2011, IIT Guwahati, Dec 08-10, 2011, Abstract id G1591.

8. **Madhuri Das,** Pranab Goswami, Electrochemical characterization and development of alcohol oxidase bioelectrode for enzymatic biosensor and biofuel cell application, 80th Annual meeting of the society of Biological Chemists, CSIR-CIMAP, Lucknow, 12th-15th November 2011, Abstract no BB 6
9. **Madhuri Das**, Pranab Goswami, Development of 3rd generation Bioanode using carbon nanotube (CNT) as a electroactive material based on immobilization of alcohol oxidase for enzymatic biofuel cell application, Summer School., IIT Guwahati, July 4-11, 2011.
10. **Madhuri Das,** Pranab Goswami, Development of Alcohol biosensor using Multiwalled carbon nanotube (MWCNT)-nafion-Polyethyleneimine (PEI) as electroactive matrix for immobilization of alcohol oxidase on electrode surface, Banglore India Bio 2011,(International conference + Trade show), Banglore International Exhibition Centre, Banglore. May 4-6 2011, Abstract No 26.
11. **Madhuri Das**, Pranab Goswami, Modified carbon nanotube and nafion composite as electro-active matrix for immobilization of cholesterol oxidase on gold electrode for bioelectrode fabrication. International Conference on Carbon Nanotechnology: Potential and Challenges, IIT Kanpur, 15-17 December, 2010.
12. Urmila Saxena, **Madhuri Das**, Seraj Ahmad, Pranab Goswami An amperometric cholesterol biosensor based on multiwalled carbon nanotube–nafion–cholesterol oxidase cholesterol esterase nanobiocomposite, International Conference on advance nano-materials and Nanotechnology, IIT Guwahati, December 9-11, 2009, Abstract No E–134.
13. Sandip Bordoloi, **Madhuri Das**, Preety Vatsyayan and Pranab Goswami. Fabrication of composite Cholesterol Oxidase Bioelectrode with carbon nanotube–based direct electron transfer for biofuel cell application. International Conference on advance nano-materials and Nanotechnology, IIT Guwahati, December 9-11, 2009 Abstract No. A-571.